Master Thesis, Department of Geosciences

# Detailed Structural Investigation of the Bjørnøyrenna Fault Complex, SW Barents Sea

**Muhammad Saqib Hameed**

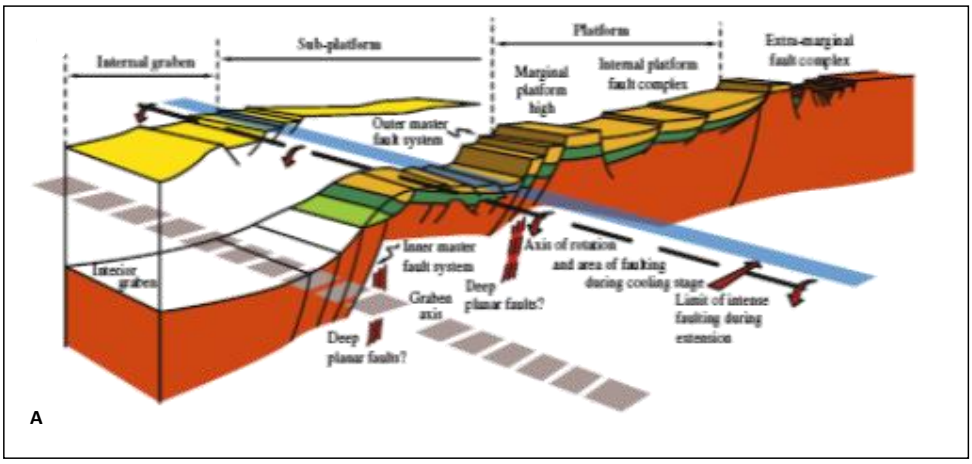


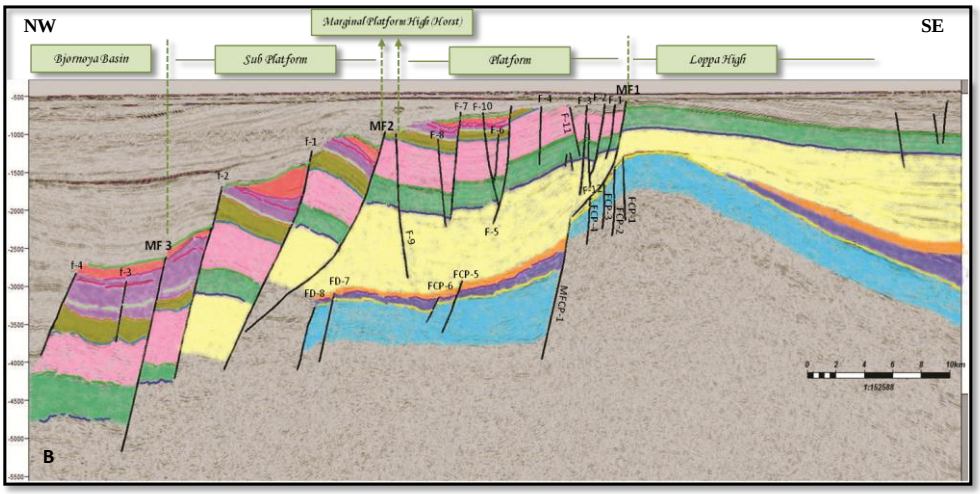


UNIVERSITY OF OSLO
FACULTY OF MATHEMATICS AND NATURAL SCIENCES

# Detailed Structural Investigation of the Bjørnøyrenna Fault Complex, SW Barents Sea

**Muhammad Saqib Hameed**

Master Thesis in Geosciences
Discipline: Petroleum Geology and Petroleum Geophysics
Department of Geosciences
Faculty of Mathematics and Natural Sciences

University of Oslo

**June 2012**

Tutor(s): **Prof. Roy Helge Gabrielsen, Prof. Jan Inge Faleide and Michel Heeremans, UiO**

# Abstract

The NE-SW and N-S trending, Bjørnøyrenna Fault Complex is obviously belongs to an extensional regime. It is comprised of three main master faults (MF1, MF2 & MF3) in the study area. This large array of master faults further characterized by different segments termed as (MF1a, MF1b; MF2a, MF2b; MF3a, MF3b & MF3c) which constitute linked fault system with variable soft-linked and hard-linked elements. In a cross-sectional view, the fault geometries exhibit a distinct contrast between deepest (late Carboniferous-early Permian) and shallowest (intra Triassic -Cretaceous) stratigraphic levels. On the basis of regional significance and thick skin nature, MFCP1 qualified as a "**First class"** fault. On the other hand, MF1 & MF2 are not basement involved but shows reactivation with time and exhibits a regional significance. Therefore, it could be termed as a combination of "**First** or **Second class"** fault.

Subsequently, the fault complex is subdivided into platform and sub platform on the basis of intrinsic fault frequency, pattern and dip dimensions of the reflection packages. On the platform, the fault at deeper level MFCP1 is characterized by planar fault geometry whereas; MF1 at shallowest level is dominated by strong listric configuration. Additionally, relatively simple listric detachment has been recognized within Permian succession. However, rotated fault blocks geometry has been recognized along planar normal faults (MF2a & MF2b) in sub platform.

Fault dating was performed by using the methods of expansion growth index and recognition of syn-rift sedimentation. On the behalf of these methods, the N-S striking, MFCP1 was active in the late Carboniferous-early Permian whereas, NE-SW striking master fault MF2a & MF2b demonstrates an age of mid/late Jurassic – early Cretaceous. Moreover, an age of MF1 could be younger than the intra Triassic.

An evidence of positive structural inversion is recognized in the present study. The analysis of such feature suggests that the strike slip movement could be responsible for the generation of this mild inversion. Therefore, an age of inversion structure can be related to the late Jurassic to the early Cretaceous.

The evolution of the Bjørnøyrenna Fault Complex was started in late Carboniferous-early Permian. The late Permian-early Triassic period was characterized by the uplift of the Loppa high and significant subsidence recognized in the fault complex. The mid-late Triassic period was characterized by growth faulting. The mid Jurassic-early Cretaceous time was marked by an extensive uplifting followed by tremendous erosion of sediments. The early cretaceous time is characterized by positive inversion resulting in strike slip movement. In addition, late Cretaceous time is followed by post rift subsidence.

# ACKNOWLEDGEMENT

I would like to express my gratitude to my supervisor Professor Roy Helge Gabrielsen for being an outstanding advisor and excellent professor. His constant encouragement, support, and invaluable suggestions made this work successful. I would also like to thank Professor Jan Inge Faleide for his guidance throughout the length of this study. I owe special thanks to Dr. Michel Heereman, co-supervisor, who helped in data management.

I would like to acknowledge Fugro & NPD for providing the seismic and well data for this study.

I am deeply and forever indebted to my parents for their love, support and encouragement throughout my entire student life.

I owe a great many thanks to a great many people who helped and supported me during the writing of this book.

# Contents

# CHAPTER 1

# INTRODUCTION

The Barents Sea is one of the largest continental shelf covering an area of 1.3 million $Km^2$ with an average water depth of 300m *(fig. 1.1)* (Dore et al., 1994). It is bounded by the north Norwegian and Russian Coasts, the Franz Joseph Land, Novaya Zemlya, Svalbard archipelagos and the eastern margin of the deep Atlantic Ocean (Dore et al., 1994).

The Barents Sea captured enormous attention of the oil industry from the last few years. The region is the best anatomized portion of the North Pole (Arctic zone) because the ice conditions are admissible, which has permitted enormous seismic acquisitions in the vicinity, particularly for the petroleum exploration. This extensive database has enhanced our apprehension of the subsurface geology. The demand has increased in the south west Barents Sea due to continued sake in petroleum exploration which promote to solve the basin dynamics of the area. This region is key area to understand the backup processes behind vertical movements, Subsidence and uplifting (Glorstad-clark et al., 2010). The exploration was exposed in 1980's in the southern Barents Sea and first discovered in 1981. A total amount of $288.5 \times 10^6$ $Sm^3$ o.e.(ca. 1.8 bn boe) has been discovered till now. About 25 discoveries have been made in the Barents Sea, most of them in the Hammerfest Basin where their reservoirs are in sandstones, mainly Jurassic as in the Snøhvit Field. Deeper discoveries have also been made, such as in the Triassic Sandstone in 7122/7-1 (Goliath Field) and 7125/4-1 (Nucula Field) (Faleide et al., 2010).

Structurally, the Barents Sea exhibits sedimentary Basins separated by deep seated fault complexes and highs. The constitution of these basins was followed by two major continental collisions and later dominated by continental separation (Dore et al., 1994). The area that has undertaken in thesis work is the NE-SW trending Bjørnøyrenna Fault Complex between 72º N, 19' E and 73º 15' N, 22º E. It exhibits a junction between the Loppa High and the Bjørnøya Basin. The faults within this province are of Paleozoic age and older provenance and were reactivated several times during the Mesozoic and Tertiary. It is likely that the fault complex is underlain by an old zone of weakness (Faleide et al., 1984; Gabrielsen, 1984; Gabrielsen et al., 1984).

The foremost objective of thesis work is to investigate the structural geometry, dating of structural events, styles and temporal evolution of the Bjørnøyrenna Fault Complex. Result of this study can lead to increase of knowledge and understanding about geometry, style and relationship between regional tectonic events and evolution of the Bjørnøyrenna Fault Complex in the southwest Barents Sea.


**Figure 1.1:** Regional setting and approximate location of the study area in orange highlighted rectangle (modified from www.wikipedia.com)

# CHAPTER 2

# Regional Tectonics & Stratigraphic Framework

## 2.1 Regional Setting

The Barents Sea is one of the largest epicontinental sea located at the north-western continental shelf of Eurasia *(fig. 1.1)*. It is restricted to the west and north by Cenozoic passive margins that formed by the extension of the Norwegian-Greenland Sea and the Eurasian Basin. Late Paleozoic to Quaternary age is dominated by sedimentary successions with having thickness more or less than 15 km (Faleide, J.I et al 1993a). The Barents Sea had been influenced by two stages of Caledonian Compressional deformation (sturt et al., 1978) and later crushed by continental separation. The first two collision event was dominated by svalbardian (Late Devonian) sinistral strike slip movements and the Kimmerian tectonic phase (Jurassic to Early Cretaceous) where as continental separation occurred around Paleocene (Gabrielsen et al., 1984).

## 2.2 Geological Provinces

The Barents Sea is split up into two main geological provinces eastern and western segment. The eastern province was influenced by late Paleozoic tectonism where as minimal deformation in Post Jurassic times while western province was affected by tectonically active mostly in Late Mesozoic and Cenozoic times.

The western Barents Sea is further subdivided into three different units *(fig. 2.1)* (Faleide et al., 1993).

(1) The Svalbard platform is covered with a relatively flat underlying sequence of Upper Paleozoic and Mesozoic, mainly Triassic sediments.
(2) The basin province Between Svalbard and the Norwegian platform Coast is characterized by a number of sub-basins and Highs and the sediments deposited in these basin are Jurassic – Cretaceous while the western side of the basin is dominated by Paleocene – Eocene Sediments.

(3) The western continental margin exhibit into three main units (a) a southern sheared margin along the Senja fracture zone; (b) a central rifted complex south- west of Bjørnøya associated with volcanism ; (c) in the north, initially sheared and later rifted margin along the Hornsund Fault Zone.

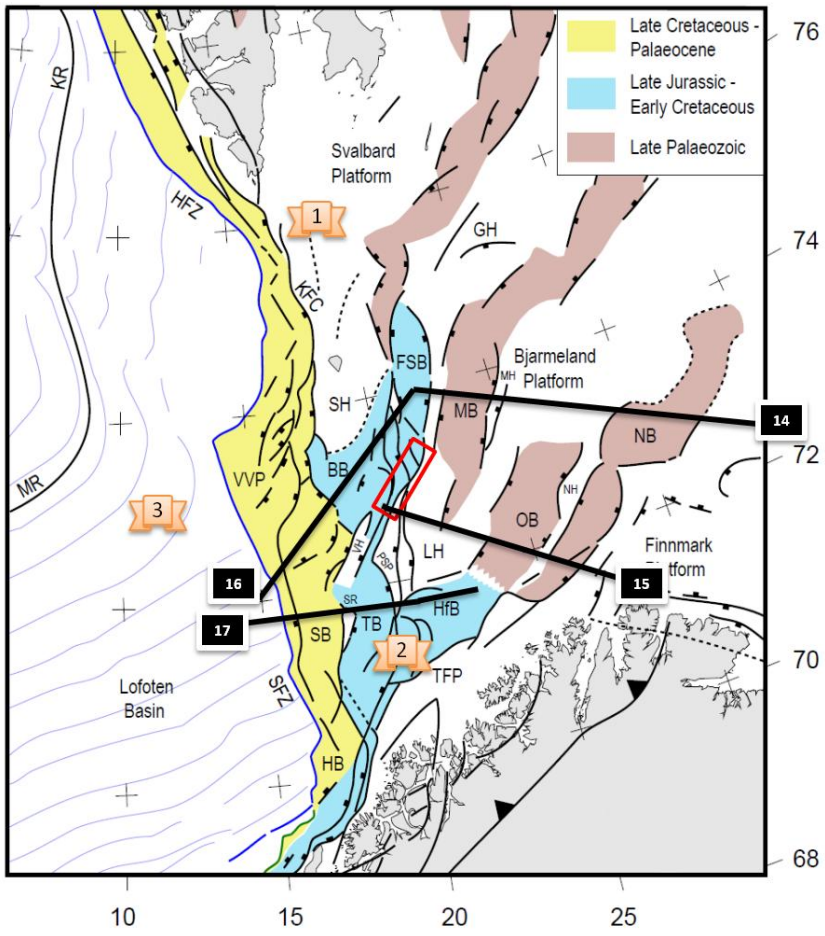


**Figure 2.1:** Structural elements of the western Barents Sea. Numbers 1-3 shows the locations of three geological provinces. Black lines illustrate seismic lines in *fig. 2.2*. Red box illustrating location of the study area of my thesis. SFZ: Senja Fracture Zone, TFFC: Troms-Finnmark Fault Complex, RLFC: Ringvassøy-Loppa Fault Complex. BFC: Bjørnøyrenna Fault Complex, LFC: Leirdjupet Fault Complex, FSB: Fingerdjupet Sub-basin GH: Gardarbanken High, HB: Harstad Basin, HFB: Hammerfest Basin, HFZ: Hornsund Fault Zone, KFC: Knølegga Fault Complex, KR: Knipovich Ridge, LH: Loppa High, MB: Maud Basin, MH: Mercurius High, MR: Mohns Ridge, NB: Nordkapp Basin, NH: Nordsel High, OB: Ottar Basin, PSP: Polheim Sub-platform, SB: Sørvestsnaget Basin, SH: Stappen High, SR: Senja Ridge, TB: Tromsø Basin, VH: Veslemøy High, VVP: Vestbakken Volcanic Province (modified from Faleide et al. 2008 and Glørstad-Clark et al. 2010)

## 2.3 Structural Elements

The Barents Sea was affected by several crustal extension and basin formation to the south west from Late Paleozoic to early Tertiary *(fig. 2.1)*. The overall trend of structures in the South west Barents Sea is NE-SW while local effect of ENW-ESW striking elements (Gabrielsen et al., 1990).The continental shelf of the Western Barents Sea is bounded by two main fault zones, the Senja Fracture Zone and Hornsund Fault Zone to the West and the Troms-Finnmark Fault Complex to the South *(fig. 2.1)* (Gabrielsen et al., 1984). The south west Barents Sea has been divided into three main segments (1,2 and 3) *(fig. 2.1).* The zones are germinated from oldest in the east to the youngest in west.

Three main basins are situated to the east of the area. The Nordkapp basin was originated in Late Paleozoic with NE-SW trend *(fig. 2.1)*. The basin exhibits a great amount of salt as salt diapirs and marginal salt pillows *(fig. 2.2)*. It is distinguished from Norsel high by the Nysleppen fault complex. The Ottar basin is located between Loppa high in the north west and Norsel high in the south east. The third, Maud basin was developed due to the evolution of svalis dome with NE to NNEW trend. It is separated by Hoop fault complex in the northwest while in the south east Mercius High distinguished it from Ottar basin *(fig. 2.1).*

The central segment of the Barents sea is dominated by Late Jurassic to early cretaceous tectonism *(fig. 2.1)*. The Tromsø basin to the west and the Loppa High to the east is distinguished by the Ringvassøy-Loppa and Senja ridge fracture zone. Along the Ringvassøy-Loppa Fault Complex there was substantial subsidence occurred during late mid Jurassic (Gabrielsen, R. et al., 1990) and the Fault complex was originated in Late Paleozoic (Gabrielsen, R. H., 1984; Gudlaugsson, S.T. et al., 1998). In the North it is separated by Veselmøy High through Bjørnøya Basin while the southeastern part is separated by the Troms Finnmark Fault complex *(fig. 2.1 & 2.2)*. The Hammerfest basin is separated through Loppa High by Asterian Fault Complex in the North where as southern limit is severalized by Finnmark Fault Complex through Troms Finnmark Fault. The Bjørnøa Basin generally located between 18 and 22 E with NE-SW trend. The Bjørnøya basin experiences large scale subsidence and sedimentation in the early Cretaceous and it is bounded to the east by the Loppa High, to the north by the Stappen High and to the North east by Fingerdjupet sub-basin (Faleide et al., 1993).

The western segment of the Barents Sea is dominated by two youngest Basins (Late Cretaceous - Paleocene). The Harstad basin is located near to the shelf edge, surrounded by oceanic crust to the west while eastern side is ceased by the southern limit of Trom-Finnmark Fault Complex. The Sørvestnaget basin is blanketed by massive Cretaceous sediments. The western limit is bounded by Senja ridge and Veselmøy High where as northern part is separated by Vestbakken volcanic province (Gabrielsen et al., 1990).

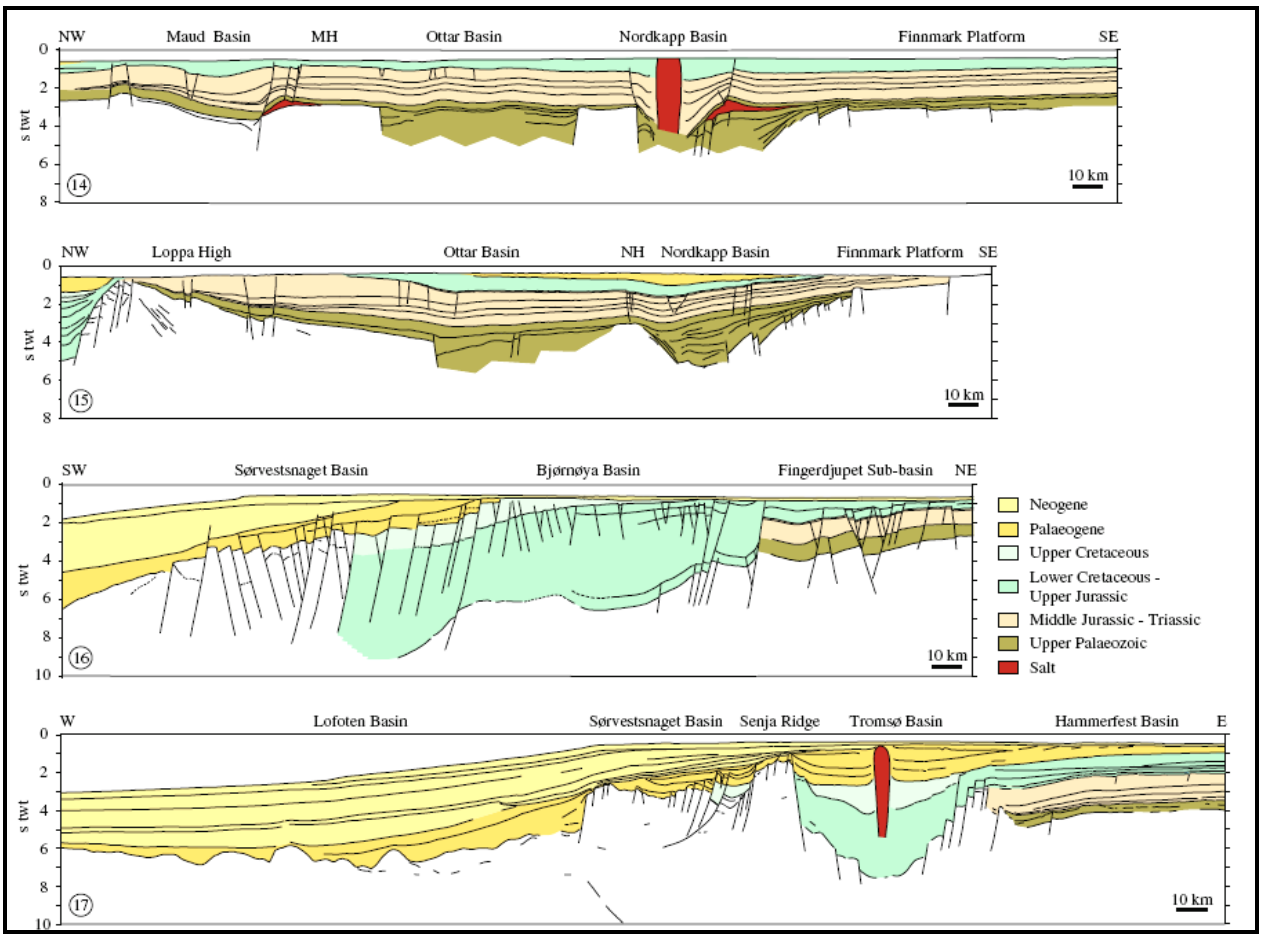


**Figure 2.2:** Regional profiles across western Barents Sea (modified from Faleide et al., 2010). See *fig. 2.1* for the location of the sections.

## 2.4 Regional Geological Evolution

The South Western Barents Sea is situated in the northern part of the post Caledonian North Atlantic rift system. The area was affected by several crustal extension and basin formation to the south west from Late Paleozoic to early Tertiary. The generalized geological evolution of the SW Barents Sea is summarized below:

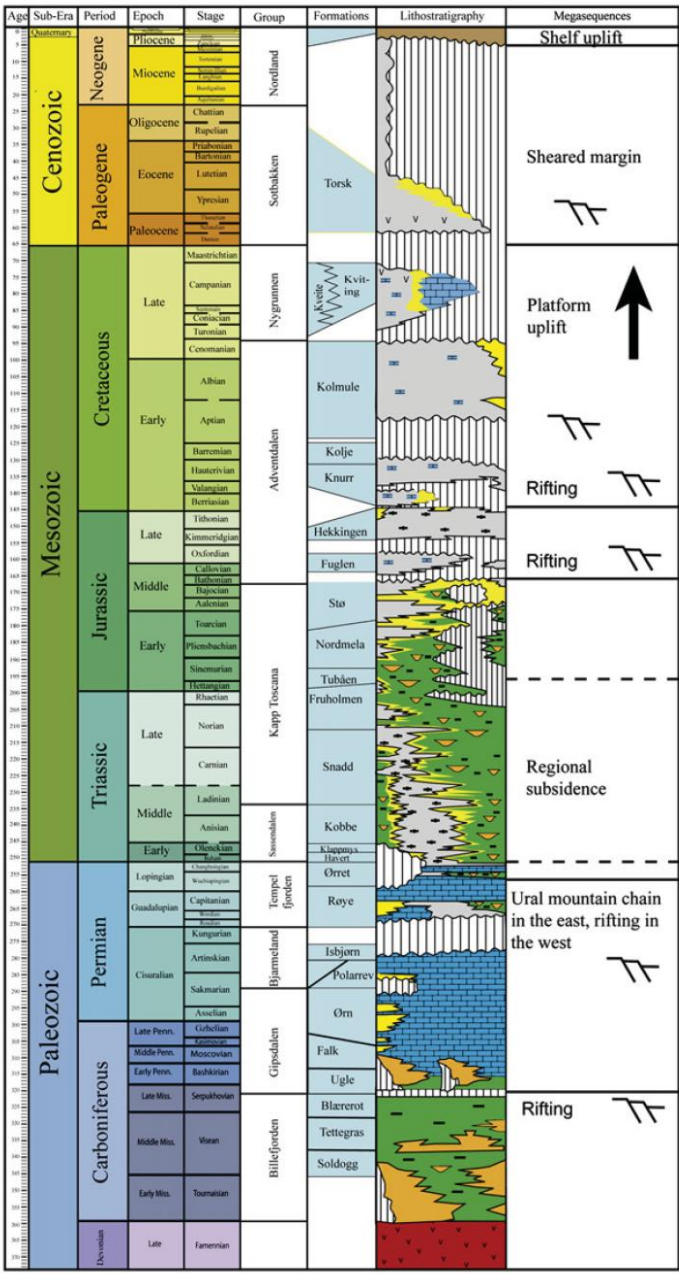


**Figure 2.3:** Generalized Stratigraphic column of the western Barents Sea (modified from Glørstad-Clark et al. 2009)

### 2.4.1 Late Paleozoic

Basically there is no direct evidence of sedimentary strata in the Barents Sea during Devonian time but still mega shear movements sustained in few paleotectonic reconstruction of the Arctic North Atlantic region (Ziegler, 1988a, 1988b, 1989). In addition to this, the Trollfjord-Komagelv Fault Zone (master strike slip fault) was active which give the image of linked strike slip and extension forming basin during the Devonian and the early Carboniferous time (Jensen & Broks 1988 and Jensen & Sørensen 1992; Gudlaugsson et al, 1998).

The latest literature on the nature of the development of the extensional structures observed and agreed by the presence of atleast two major extensional phases. The first one in the late Devonian to the early-middle Carboniferous times and the second one is in Permian to the early Triassic times (Lippard and Roberts, 1987; Gabrielsen et al., 1990; Dengo and Røssland, 1992; Jensen & Sørensen, 1992; Nøttvedt et al., 1993a; Gudlaugsson et al, 1998).

In the late Devonian, the compressional regime switch into left lateral shear system and strike slip movements occurred in the Arctic-North Atlantic region. During the Svalbardian (Ellesmerian) phase transpression and transtension led to the formation of Graben (Harland, 1973; Ziegler, 1978; Gudlaugsson et al, 1998).

The late Devonian to middle Carboniferous rift phase lead to the formation of interconnected extensional basins occupied with syn-rift deposits and separated by fault bounded highs (Lippard and Roberts, 1987; Gabrielsen et al., 1990; Dengo and Røssland, 1992; Jensen and Sørensen, 1992; Breivik et al., 1995; Gudlaugsson et al, 1998). Most of the Southwestern Barents Sea was highlighted by north-east to north structural trend. Moreover, the Tromsø, Bjørnøya, Nordkapp, Fingerdjupet, Maud and Ottar basins have been formed during this stage. In addition to this Hammerfest basin also started to form at this stage (Dengo and Røssland, 1992; Jensen and Sørensen, 1992; Bugge and Fanavoll, 1995; Breivik et al., 1995; Gudlaugsson et al, 1998). The Upper Devonian basin fill is composed of clastics, Carbonates and Evaporates. A collection of rocks of same age is found in Pechora Basin.

The movements of fault become terminated in the eastern side at the end of the Carboniferous period and most of the structure was occupied by a platform succession of the late

Carboniferous-Permian age (Stemmerik and Worsley, 1989, 1995; Gabrielsen et al., 1990; Dengo and Røssland, 1992; Stemmerik and Larssen, 1992; Bruce and Toomey, 1993; cecchi, 1993; Nilsen et al., 1993; Nøttvedt et al., 1993a; Bugge et al., 1995; Cecchi et al., 1995; Stemmerik et al., 1995; Gudlaugsson et al, 1998). The lower most part of Gipsdalen Group is followed by dolomite and evaporite passes while upper part contains massive deposit of limestone. The late Carboniferous-earliest Permian was typified by widespread deposition of evaporate layer (Gerard and buhrig, 1990). During the deposition of cherty limestone and shales of the Tempelfjorden Group marked significant change in type of sedimentation which label the initial evolution of regional sag basin which started to subside in the late Permian age (Stemmerik and Worsley, 1989; Dengo and Røssland, 1992; Gudlaugsson et al, 1998). Block faulting, uplift and erosion was followed by rift system in the western part of the Barents Sea in the Permian-early Triassic times. Regionally this event correspond to the formation of Sequence boundary (Berglund et al., 1986; Riis et al., 1986; Stemmerik and Worsley, 1989, 1995; Gabrielsen et al., 1990; Johansen et al., 1994a; Gudlaugsson et al, 1998).

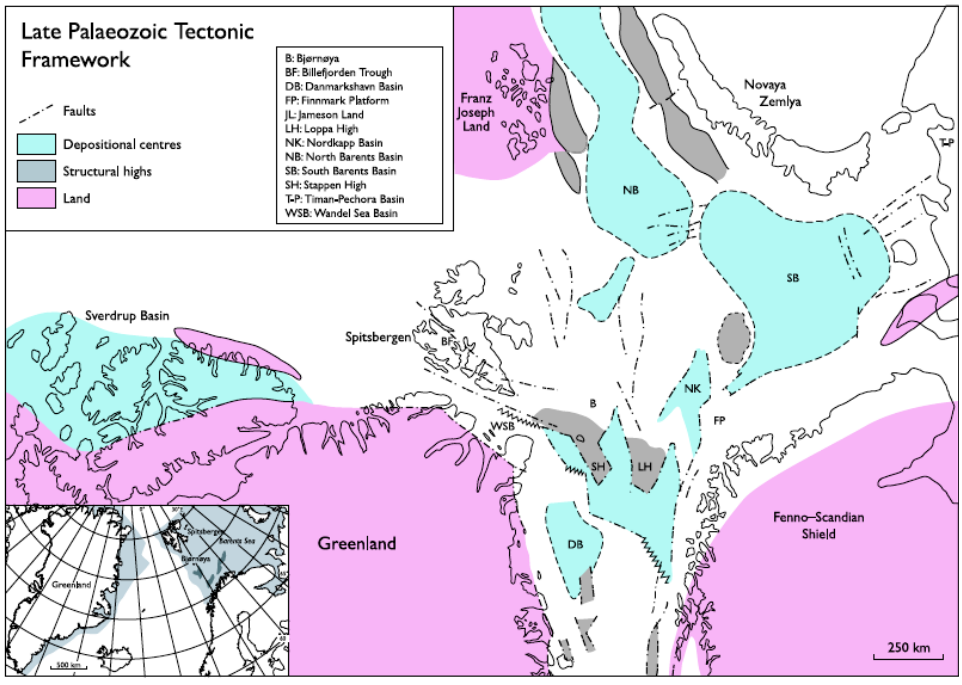


**Figure 2.4:** Tectonic settings during late Paleozoic (Stemmerik, L. & Worsley, D 2005)

### 2.4.2 Mesozoic

During Mesozoic, the Middle-Late Jurassic period was dominated by regional extension and minor Strike slip fault system. Due to extensive extension, rotational fault blocks get subsided in the upper Jurassic time and rift basin extent from Rockall Trough to south-western Barents Sea and further ramificate into the North Sea. At this time Barents Sea was rifted from the Hammerfest and Bjørnøya Basin along pre-existing framework. Due to this rifting the blocks get faulted in east and north-east direction and upper Jurassic shale deposited between titled fault blocks. The subsidence of the Tromsø and Bjørnøya Basin was renewed at this time (Faleide et al 1993a).


**Figure 2.5:** Tectonic setting during Middle Jurassic time (Faleide *et al.,* 1991).

During the early cretaceous time the Harstad, Tromsø and Bjørnøya basin was expanded (stretching & thinning) due to the continuation of both North Atlantic rift basin into south-western Barents Sea and the opening of Amerasia Basin. This time was indicated by three tectonic phases which impact the Hammerfest, Tromsø and Bjørnøya Basin. The first two phases was, Berriasian/valanginian and Hauterivian/Barremian where Tromsø and Bjørnøya Basin was

strongly influenced by these two phases while Hammerfest Basin was least affected. The thickness of Kolje Formation (Barremian) increases towards the west of Hammerfest Basin into Ringvassøy-Loppa Fault complex which certify the thermal subsidence in the centre of Tromsø Basin. The Aptian strata get faulted along Ringvassøy-Loppa Fault complex which further terminate in the western side of the basin signifying the formation of deep water elastic fans due to the uplift of the Loppa high. To the north, the footwall of Leirdjupet Fault Complex undergone uplift and erosion showed by the sedimentary strata onlapping a tilted fault block in Bjørnøya Basin and also affect the Fingerdjupet Sub-basin to the east (Faleide *et al.*, 1991).

In short, the early Cretaceous phase was indicated by rapid subsidence and deposition of 5-6 km massive sequence (kolmule Formation) in Bjørnøya, Tromsø and Harstad Basin. The deposition of these large sequences to the north Tromsø and central Bjørnøya Basin with Veselmøy High and Senja ridge signifying a large scale extension characterizing sinistral transpression strike slip movement along Bjørnøyrenna Fault Complex in west and west-north-west trend (Faleide *et al.*, 1991).

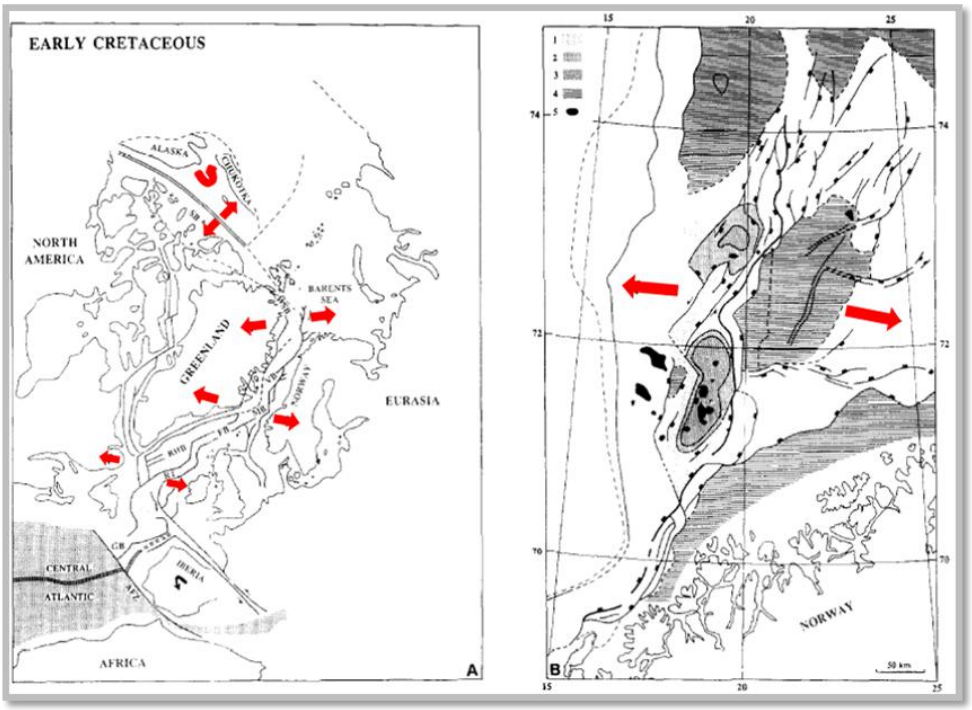


**Figure 2.6:** Tectonic setting during Early Cretaceous (Faleide *et al.*, 1991).

During the late Cretaceous most of deep and broad basins ended at the De Geer Zone indicating the formation of pull apart basins in Wandel Sea and south Western Barents Sea due to dextral oblique slip (Faleide *et al.*, 1991).

Along rift-shear intersection, Sørvestsnaget Basin and Harstad Basin situated which contain deep late Cretaceous Basins. The gesture in De Geer Zone typifying an event of uplift and faulting in Andoya (Dalland, 1981) during Santonian (86-87 Ma). The Senja Ridge divided the Tromsø and Sørvestsnaget Basin dramatically, where as these basins subsided during late Cretaceous while eastern side is dominated by large evaporites. Late cretaceous extension typifying normal faults where throws less than 300m at Veslemøy High and in the Bjørnøya basin (Faleide *et al.*, 1991).

Thus the late Cretaceous was mostly dominated by extension but there was an evidence of wrench forming structure along larger faults indicating Compressional deformation (Gabrielsen et al., 1990). At this stage most of the subsidence occurred in the tromsø and Sørvestsnaget Basins is due to the salt movements.

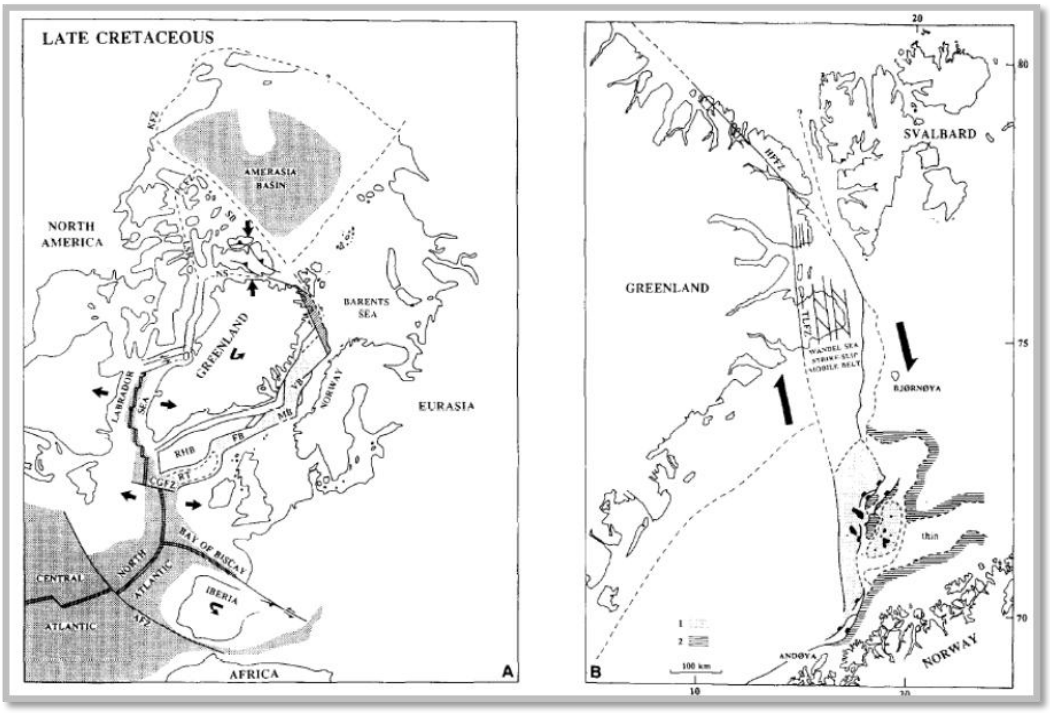


**Figure 2.7:** Tectonic setting during Late Cretaceous (Faleide *et al.*, 1991).

### 2.4.3 Cenozoic

Basically the Cretaceous-Tertiary transformation marks the time gap acting as a sequence boundary on a regional scale and the whole western Barents Sea was blanketed by sheet like sequence in Late Paleocene. The provenance of the sediments in Tromsø Basin was Loppa High and locally the faulting occurred along the western side of the Senja Ridge during the late Paleocene (Faleide *et al.,* 1993).

The Eocene age was dominated by the opening of Norwegian-Greenland Sea and Eurasia basin and shear margin developed along western Barents Sea with in De Geer Zone (Faleide *et al.,* 1991). Senja fracture zone and Hornsund Fault Zone inducing transpressional and transtensional settings due to transform movements. Due to transtension Senja Fracture Zone developed a leaky transform fault (Reksnes and Vågnes, 1985: Eldholm et al., 1987; Faleide *et al.,* 1993). At this stage Senja fracture zone was uplifted, eroded and sediments prograde to the eastward in Tromsø Basin. Instead, the northern part of Sørvestsnaget Basin was developed in Pull apart settings in response to releasing band resulted extensional faulting (Faleide et al., 1991). In addition, the south of Harstad Basin dominated by the tertiary uplift and erosion, give rise a thin Paleocene succession.

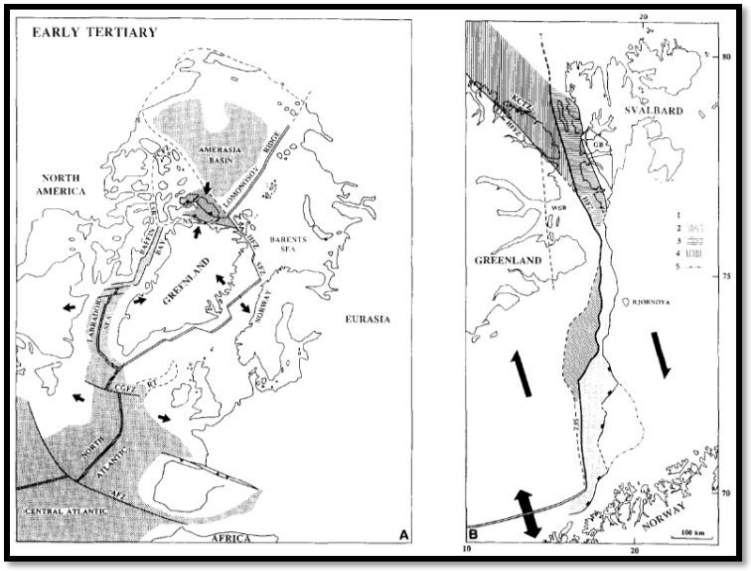


**Figure 2.8:** Tectonic setting during Early Tertiary (Faleide *et al.,* 1991).

The Oligocene time demonstrate a change in plate movement in the south western Barents Sea as indicated by regeneration of mostly Eocene faults and volcanism occurred in the Vestbakken volcanic Province (Faleide et al., 1988). During the Oligocene the margin was tectonically quiet and the Barents Sea was followed by regional subsidence, causing a massive formation of post Oligocene sediments in wedge shaped which mainly consist of Pliocene-Pleistocene deposits through Glaciers (Faleide *et al.,* 1991).

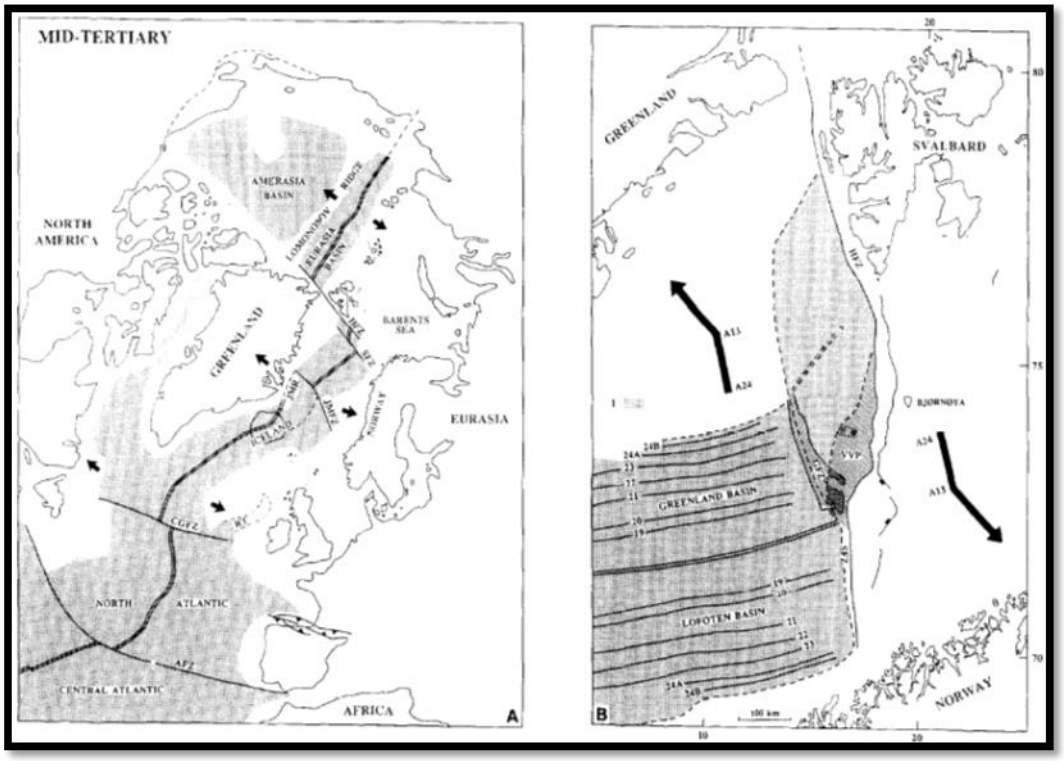


**Figure 2.9:** Tectonic setting during Mid-Tertiary (Faleide *et al.,* 1991).

## 2.5 Bjørnøyrenna Fault Complex (An Overview)

The Bjørnøyrenna Fault Complex is situated between 72º N, 19' E and 73º 15' N, 22º E with general NE-SW trend. The fault complex is bounded by the Loppa High to the south east where as Bjørnøya Basin to the southwest.*(fig. 2.10)*.

The Bjørnøyrenna Fault Complex is the northeast extension of Ringsvassøy-Loppa Fault Complex. It exhibit very complex geometry and the fault has undergone multiple phase of deformation with time. Generally the complex is defined by an extensional origin and differentiated by listric fault geometries which get flatten into detachment in Permian rocks (Faleide *et al.,* 1993). Moreover, it lies over crustal zone of weakness. In addition the faults have been experienced strong deformation of the footwall block, reverse faults and deformed fault planes (Gabrielsen *et al.,* 1984). Across the Bjørnøyrenna Fault complex, displacement was vertical which represents about 6 second (TWT) on the Upper Triassic level *(fig. 2.10)*. However the throw terminates to the North and South (Gabrielsen et al., 1990).

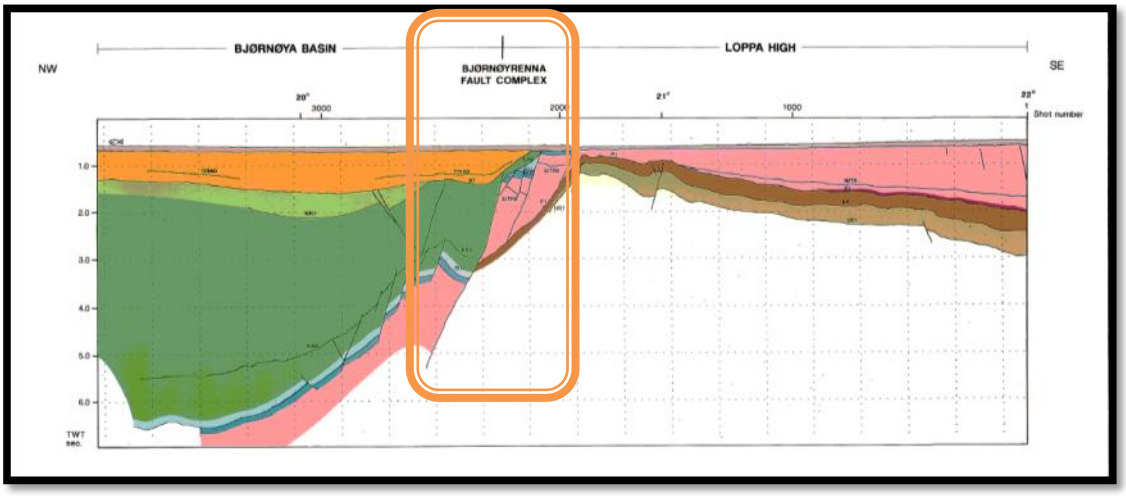


**Figure 2.10:** Showing location of Bjørnøyrenna Fault Complex (PROFILE D-10-84) color codes: Grey (Quaternary), Orange (Tertiary), Yellow Green (Upper Cretaceous), Green (Lower Cretaceous), Light blue and blue (Base of Upper Jurassic), Pink (Triassic), Violet (Top Permian), Brown (Base of Permian), Olive (Carboniferous) (Modified from Gabrielsen et al., 1990).

According to Faleide et al., 1993, the early cretaceous age is dominated by downward faulting along the Bjørnøyrenna Fault Complex while extensive uplift and Erosion encountered in Tertiary. But according to Gabrielsen et al., 1997 there were two episodes of inversion in the Bjørnøyrenna Fault Complex. The early cretaceous time is dominated by strike slip movement where as the late Cretaceous- early Tertiary age experienced compressional inversion with orientation of NW-SE.

## 2.6 Loppa High

The Loppa High is located between 71°50'N, 20°E and 71°55'N,22°40'E and it resemble to a daimond shaped structure . It is separated from the Hammerfest basin in the south by Asterian fault Complex. The western limit of the Loppa High is separated by the Ringsvassøy-Loppa and the Bjørnøyrenna Fault Complex through Trømso and the Bjørnøya basin *(fig. 2.10).* The high comprised of polhem subplatform. The subplatform separated from the selis ridge by Jason Fault Complex and exhibit listric fault geometry (Gabrielsen et al., 1990).

The Loppa High was originated in Carboniferous rift topograpgy followed by reactivation during the late Permian and early triassic which resulted several phases of uplift, subsidence followed by tilting and erosion(1990; clark et al 2010).

## 2.7 Bjørnøya Basin

The Bjørnøya basin is placed between 72°30' and 74°N and between 18° and 22°E. The deep western part of the basin is distinguished by the Leirdjupet Fault Complex while shallowest (eastern) part is separated by Fingerdjupet subbasin.

Most of the deposition in the basin is of Early Creatceous in age and extensive deformation occurred along the Bjørnøyrenna fault Complex and Stappen High *(fig. 2.10).* The top most part of the basin succession is heavily eroded while the centre of the basin is quite stable(Gabrielsen et al., 1990; Faleide et al., 1993).

# CHAPTER 3

# SEISMIC INTERPRETATION

The generalized workflow of the study area is summarized in *fig 3.1*

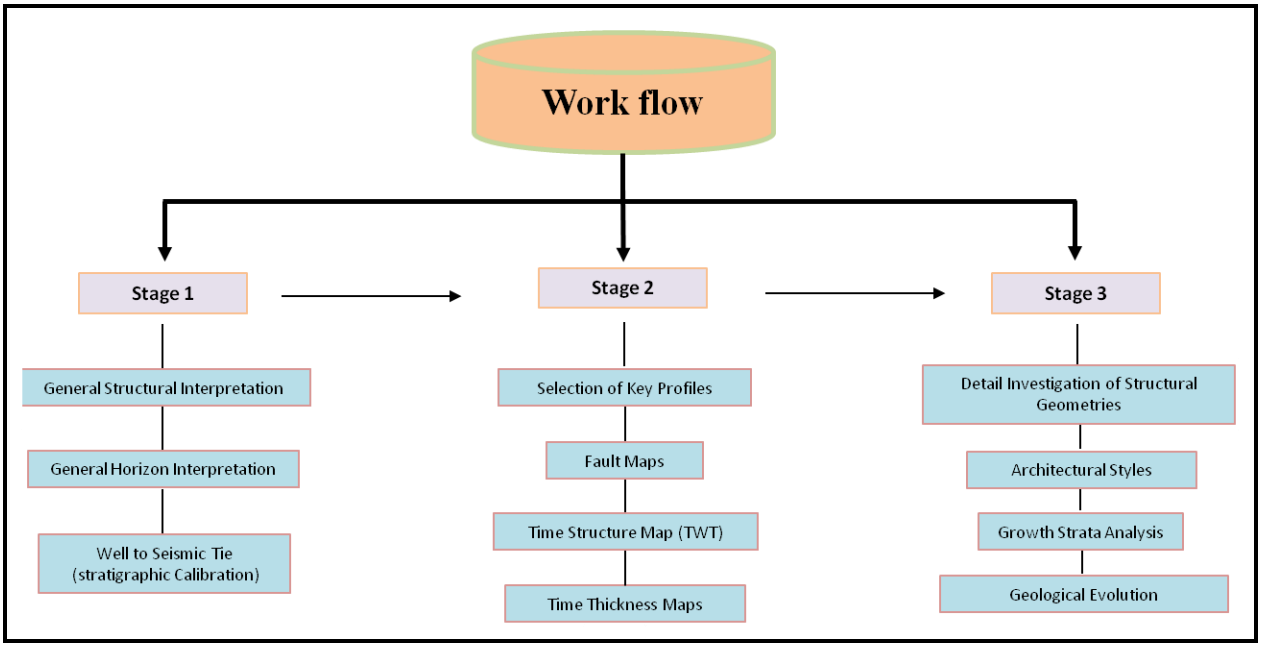


**Figure 3.1:** Generalized workflow of the study.

## 3.1 Seismic Data

The data set constitutes of a grid of high resolution 2D seismic reflection lines and well logs (*fig. 3.1*). The 2D seismic lines were provided by Fugro & TGS containing both dip and strike lines and well data from the Norwegian Petroleum Directorate (NPD). The dip lines are oriented NW-SE while strike lines shows E-W orientation. These seismic reflection profiles were used to examine broad and detailed structural investigation of the Bjørnøyrenna Fault complex.

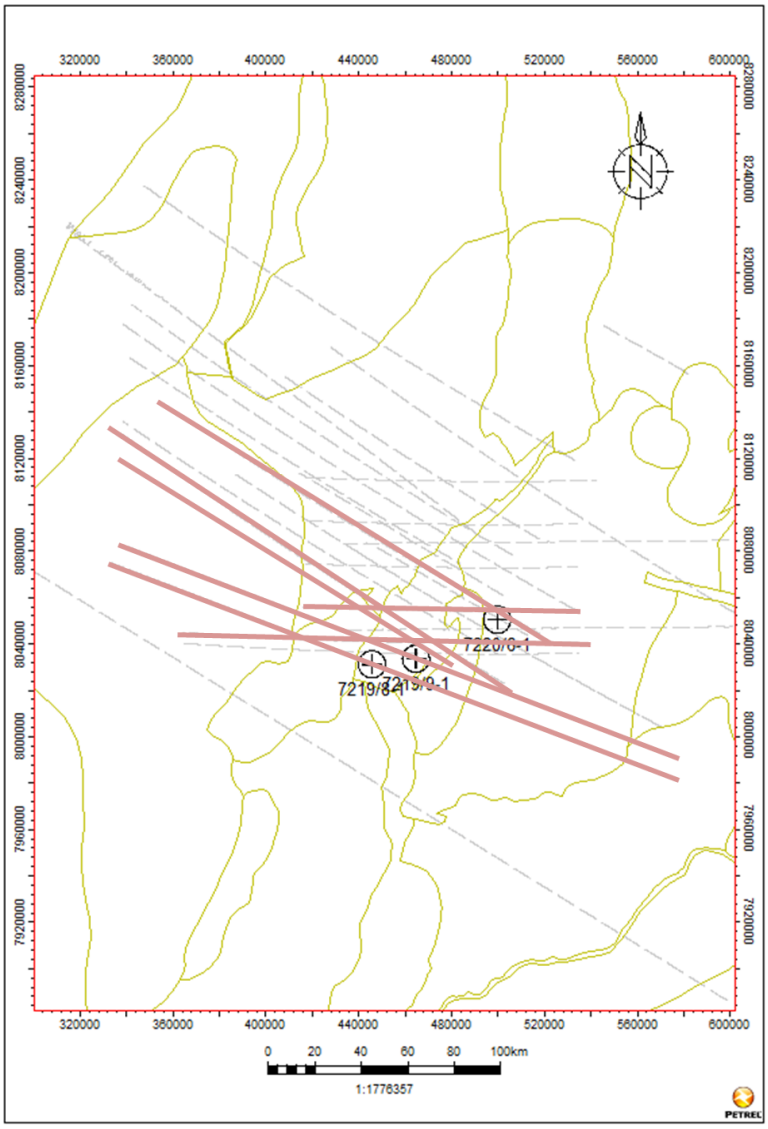


**Figure 3.2**: Base map of the study area shows location of seismic lines and well logs used in the study. Pink lines show the location of the key profiles.

Three Wells (7219/9-1, 7219/8-1S, 7220/6-1) were used in the study area for the stratigraphic calibration and well to seismic tie (*fig. 3.1*). The general and Lithostratigraphic information have been taken from NPD *(Table 3.1 & 3.2*). The well 7219/9-1 was drilled in 1987 within the vicinity of the Bjørnøyrenna Fault Complex and penetrated up to the Snadd Formation (Mid Triassic) with total Depth (TD) of 4300m (RKB) (*Table 3.1).* The well 7219/8-1S was drilled in 1992, also located within study area on rotated fault blocks and the oldest penetrated formation is of early Jurassic age (Stø Formation) with total depth (TD) of 4611m (RKB) (*Table 3.1).*

| Wellbore name | 7219/9-1 | 7219/8-1 S |
|---|---|---|
| Main Area | Barents Sea | Barents Sea |
| Seismic Location | MN 85 105 SP. 1125 | SG-9106-449 & SP 550 |
| NS degree | 72° 24' 0.78" N | 72° 22' 28.32" N |
| Drilling Operator | Norsk Hydro Production AS | Saga Petroleum AS |
| EW degree | 19°57'11.68" E | 19°23'40.24" E |
| Drilling Days | 101 | 83 |
| Completion Date | 25.02.1988 | 26.12.1992 |
| Type | Exploration | Exploration |
| Purpose | Wildcat | Wildcat |
| Status | P & A | P & A |
| Discovery wellbore | No | No |
| Kelly bushing elevation (m) | 23.0 | 24.0 |
| Water depth (m) | 356.0 | 369.0 |
| Total depth (MD) [m RKB] | 4300.0 | 4611.0 |
| Final Vertical depth (TVD) [m RKB] | 4286.0 | 4404 |
| Bottom hole temperature [°C] | 145 | 165 |
| Oldest penetrated age | Late Triassic | Early Jurassic |
| Oldest penetrated formation | Snadd formation | Stø Formation |

**Table 3.1:** Additional information of well logs used in the stratigraphic calibration (NPD Website).

The third well 7220/6-1 was drilled in 2005 in which the bore hole has penetrated up to the Basement (Pre- Devonian) to a total depth of 1540m (RKB) (*Table 3.2*). The well is located on the Loppa High, eastern part of the study area. This well was used to examine the Lithostratigraphic correlation across the Loppa High and the Bjørnøyrenna Fault Complex.

However late Jurassic to Paleogene sequences is missing on the high and Nordland group directly overlain on Kapp Toscana Group.

| Wellbore Name | 7220/6-1 |
|---|---|
| Main Area | Barents Sea |
| Location | NH0352-inline 8352 & x-line 5106 |
| NS degree | 72° 33' 12.56" N |
| EW degree | 20° 59' 26.86" E |
| Drilling Operator | Norsk Hydro Production |
| Drilling Days | 69 |
| Completion Date | 29.03.2005 |
| Type | Exploration |
| Purpose | Wildcat |
| Content | Oil Shows |
| Status | P & A |
| Discovery wellbore | No |
| Kelly bushing elevation (m) | 25 |
| Water depth (m) | 368 |
| Total depth (MD) [m RKB] | 1540 |
| Final Vertical depth (TVD) [m RKB] | 1540 |
| Bottom hole temperature [°C] | 46 |
| Oldest penetrated age | Pre-Devonian |
| Oldest penetrated formation | Basement |

**Table 3.2:** Additional information of boreholes used in the stratigraphic calibration (NPD Website)

| AGE | | GROUP/FORMATION | 7219/9-1 | 7220/6-1 | 7219/8-1S |
|---|---|---|---|---|---|
| Sub-Era | Period | | Top Depth (m) | Top Depth (m) | Top Depth (m) |
| Cenozoic | Neogene | Nordland Group | 379 | 394 | 393 |
| | Paleogene | Søtbakken Group | 483 | Missing | 554 |
| | | Tørsk Formation | 483 | | 554 |
| Mesozoic | Cretaceous | Adventalen Group | 1468 | | 1545 |
| | | Kolmule Formation | 1468 | | 1545 |
| | | Kolje Formation | | | 2080 |
| | | Knurr Formation | 1836 | | 2494 |
| | Jurassic | Hekkingen Formation | 1893 | | 3472 |
| | | Fuglen Formation | 1919 | | 4328 |
| | | Kapp Toscana Group | 1951 | 476 | 4521 |
| | | Stø Formation | 1951 | Missing | 4521 |
| | | Nordmela Formation | 2062 | | |
| | | Tubåen Formation | 2206 | | |
| | Triassic | Fruholmen Formation | 2305 | | |
| | | Snadd Formation | 2877 | 476 | |
| Paleozoic | Permian | Gipsdalen GrouP | | 1138 | |
| | | Ørn Formation | | 1138 | |
| | Carboniferous | Falk Formation | | 1436 | |
| | | Basement | | 1483 | |

**Table 3.3:** Well Tops used in the study, highlighted formations have been interpreted on 2D seismic reflection profiles.

## 3.2 Interpretation Tool

Petrel 2011 has been utilized for seismic interpretation during thesis work and it's a property of schlumberger. The application of this software is window based which provide a full spectrum of operations including 2D/3D interpretation, well log correlation, reservoir modeling, reservoir simulation, volumetric calculation and subsurface geological mapping (www.slb.com).

## 3.3 Interpretation Procedure

The first step was started by loading of the 2D seismic data in order to persue thesis work. Afterwards, a general overview of the data set has been carried out to familiarize with the structural elements and regional geological settings of the study area.

The next step was structural interpretation of seismic lines by using Petrel 2011 which then led to the horizon interpretation. To distinguish different formations by means of seismic reflection is an important question in interpreting seismic reflection data. For this purpose, calibration of seismic to well tie at various locations, well tops and check-shot surveys were imported in ASCII format. Once wells were loaded and displayed correctly, subsequently the actual interpretation starts by interpreting pre decided reflections and it established a stratigraphic frame block for the main interpretation as seen in *(fig. 3.4).*

Due to limitation of this software (Petrel 2011), manual interpretation of seismic lines was carried out to optimize the fault geometry and its details. Additionally, eight reflectors were used to interpret on the selected seismic lines with support of well logs. The reflectors with different color codes are presented in *fig. 3.3*.

| Reflectors | FORMATION | Age | Color |
|---|---|---|---|
| Early Cretaceous | Knurr Formation | 130.0 | |
| Base Cretaceous | Hekkingen Formation | 145.5 | |
| Upper Mid Jurassic | Fuglen Formation | 155.6 | |
| Early Jurassic | Tubaen Formation | 189.6 | |
| Base Jurassic | Fruholmen Formation | 196.5 | |
| Late Triassic | Snadd Formation | 203 | |
| Mid-Triassic | | | |
| Early Permian | Gipsdalen Gp | 284.4 | |

**Figure 3.3:** Color codes of the interpreted reflections in the study area

Lithostratigraphic correlation has been actualized across the Loppa High and the Bjørnøyrenna Fault Complex to examine the behavior of sedimentary packages and structural styles within the study area. The Loppa High is located at the eastern corner of seismic section whereas; western part is dominated by the Bjørnøyrenna Fault Complex. The reflectors are marked on the basis of well based information while deep seismic reflections are marked by picking the continuous train of wavelets running across the section. Confusion arise in marking the continuity because the wavelets or the traces tend to mix up or the sequence might break due to subsurface structural changes or abrupt lithological changes or the most common problem faced is the presence of different types of noises, such noises causes the distortion of the signal.

Although the resolution was not very high at deeper level so it was not easy to predict the Carboniferous - early Permian sequence at greater depth. To do so, some previous published work has been taken into account to build the late Carboniferous- early Permian sequences within study area (Glørstad-clark et al., 2010 & 2011). An uneven thickness distribution of the late mid Carboniferous-early Permian has been observed across the profile *(fig. 3.4)*. The sedimentary packages of the Bjarmeland Group and Tempelfjorden Group are onlapping toward the crest of the Loppa high, which is characterized by an angular unconformity *(fig. 3.4)*. At the

top of the Loppa high, the sedimentary succession of the early-mid Permian thin out and truncated. Only intra Triassic sequences are present just above Gipsdalen Group whereas, the Søtbakken Group directly overlain on Triassic succession which indicates an episode of erosion or non deposition followed by uplifting *(fig. 3.4, Table 3.3)*. The most prominent feature in this profile is that the only intra-Triassic succession is well preserved and constitute by constant thickness across the Loppa High and the Bjørnøyrenna Fault Complex. On the other hand, the Jurassic and the early Cretaceous sequences are well preserved on the western flank of the Bjørnøyrenna Fault Complex but completely disappeared on the eastern part of the fault complex and at the hinge of the Loppa High. Moreover, a valuable thickness has been observed between the intra-triassic and the intra Permian packages across the seismic section *(fig. 3.4)*.

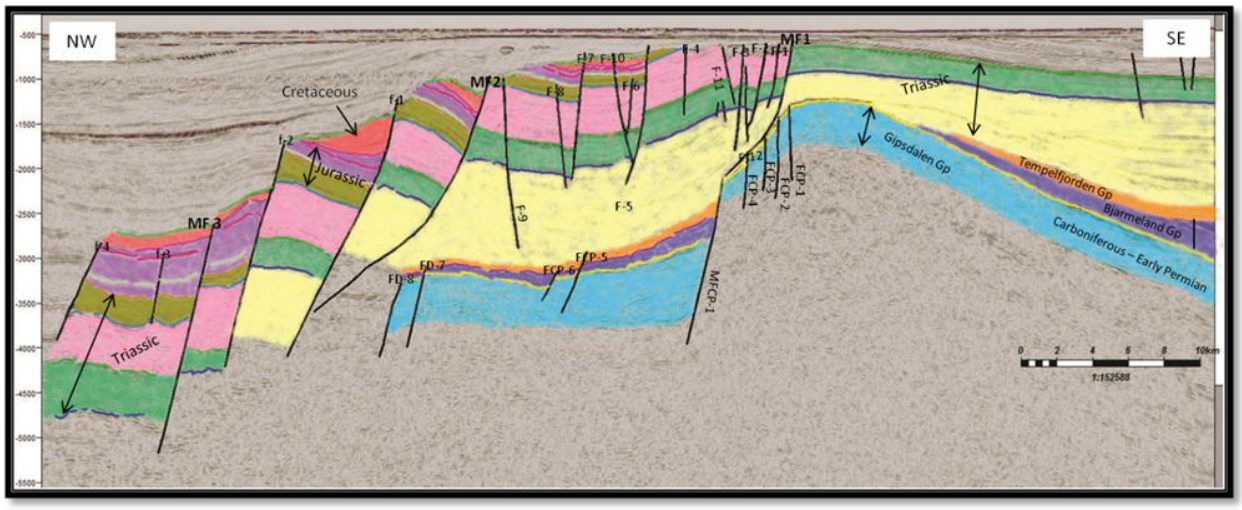


**Figure 3.4:** Lithostratigraphic correlation of regional seismic profile across the Loppa High and the Bjørnøyrenna Fault Complex.

One of the deepest reflections marked in the study area is of mid-Carboniferous in age. The reflection is represented by the Falk Formation *(fig. 3.5)*. At the Loppa High, the reflection is marked by the well base information but within fault complex no well based inofrmation exist at much deeper level. Thus, reflection within fault complex is marked on the basis of acoustic impedance contrast and by previous published work (Glørstad-clark et al, 2010 & 2011;). The formation predominantly consists of mixture of shallow sandstone, marine sandstone and shallow marine carbonates (Larssen et al., 2002). In the study area, this reflection exhibits positive amplitude as shown in *(fig. 3.5*). It has been marked between 1170-1190 ms TWT at the Loppa

High while on the Bjørnøyrenna Fault Complex this reflection has been interpreted in the range of 3700-3750 ms TWT approximately in the *(fig. 3.5)*.

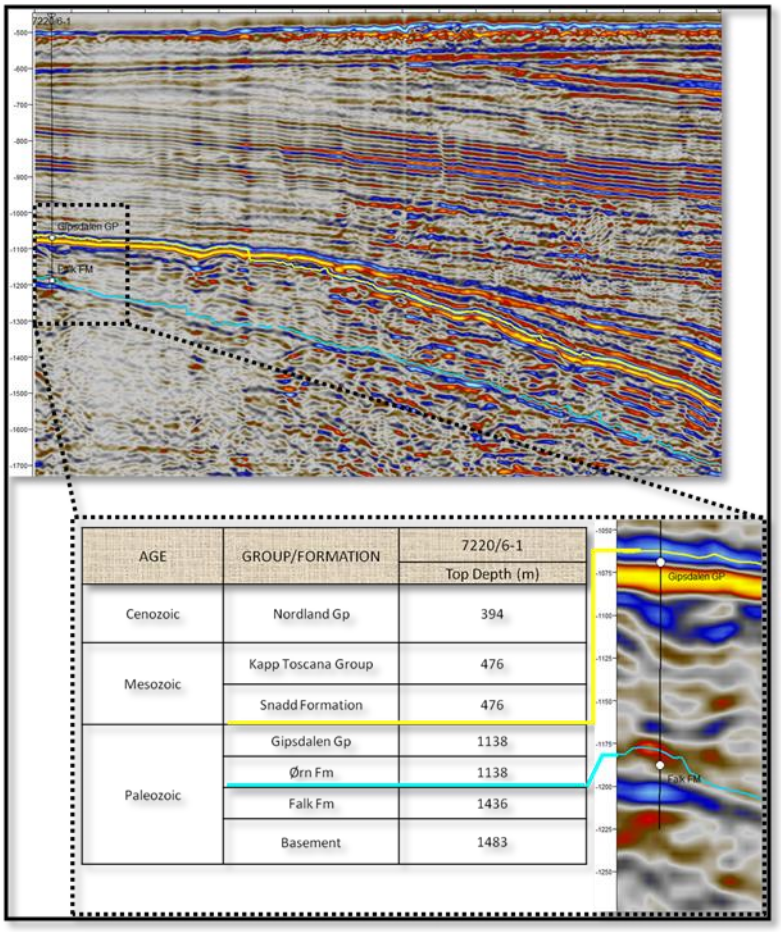


**Figure 3.5:** Seismic tie to well 7220/6-1, located at the crest of Loppa high.

Early Permian reflection is represented by the Gipsdalen Gp *(fig 3.5, table 3.3)*. This Group is interpreted both at the Loppa high and within the Bjørnøyrenna Fault Complex. But there is no deep well which is penetrated up to Permian level in the Bjørnøyrenna Fault Complex. Thus, it is marked on the basis of acoustic impedance contrast and by previous published research work (Evy Glørstad-clark et al., 2010 & 2011). Generally the Gipsdalen group consists of three main Formations namely, Ørn Formation, Falk Formation and the Ugle Formation. The group is comprised of metre-thick to rarely tens of meter thick generally showing continental red bed sandstones, siltstone, and conglomerate is dominating at the basal part of the succession while the upper part is dominated by Limestone and dolomite with minor evaporites on the Platform

area (Larssen et al., 2002). In the study area this reflection has been marked between 1240-1250 ms TWT at the Loppa High while on the Bjørnøyrenna Fault Complex, it has been marked between 2850-2900 ms TWT approximately and generally exhibits strong negative amplitude at the crest of Loppa high as shown in the *(fig. 3.5).*

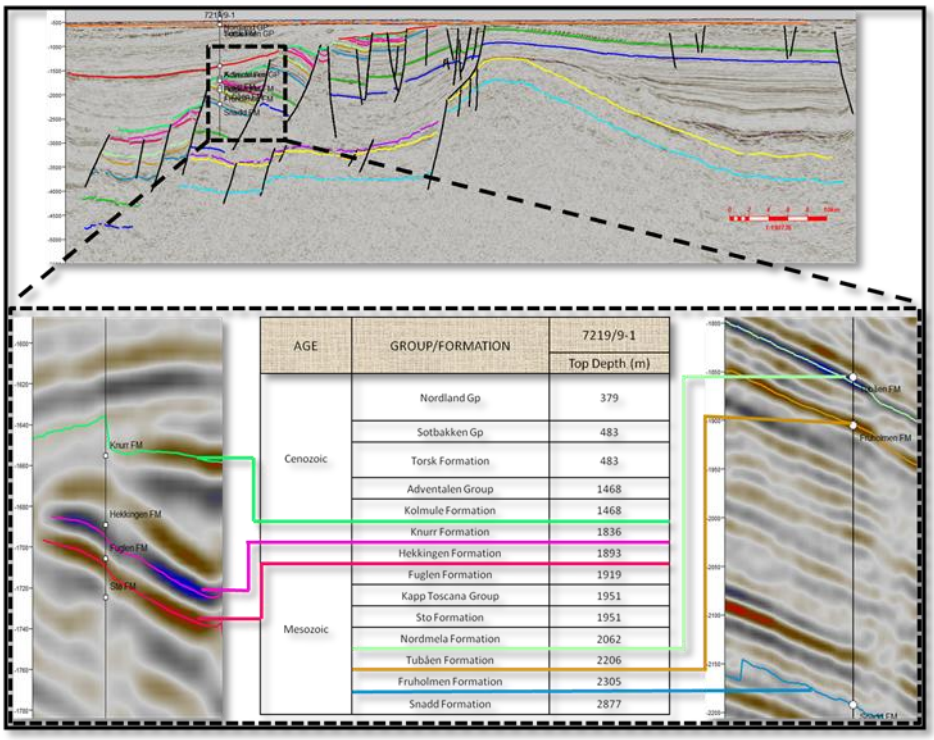


**Figure 3.6:** Seismic tie to well 7219/9-1, located within Bjørnøyrenna Fault Complex

Late Triassic reflection is characterized by Fruholmen Formation which exhibits a strong positive reflection with high amplitude *(fig. 3.6)*. The thickness of this formation is more or less constant throughout the study area. It has been marked on seismic section between 1850-2150 ms TWT in the fault complex *(fig. 3.6)*. The formation consists of shale with interbedded sandstone and coal. On the basis of lithological contrast, the formation is comprised of three main members namely; Akkar, Reke and Krabbe (Larssen et al., 2002).

The mid-Triassic reflection is represented by Snadd Formation and its one of the reflection which constitutes valuable thickness within fault complex. The formation predominantly comprised of grey shale with interbeds of siltstone and sandstone (Dalland et al., 1988). In the present study,

the reflector exhibit strong negative amplitude and it has been interpreted between 2180-2200 ms TWT *(fig. 3.6).*

The early Jurassic reflection is represented by Tubåen Formation *(fig. 3.6, table 3.3).* This formation is only marked within fault complex and it is not present at the Loppa High. The formation is comprised of sandstone, shale with minor deposition of coal (Larssen et al., 2002). On a seismic section, the reflection has been marked between 2000-2200 ms TWT. Additionally, the reflection is characterized by strong-moderate, negative amplitude *(fig. 3.6).*

The Upper mid Jurassic reflection is dominated by Fuglen Formation *(fig. 3.6, table 3.3)* that has been marked on seismic section between 1700-1800 ms TWT. The formation is composed of pyritic mudstone with thin intercalations of Limestone. The reflector generally exhibits strong positive character as seen in *(fig. 3.6, 3.7).*

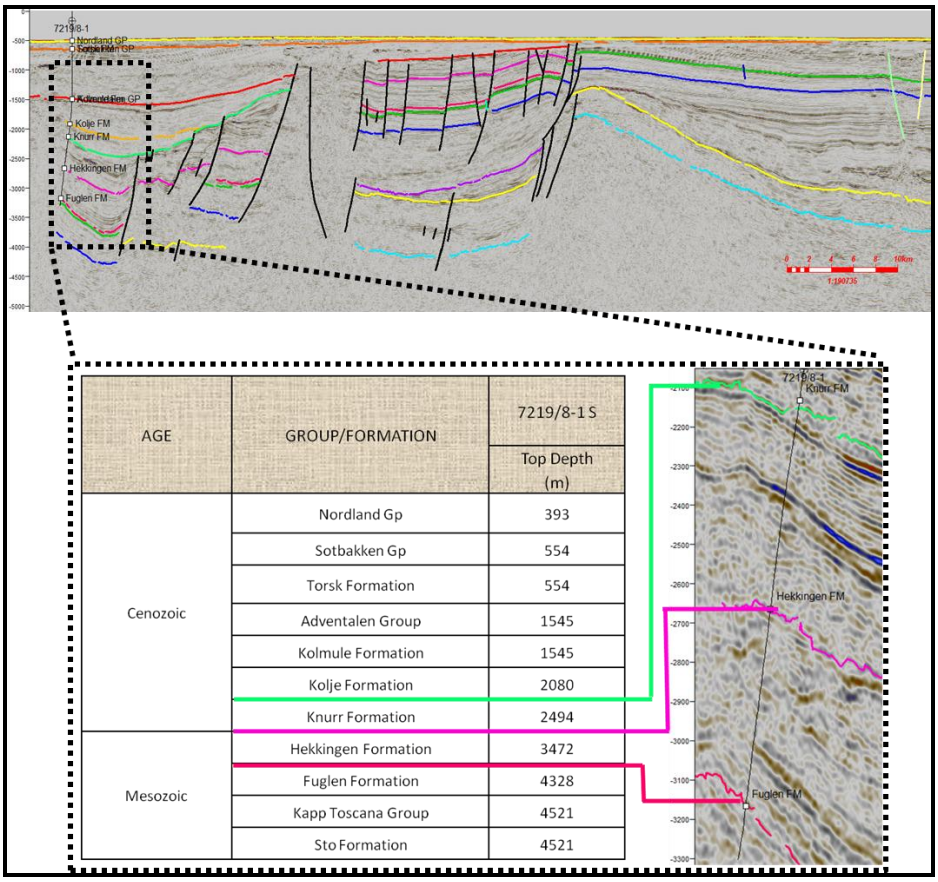


| AGE | GROUP/FORMATION | 7219/8-1 S Top Depth (m) |
|---|---|---|
| Cenozoic | Nordland Gp | 393 |
| | Sotbakken Gp | 554 |
| | Torsk Formation | 554 |
| | Adventalen Group | 1545 |
| | Kolmule Formation | 1545 |
| | Kolje Formation | 2080 |
| | Knurr Formation | 2494 |
| Mesozoic | Hekkingen Formation | 3472 |
| | Fuglen Formation | 4328 |
| | Kapp Toscana Group | 4521 |
| | Sto Formation | 4521 |

**Figure 3.7:** Seismic tie to well 7219/8-1S, located within Bjørnøyrenna Fault Complex.

The base cretaceous is represented by Hekkingen Formation. On the eastern flank of the fault complex, the formation is eroded due to uplifting while its easily marked on the western flank of the fault complex between 1750-2000 ms TWT *(fig. 3.6)*. The formation predominantly consists of grey to dark grey shale and claystone with thin intercalations of limestone, dolomite, siltstone and sandstone (Larssen et al., 2002). The reflection is generally characterized by strong-moderate and high-medium frequency *(fig. 3.6, 3.7)*.

The early cretaceous reflection shows strong, high amplitude positive reflection marked by Knurr Formation on the seismic profile between 1600-1700 ms TWT *(fig. 3.6 & 3.7)*. The formation has experienced an extensive erosion and acting as a wedge shaped deposit which is a clearly indication of syn-rift sediments. It is dominantly composed of brown claystone with beddings of limestone and dolomite (Larssen et al., 2002).

### 3.4 Geometrical and Structural Interpretation of the faults maps and Key seismic lines

This section is primarily used to define all the structural elements and sub features within the study area. Therefore, 2D seismic dip lines have been selected as the most exact representation of the cross-sectional view for the examination of the structural elements. Seven 2D seismic lines as key profiles *(fig. 3.2, 3.8 & 3.9)* have been selected for the better understanding of the behaviour of structures and geometries within the Bjørnøyrenna Fault Complex. Hence, two Key profiles from segment 1, four key profiles from segment 2 and one key profile from Segment 3 have been selected to describe each segment in detail *(fig. 3.8, & 3.9).*

Based on the structural interpretation, the Bjørnøyrenna Fault Complex is subdivided into three main segments *(fig. 3.8 & 3.9)*. Segment 1 constitutes the southernmost part of the fault complex in the study area. Three main master faults (MF-1a, MF-2a & MF-3a) are recognized here *(fig. 3.8).* MF-1a defining the easternmost boundary fault separating the western part of the Loppa High with N-S strike. MF-1a seems to be continuing on part of the unbroken master fault that can be traced into segment 2 & 3 as well. However, MF-2a & MF-3a striking NE-SW are embedded in the structural sub-platform constituting the hanging wall of the MF-1a. Additionally, MF-3a distinguished the western boundary of the fault complex by the deep Bjørnøya Basin.

Segment 2 is located in the central part of the fault complex encompassing all the three master faults (MF-1a, MF-2b & MF-3b) *(fig. 3.8)*. The N-S, MF-1a exhibits the eastern boundary of the fault complex distinguishing it from the western part of the Loppa High. MF-2b is changing its strike from NNW-SSE to NE-SW and it seems to be continued in segment 3 as well (*Fig. 3.1)*. MF-3b is characterized by a NE-SW trend and separated the western boundary of the fault complex by deep Bjørnøya Basin. The magnitude of dip slip of MF-2b is greater than MF-1a & MF-3b. Comparatively, the frequency of faulting is higher in segment 1 & 2 than segment 3 *(fig. 3.8).*

The northern part of the fault complex is defined by segment 3; consists of three main master faults *(fig. 3.8)*. In this segment, MF-1a get segmented due to change in strike from N-S to NE-SW and further extended by MF-1b *(fig. 3.8)*. MF-1b is define by the eastern boundary of the fault complex separates the western part of the Loppa High and exhibits NE-SW structural trend.

MF-2b is characterized by NNE-SSW structural trend. Moreover, MF-3c separating the western margin of the fault complex by deep Bjørnøya Basin with general NE-SW structural trend. This segment is also terminated at the eastern margin of the Fingerdjupet sub-basin *(Fig. 3.8 & 3.9*).

The time structure map at the intra Triassic level generally shows westward deepening of reflections indicated by color variations from shallow to deep *(fig. 3.9)*. This is one of the two reflections that are interpreted both on the Loppa High and within the Bjørnøyrenna Fault Complex *(fig. 3.9 & 3.10)*. The displacement pattern along master faults (MF-1, MF-2 and MF-3) is not uniform in all three segments and the greatest vertical separation is observed along MF-2 at the intra Triassic level on the entire key profiles (1-7)*(fig. 3.9).* However, MF1 shows comparatively less vertical separation than MF2 while MF3 shows the least vertical displacement as interpreted on key profiles (1-7). The deepest part is located in the south-western quadrant of the map shown by purple in color indicating greatest time values *(fig. 3.9).*

The fault map at the intra-Triassic level demonstrates high frequency of faulting and thus it is affected by three main master faults (MF-1, MF-2 and MF-3), trending N-S, NE-SW and NW-SE respectively, as discussed above in detail *(fig. 3.8)*. Therefore, each of these master faults is further characterized by different segments termed as (MF-1a, MF-1b; MF-2a, Mf-2b and MF-3a, MF-3b, MF-3c) *(fig. 3.8).* The overlapping relation has been noticed between large array of master faults which will further discuss in detail in chapter 4 (section 4.1). Hence the connection between MF1a & MF1b is seems to be soft-linked segments whereas, MF2a and MF2b is dominated by hard-linked segment *(fig. 3.8 & 4.1)*. Moreover, Small west-dipping normal faults are also interpreted between the fault segments MF-2a & MF-2b at key profiles 6, which bring both master faults in communication *(fig. 3.8).*

At the intra-Triassic reflection, MF-1a dips to the west and it is found to be structurally unbroken master fault in the study area. MF-2a shows dip to the NW whereas; MF2b varies its dip from SW to NW. However, MF-3 is dipping towards NW in all three structural segments *(fig. 3.8).* A number of small normal faults also interpreted between these master faults which generally shows dip towards NW and W, are termed as synthetic with respect to the master faults. The other set of small normal faults shows dip towards SE and E, are termed as antithetic with the reference of master faults *(fig. 3.8)*. The structures in the hanging wall of the MF1 are more

deformed than MF2 and MF3, by the synthetic and antithetic behavior of small normal faults *(fig. 3.8)*. In addition, Splay faults are also observed particularly along small normal faults at the hanging wall of MF-1a, as interpreted on key profiles 1 & 2. Fault splays have been also branches out from MF3b and 3c as illustrated in *(fig. 3.8)*.

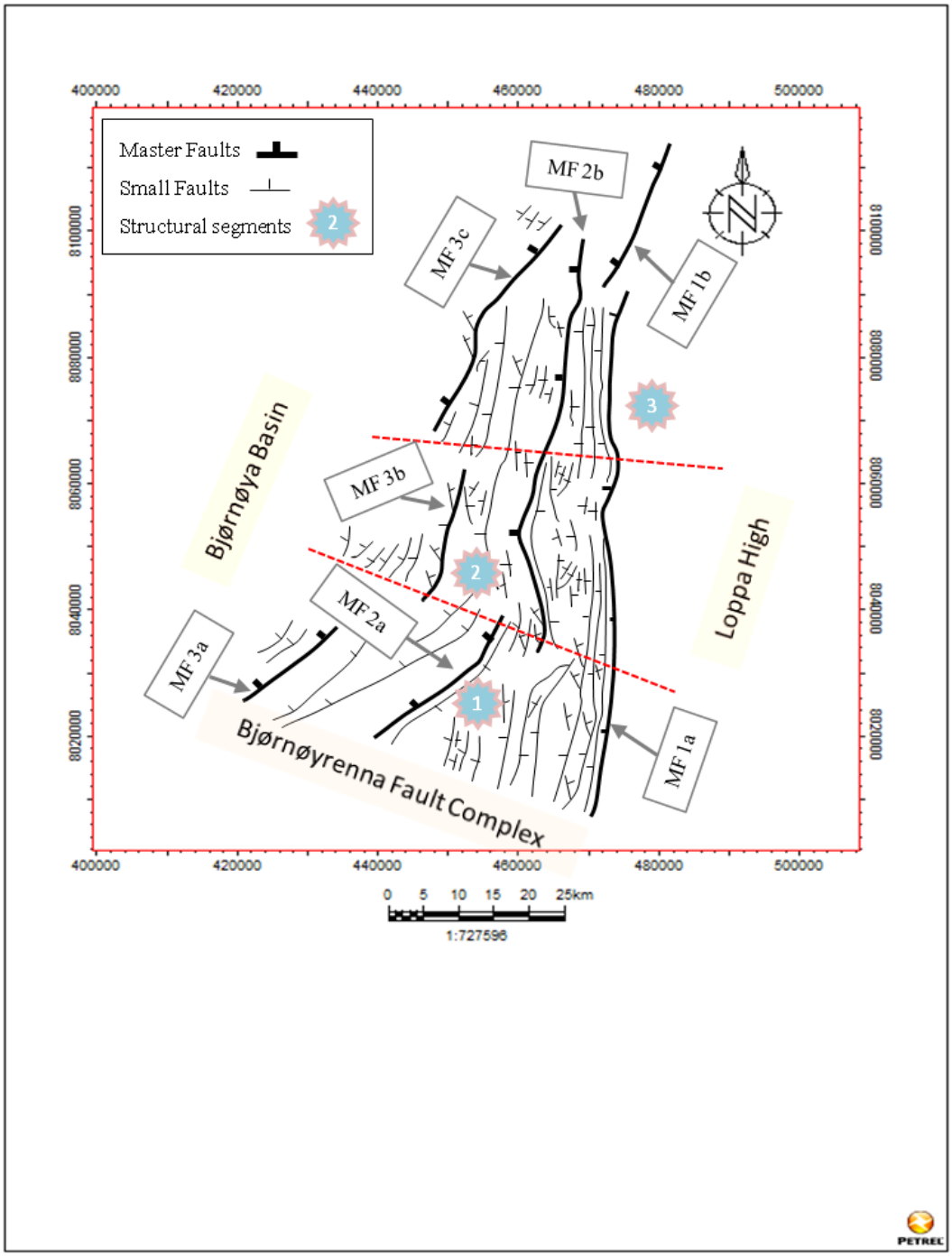


**Figure 3.8:** Fault map at intra Triassic level showing the main structural segments of the Bjørnøyrenna Fautl Complex. Descriptions of the system for naming of the faults and the principles for identifying the main structural elements are described in the main text.

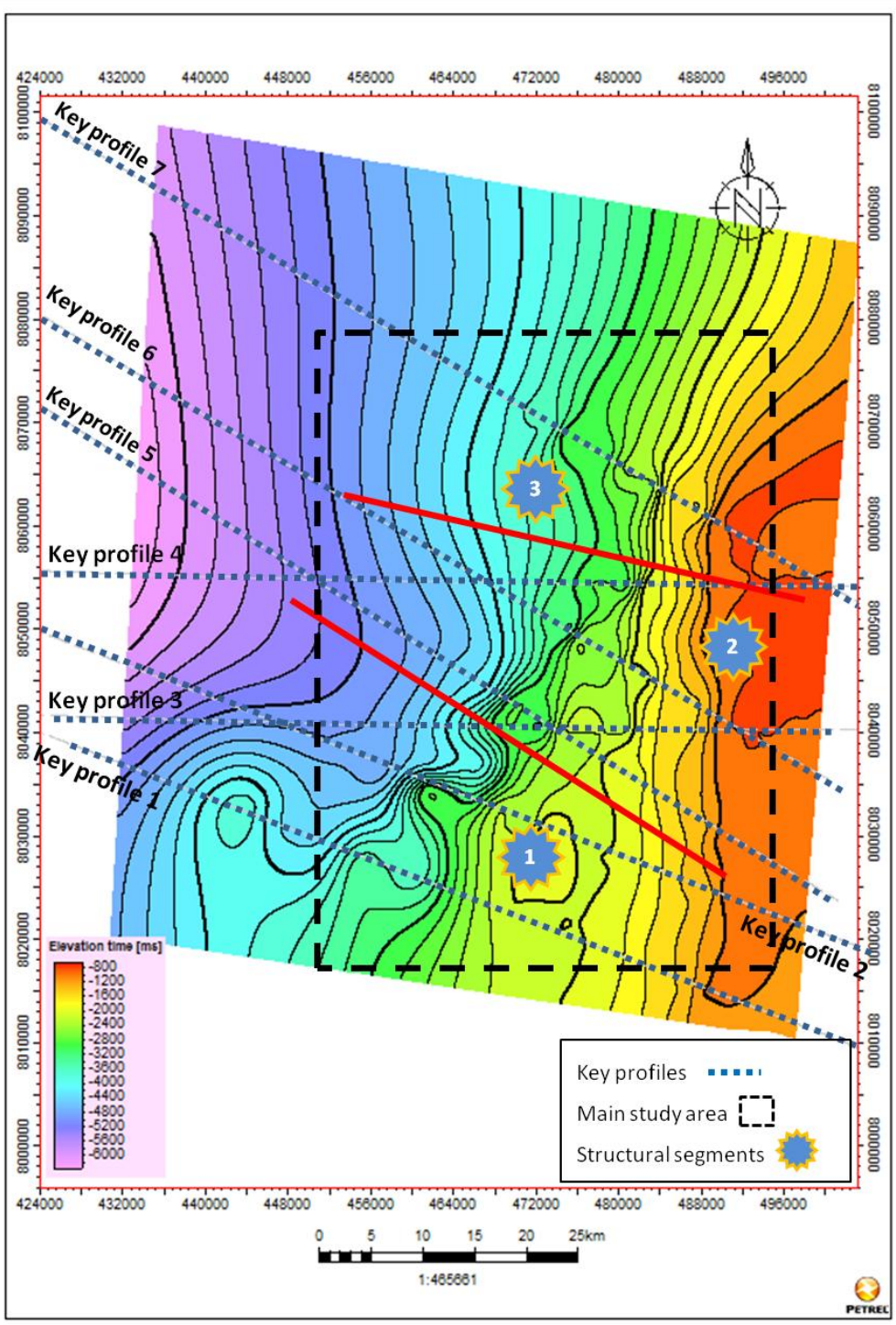


**Figure 3.9:** Time structure map contouring (TWT) at intra Triassic level showing the main structural segments of the study area. Position of key reflection seismic lines are shown by blue stripped lines.

According to the strategy for the structural descriptions and analysis as given above, description of the key seismic lines are given in the following. First, a general description of the main structural elements as seen in the cross section is given *(Fig. 3.10 a,b)* and thereafter detailed description of the key profiles from segments 1, 2 and 3 *(fig. 3.9)* are presented.

In seismic reflection profiles, the Bjørnøyrenna Fault Complex is divided into two main structural subareas, termed as the upper fault terrace and the lower fault terrace *(fig. 3.10 b)*. Both fault terraces are recognized on the basis of relative position to the matser fault MF1, intrinsic fault frequency, pattern and internal systematic changes with dip dimensions of the reflection packages, presumeably reflecting variations of the master fault planes . Thus, *the* ***upper terrace*** is confined between master faults MF1 and MF2. This element is characterized by southwesterly dipping reflections. *The* ***lower terrace*** is composed of series of rotated fault blocks and bounded by MF2 and MF3. The reflection pacakes in this unit dip towards the southeast *(Fig. 3.10 a,b).*

Furthermore, by comparison of fault frequency and geometry, the striking contrast exist in structural trend between the deeper (intra Carboniferous - mid Permian) and the upper (Triassic - early Cretaceous) levels *(fig. 3.10 a,b).* These contrasts are analyzed in more detail separately below.

On key seismic reflection profiles, the faults of upper terrace are indicated by “F” with numeric index (1,2,3.....n) whereas lower fault terrace demonstrating by “f” with numeric index (1,2,3.....n). Furthermore, faults situated at the deepest stratigraphic levels (Late Carboniferous to Permian) are identified by the term “FCP” followed by a numeric index (1,2,...n) indicating their relative position. In addition, the faults located at the Loppa high is presented by “FLH” with numeric index (1,2,...n) (*Fig. 3.10 a,b*). The same pattern will be followed for all the key profiles (1-7).

Generally, the thickness between lower to middle Triassic, middle Triassic to lower Jurassic and Lower Jurassic to base Cretaceous is more or less constant throughout on all the Key profiles. Although the succession of base Cretaceous to early Cretaceous are well preserved in Lower fault terraces but did not found at upper fault terrace which suggest that there was an episode of erosion or non deposition due to extensive uplifting *(fig. 3.4, 3.10 a,b).*

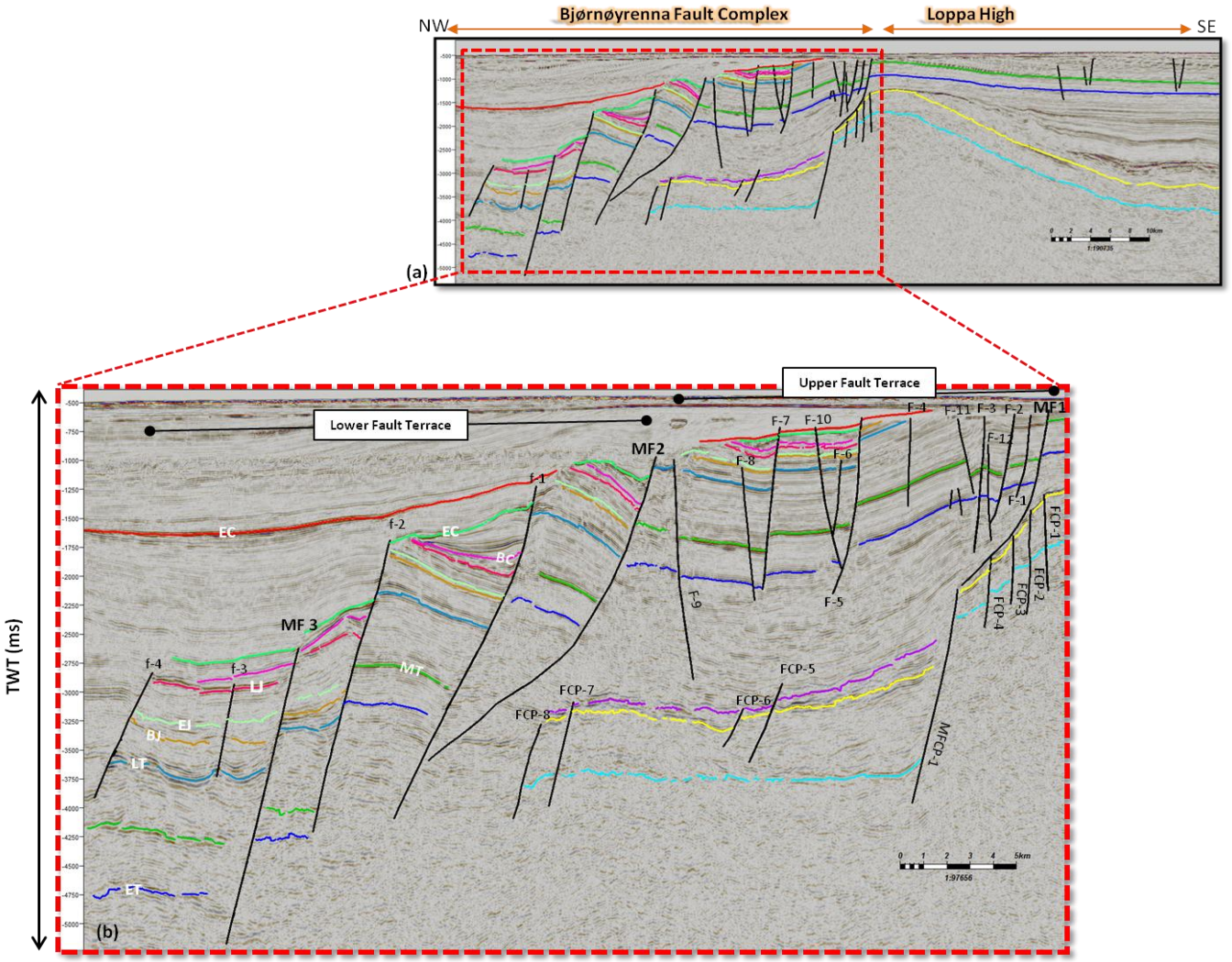


**Figure 3.10:** Generalized seismic section showing subareas along fault segments (MF-1, MF-2, MF-3). (b) Zoomed part of (a) represented by red square. See Figs. 3.8 & 3.9 for location of the line. EC: Early Cretaceous, BC: Base Cretaceous, LJ: Late Jurassic, EJ: Early Jurassic, BJ: Base Jurassic, MT: Mid Triassic, LT, Late Triassic, ET: Early Triassic, MP: Mid Permian, EP: Early Permian, IC: Intra

### 3.4.1 Key Profile 1

This dip line is situated at the southern corner of the study area in segment 1 with an orientation of NW-SE *(fig. 3.8 & 3.9).* The eastern main boundary fault MF-1a is located in the upper terrace as discussed above. MF-1a displays a distinct contrast in fault geometry when the deeper and shallower sections are compared. Thus, its deeper section (MFCP-1) is characterized by a planar geometry, whereas the shallowest section (MF-1a) has a strong listric configuration *(fig. 3.11 a,b).* MF-1a shows a large vertical separation of about 1.38 s TWT at intra-Permian level while at shallowest level, the vertical separation is reduced to 0.2 s TWT with reference to intra Triassic level *(fig. 3.11b).* MF-1a cuts the stratigraphic succession from the intra Triassic level down-section to the early Permian and is therefore termed as ***First*** *or* ***Second-class*** fault (Gabrielsen et al., 1984). On the other hand, MFCP-1 exhibits thick skin nature and imparts a significant role in the development of the Loppa High. Hence it could be termed as ***First-class*** fault *(fig. 3.11b)* (Gabrielsen et al., 1984).

MF-2a shows planar fault geometry along rotated fault blocks. MF2a cut the stratigraphic succession from the early Cretaceous down to the Intra Triassic level and experienced large vertical displacement. A wedge-shaped geometry has been observed along MF-2a between base Cretaceous to early Cretaceous which is a clear indication of Syn-rift sedimentation *(fig. 3.11b).* Moreover, MF-3a is characterized by normal faulting and it shows a vertical separation of about 0.1 s TWT at base cretaceous level which is comparatively less than MF-2a and MF-1a in segment 1 *(fig. 3.11b).*

It can observe that the concentration of faults in upper terrace is higher as compared to lower terrace and generally reflections are dipping toward southwest (*fig. 3.11b).* Most of the faults with in Upper terrace (F-1 to F-9) are synthetic to the MF-1a whereas some other faults (F-10 to F-14) acting as antithetic to the MF-1a. A noteworthy feature as roll-over fold has been observed at the hanging wall of MF-1a. Some deep seated faults including (FCP-2 to FCP-5) have also been interpreted at intra-Carboniferous to intra-Permian level which generally behaves as synthetic to MFCP-1 (*fig. 3.11b).* These deep faults doesn't continue upward to younger successions, so this disconnection indicating that these both faulting were result of different

tectonic phases. Along MFCP-1, drag fold is observed which exhibits a synclinal feature at the hanging wall while anticline is found to be associated at the foot wall (*fig. 3.11b).*

The lower fault terrace is bounded between MF-2a and MF-3a, signifying rotated fault blocks geometry along the planar normal faults as discussed above. In the lower terrace, most of the faults (f-1 to f-4) are synthetic to MF-2a and the reflections are dipping toward Southeast (*fig. 3.11b).* A syncline is formed at the hanging of wall of MF3a which is a prominent representation of Normal drag fold geometry.

The fault frequency decreases towards the footwall of the MF1a where Loppa High is situated. Only the intra Triassic successions had experienced minor faulting and show planar fault geometry. Most of the faults (FLH1-FLH3) are antithetic to the MF-1a while only one fault (FLH4) is acting as synthetic to MF-1a *(Fig. 3.11a).*

At the western edge of the Loppa High, early Tertiary sequences directly overlain on the Triassic succession which clearly illustrates that the succession ranging from the late Triassic to the late Cretaceous is missing. On the other hand, constant thickness is observed between the intra Triassic succession within fault complex and the Loppa High while Jurassic and Cretaceous reflections are absent on both locations due to an extensive erosion followed by uplifting (*fig. 3.11b).*

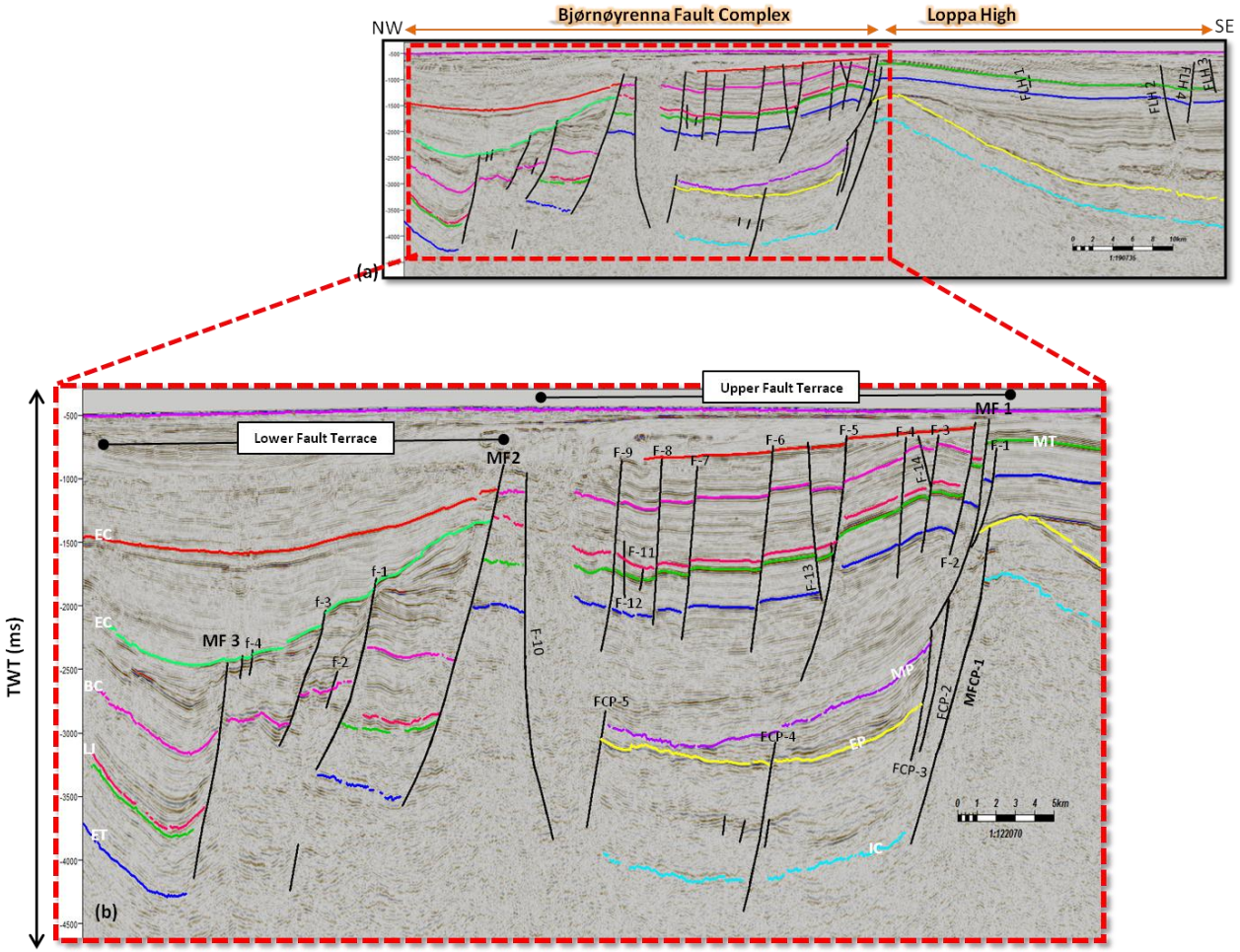


**Figure 3.11(a)**: Key Profile 1 along the fault segments MF1, MF2 & MF3. **(b)** Zoomed-in part of (a) shown by red square. See Figs. 3.8 & 3.9 for location of the line. EC: Early Cretaceous, BC: Base Cretaceous, LJ: Late Jurassic, MT: Mid Triassic, ET: Early Triassic, MP: Mid Permian, EP: Early Permian, IC: Intra Carboniferous.

### 3.4.2 Key Profile 2

The orientation of this dip line is NW-SE, located to the southern corner of the study area in segment 1 *(fig. 3.8 & 3.9)*. This seismic reflection profile is located at a distance of 9 Km from key profile 1. The eastern main boundary fault MF-1a striking N-S with general southwest dip that varies with depth. MF-1a displays a distinct contrast in fault geometry when the deeper and shallower sections are compared. Thus, its deeper section is characterized by a planar geometry, whereas the shallowest section shows a concave upward listric configuration *(fig. 3.12b)*. MF-1a shows a large vertical displacement of about 0.7 s TWT at intra-Permian level whereas it reduced to 0.33 s TWT at mid-Triassic level. It cuts the stratigraphic succession from intra Triassic down to early Permian and is therefore termed as ***First*** *or* ***Second-class*** fault (Gabrielsen et al., 1984). In addition, the MFCP-1 imparts a significant role in the development of the Loppa High and it is rooted down to the basement indicated by thick skin nature. Hence it could be termed as ***First-class fault*** (*fig. 3.12b)*(Gabrielsen et al., 1984).

MF-2a shows planar fault geometry along rotated fault block. It also experienced a large vertical throw as compare to MF-1a in this seismic reflection profile. The displacement along MF-2a is estimated to be 0.13 s TWT at late-Jurassic level (*fig. 3.12b)*. MF-2a cut the stratigraphic succession from the early Cretaceous down to the Intra Triassic level. Along MF-2a, wedge shaped geometry is observed between base Cretaceous to the early Cretaceous indicating the onset of Syn-rift sedimentation (*fig. 3.12 a,b)*. Moreover, MF-3a acts as a western boundary fault and is characterized by planar normal fault geometry. MF3a experienced a vertical separation of about 0.24 s TWT at the base Jurassic level (*fig. 3.12b)*.

The concentration of faulting in Upper terrace is higher as compared to lower terrace and generally reflections are dipping toward southwest. Most of the faults with in Upper terrace (F-1 to F-7) are synthetic to the MF-1a while faults (F-8 to F-13) acting as antithetic to the MF-1a (*fig. 3.12b)*. A noteworthy feature as roll-over fold has been interpreted at the hanging wall of MF-1a. Moreover, at deeper level the faults (FCP-1 to FCP-8) are synthetic to the planar MFCP-1. These deep faults didn't continue upward to younger successions, so this disconnection indicating that these both faulting has been occurred at different tectonic phases. The most prominent feature

has been observed along MFCP-1 is the presence of drag fold, which displays a syncline at the hanging wall whereas, anticline is established at the footwall (*fig. 3.12b).*

The lower terrace is characterized by rotated fault blocks geometry along the planar faults and it is limited between MF-2a and MF-3a *(fig. 3.12 a,b).* In lower terrace, the faults (f-1 & f-2) are synthetic to MF-2a whereas (f3 & f4) are synthetic to MF-3a. In addition, the reflections are dipping toward Southeast in this terrace.

The population of faulting decreases towards the footwall where Loppa High is located. Only intra Triassic sequences had experienced minor faulting and it shows planar geometry. Most of the faults (FLH-1 to FLH-3) are antithetic to the MF-1a while faults (FLH-4 & 5) are synthetic to MF-1a (*fig. 3.12 a,).*

The early Tertiary sequences are directly overlain on the Triassic succession at the hinge of the Loppa High which clearly demonstrates the succession ranging from the late Triassic-late Cretaceous is missing. On the other hand, a constant thickness has been observed between the Triassic succession within fault complex and the Loppa High while Jurassic and Cretaceous reflections disappeared in the upper terrace due to erosion followed by Uplifting. Similarly, these successions are well preserved in lower fault terrace (*fig. 3.12b).*

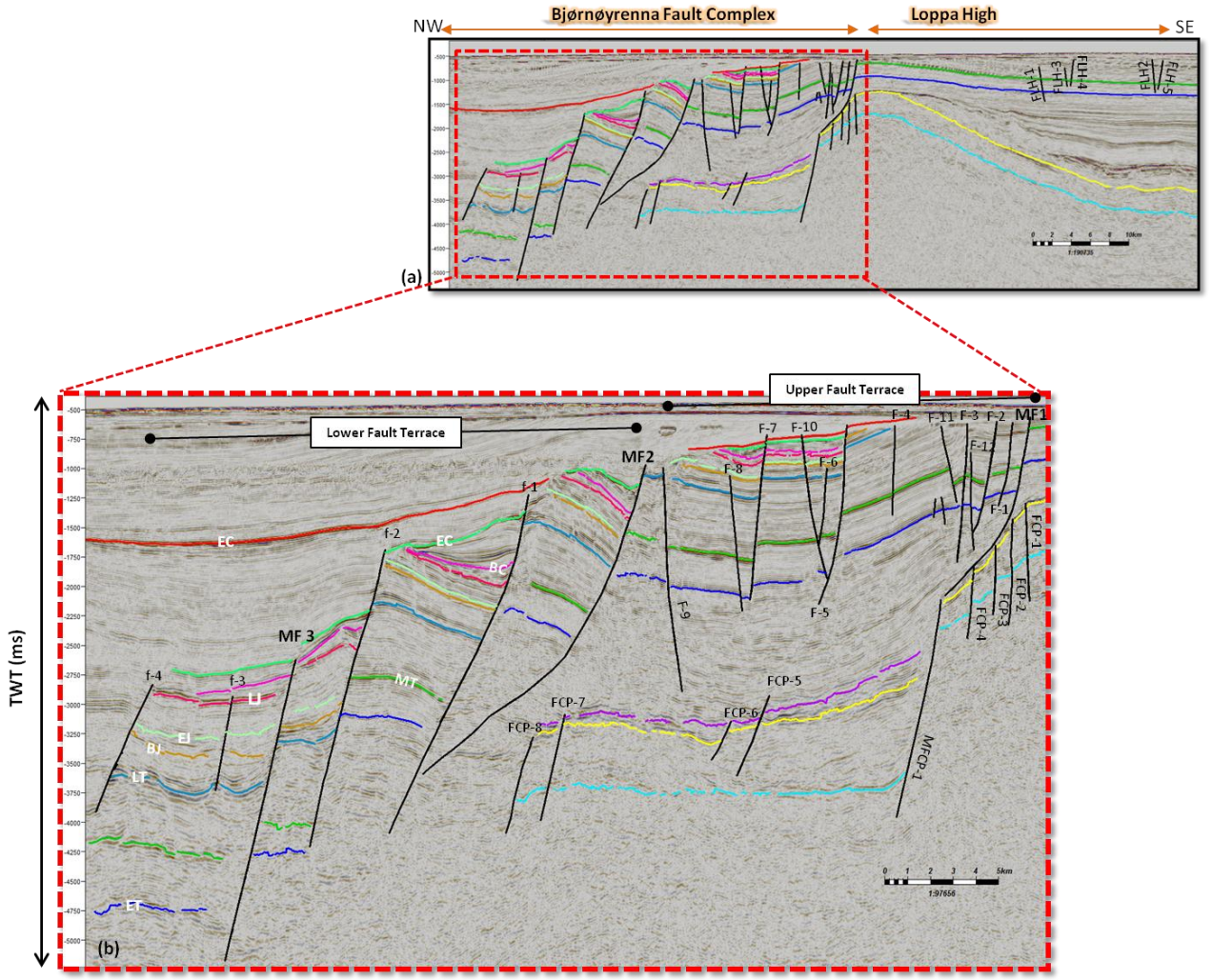


**Figure 3.12(a)**: Key Profile 2 along the fault segments MF1, MF2 & MF3. **(b)** Zoomed-in part of (a) shown by red square. See Figs. 3.8 & 3.9 for location of the line. EC: Early Cretaceous, BC: Base Cretaceous, LJ: Late Jurassic, EJ: Early Jurassic, BJ: Base Jurassic, LT: Late Triassic, MT: Mid Triassic, ET: Early Triassic, MP: Mid Permian, EP: Early Permian, IC: Intra Carboniferous.

### 3.4.3 Key Profile 3

This 2D seismic line belongs to the central part of the study area in segment 2 and is oriented W-E *(fig. 3.8 & 3.9).* The eastern main boundary fault MF-1a exhibits a distinct contrast in fault geometry when deeper and shallower levels are concerned. Thus, its deeper section is characterized by planar fault geometry, whereas the shallowest section has a strong listric configuration. MF-1a indicates a large vertical separation of about 1.22 s TWT at the intra-Permian level whereas the throw reduced to 0.15 s TWT at the upper-Triassic level *(fig. 3.13 a,b).* MF-1a cuts the stratigraphic succession from intra Triassic down to early Permian and is therefore termed as ***First*** *or* ***Second-class*** fault (Gabrielsen et al., 1984). On the other hand, MFCP-1 striking N-S and dominating a major role in the evolution of the Loppa High and this fault is rooted down to basement indicating thick skin tectonic. Therefore it is termed as ***First class*** *fault (fig. 3.13 a,b)* (Gabrielsen et al., 1984).

MF-2a shows planar fault geometry along rotated fault blocks. The vertical separation of about 0.4 s TWT has been examined at early-Jurassic level. MF-2a cut the stratigraphic succession from early Cretaceous down to Intra Triassic level. A wedge-shaped geometry has been observed along MF-2a which suggests syn-rift deposition between the base Cretaceous to early Cretaceous level *(fig. 3.13 a,b).* Similarly, MF-3a distinguishing the western boundary of the fault complex by deep Bjørnøya Basin and is characterized by normal fault.

The population of faulting in Upper terrace is tremendous as compared to lower terrace and generally reflections are dipping toward southwest. Most of the faults within Upper terrace (F-1 to F-7) are synthetic to the MF-1a whereas some other faults (F-8 to F-14) acting as antithetic to the MF-1a *(fig. 3.13b).* In addition, (F-4 & F-5) has been branches out form F-9. The behavior of structural patterns in this segment is seemed to be different from previous seismic lines of segment 1. A noteworthy feature has been interpreted in the proximate vicinity in the hanging wall of MF1a, is the existence of rollover fold *(fig. 3.13b).* The faults at deeper level including (FCP-1 to FCP-6) are synthetic to MFCP-1. These deep seated faults didn't continue upward to younger successions, so this disconnection indicating that these both faulting has been occurred at different tectonic phase. The most pronounced feature has been examined in the close vicinity

of MFCP-1 is the ubiquity of drag fold which shows a syncline at the hanging wall and anticline the footwall *(fig. 3.13 a,b).*

The lower terrace exhibits rotated fault block geometry along the planar faults and it is bounded between MF-2b and MF-3b. In lower terrace most of the faults (f-1 to f-5) are synthetic to MF-2a and the reflections are dipping toward Southeast *(fig. 3.13b).*

The Loppa high is comparatively less faulted than other key profiles described earlier. Only mid Triassic reflection affected by faulting and it exhibit planar fault geometry. Only one small fault is tend to be antithetic to the MF1a *(fig. 3.13 a).*

The early mid Jurassic to late Cretaceous successions disappeared, particularly in the upper fault terrace and at the western edge of the Loppa High. This disappearance suggests an episode of erosion or non deposition followed by uplifting *(fig. 3.13 a,b).*

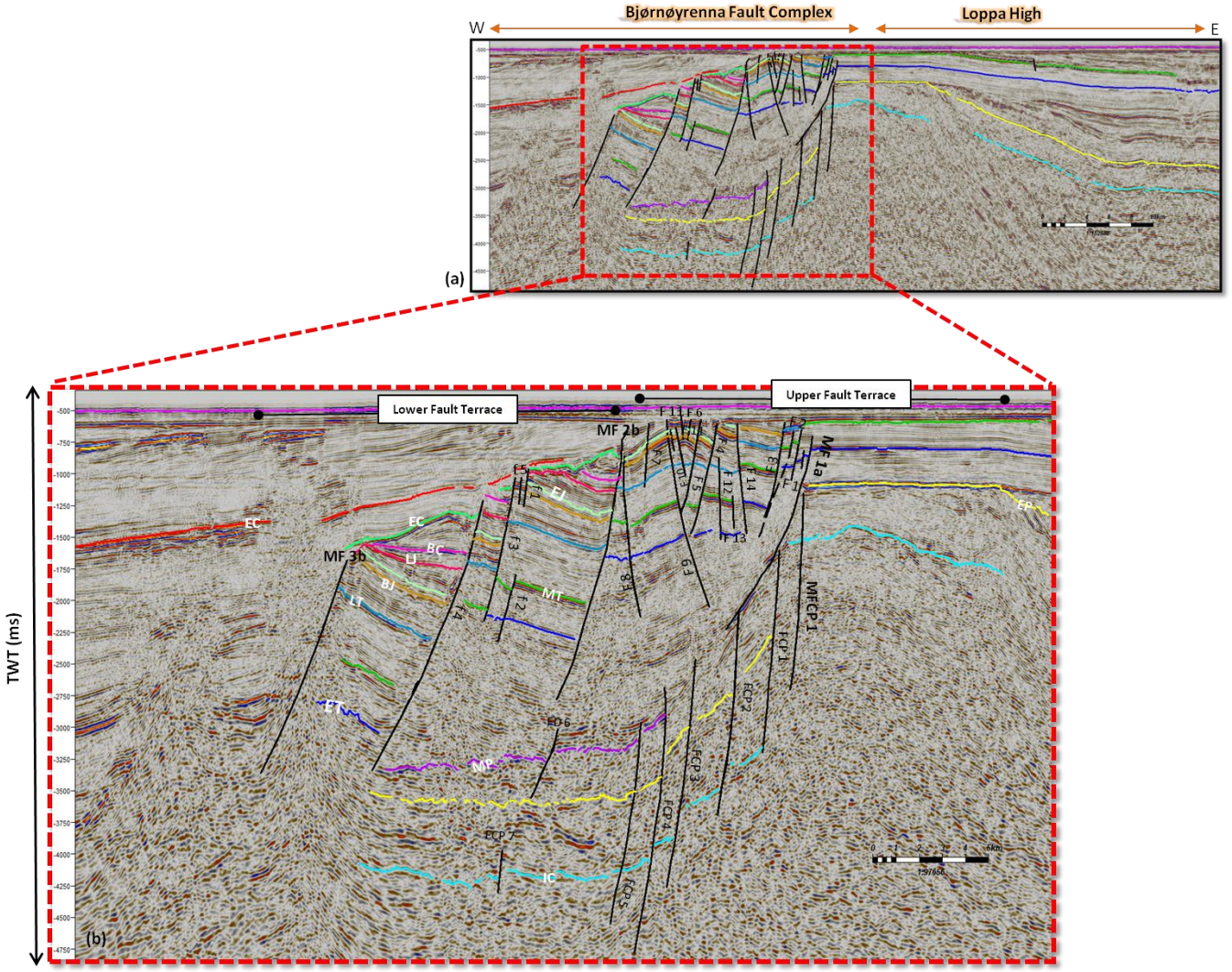


**Figure 3.13(a)**: Key Profile 3 along the fault segments MF1, MF2 & MF3. **(b)** Zoomed-in part of (a) shown by red square. See Figs. 3.8 & 3.9 for location of the line. EC: Early Cretaceous, BC: Base Cretaceous, LJ: Late Jurassic, EJ: Early Jurassic, BJ: Base Jurassic, LT: Late Triassic, MT: Mid Triassic, ET: Early Triassic, MP: Mid Permian, EP: Early Permian, IC: Intra Carboniferous.

### 3.4.4 Key Profile 4

The orientation of 2D seismic line is W-E, located at the central part of the study area in segment 2 *(fig. 3.8 & 3.9)*. The eastern main boundary fault MF-1a shows N-S structural trend with general westward dip that varies with depth. MF-1a displays a distinct contrast in fault geometry when the deeper and shallower levels are compared. Thus, its deeper level is characterized by a planar geometry, whereas the shallowest section has a strong listric configuration *(fig. 3.14 a,b).* MF-1a shows a large vertical displacement of about 1.4 s TWT at the intra-Permian level and cuts the stratigraphic succession from the intra Triassic down to the early Permian. Therefore it is termed as ***First*** *or* ***Second-class*** faults (Gabrielsen et al., 1984). At deeper level, MFCP-1 display a dominant part in the development of the Loppa High and this fault is seated to basement level dominated by thick skin nature, hence it is termed as ***First class*** fault *(fig. 3.14 a,b)*(Gabrielsen et al., 1984).

MF-2a is indicated by planar fault geometry along rotated fault blocks. It experienced a large vertical throw as compared to MF-1a particularly in this reflection profile *(fig. 3.14 a,b)*. The displacement along MF-2a is estimated to be 0.24 s TWT at the early-Jurassic level followed by NE-SW trend in strike dimension. MF-2a cuts the stratigraphic succession from the early Cretaceous down to the Intra Triassic level. A wedge-shaped geometry has been observed along MF-2a between base Cretaceous to the early Cretaceous which is a clear indication of Syn-rift deposition *(fig. 3.14b)*. On the other hand, MF-3a is characterized by normal fault and distinguishing the western boundary of the fault complex by deep Bjørnøya Basin as mentioned above.

Upper terrace is densely faulted as compared to lower terrace and generally reflections are dipping toward southwest. Most of the faults in Upper terrace (F-1 to F-6) are synthetic to the MF-1a while faults (F-7 to F-9) acting as antithetic to the MF-1a. A noticeable feature is observed along MF1a is the presence of rollover fold *(fig. 3.14b)*. The faults at deeper level (FCP-1 to FCP-4) are synthetic to the planar MFCP-1 *(Fig. 4b).* These deep seated faults cut the stratigraphic succession from the intra-Carboniferous to the early-Permian and didn't continued upward to younger successions, so this disconnection indicating that these both faulting was a

result of different tectonic phase. A syncline is observed at the hanging wall while anticline is established at the footwall of the MFCP-1 which exhibits remarkable feature of drag fold *(fig. 3.14b).*

The lower fault terrace is restricted between MF2a and MF3a, illustrated by rotated fault blocks geometry. Predominantly, reflections are dipping toward Southeast in this terrace. Most of the faults in lower terrace (f-1 & f-2) are antithetic to MF-2a whereas f-3 shows synthetic behavior to MF-2b *(fig. 3.14b).*

The succession ranging from late Triassic to late Cretaceous is absent both at the western corner of the Loppa High and in upper terrace of the fault complex. This implies an episode of erosion or non deposition in this age followed by uplifting. On the other hand, a remarkable thickness has been observed between intra Triassic successions and this is the only one reflection which is completely well preserved throughout the study area *(fig. 3.14 a,b).*

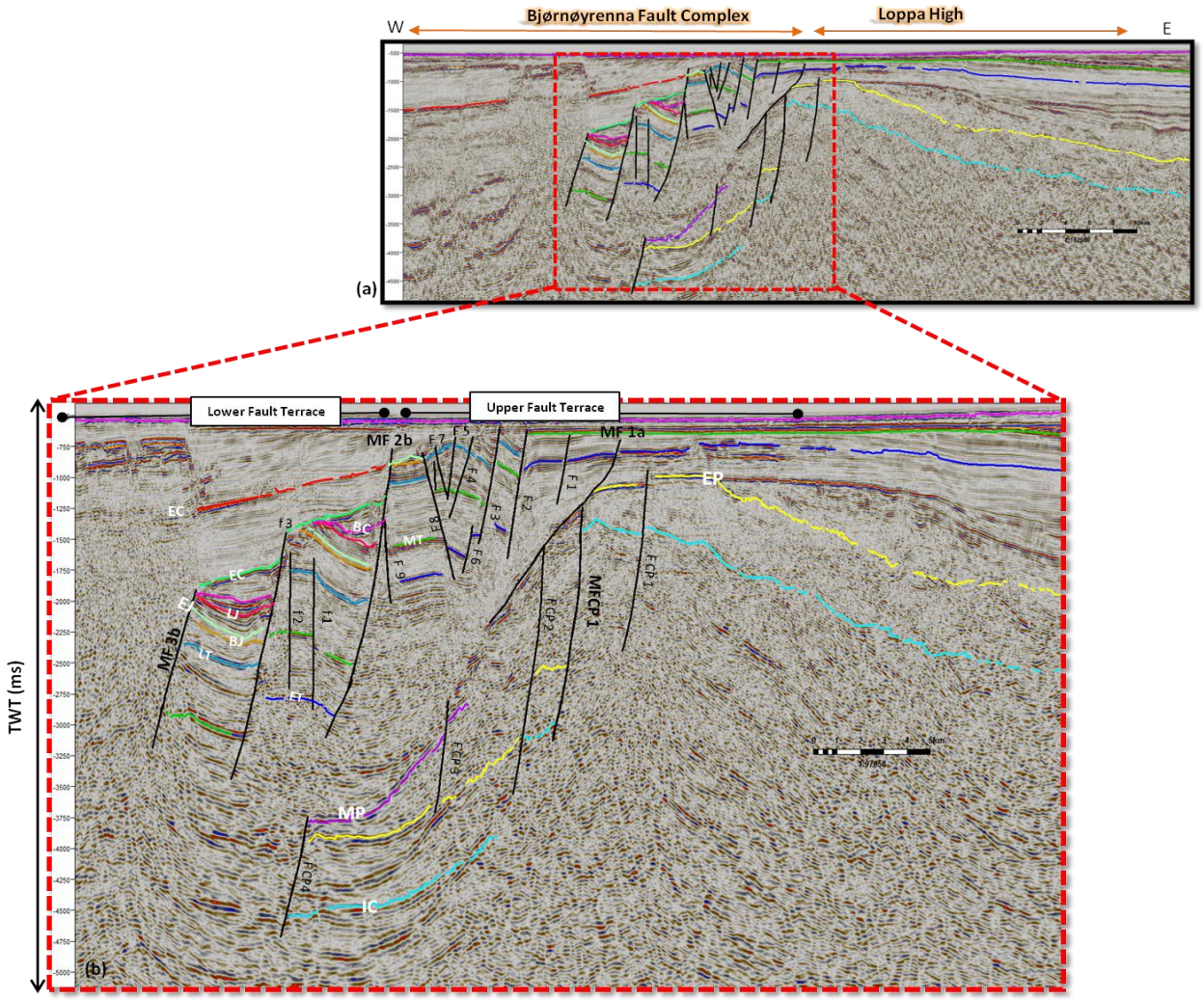


**Figure 3.14(a)**: Key Profile 4 along the fault segments MF1, MF2 & MF3. **(b)** Zoomed-in part of (a) shown by red square. See Figs. 3.8 & 3.9 for location of the line. EC: Early Cretaceous, BC: Base Cretaceous, LJ: Late Jurassic, EJ: Early Jurassic, BJ: Base Jurassic, LT: Late Triassic, MT: Mid Triassic, ET: Early Triassic, MP: Mid Permian, EP: Early Permian, IC: Intra Carboniferous.

### 3.4.5 Key Profile 5

This seismic line belongs to the central part of the study area in segment 2 and is oriented NW-SE *(fig. 3.8 & 3.9)*. The eastern main boundary fault MF-1a exhibits N-S structural trend in strike with general westward dip that varies with depth. MF-1a prescribed a distinct diversity in fault geometry when the deeper and shallower sections are concerned. Thus, its deeper level is described by a planar geometry, whereas the shallowest level shows strong listric configuration. MF-1a shows a large vertical separation of about 0.9 s TWT at intra-Permian level whereas it reduced to 0.1 s TWT at intra-Triassic level *(fig. 3.15 a,b)*. MF-1a cuts the stratigraphic succession from intra Triassic down to early Permian and is therefore termed as **First** or **Second-class** fault (Gabrielsen et al., 1984). The MFCP-1 constitutes N-S orientation with general westward dip. MFCP-1 greatly influenced the mid Carboniferous to intra Permian succession and imparts a considerable role in the development of the Loppa High. This fault is seated up to basement level and demonstrates thick skin nature. Therefore, it is termed as **First class fault** *(fig. 3.15 a,b)* (Gabrielsen et al., 1984).

MF-2b is defined by planar fault geometry along rotated fault block. Comparatively, a large vertical throw has been examined along MF2b than MF1a particularly in this key profile . The displacement along MF-2a is estimated to be 0.13 s TWT at base-Cretaceous level and followed by NE-SW strike *(fig. 3.15b)*. MF-2a cuts the stratigraphic succession from the early Cretaceous down to the Intra Triassic level. A wedge-shaped geometry has been observed along MF-2a between base Cretaceous to the early Cretaceous which demonstrate Syn-rift sedimentation. Simultaneously, MF-3b is characterized by normal fault shows large vertical separation than MF2b and it is estimated to be 0.6 s TWT at early-Cretaceous level *(fig. 3.15b)*.

The concentration of faulting in Upper terrace is higher as compared to lower terrace and generally reflections are dipping toward southwest. Most of the faults with in Upper terrace (F-1 to F-10) are synthetic to the MF-1a while faults (F-11 to F-20) acting as antithetic to the MF-1a. Additionally (F-20 & F-21) and (F-12 & F-13) acting as splay faults that branches out from F-8 and F-6 *(fig. 3.15b)*. A noteworthy feature has been examined near the vicinity of MF1a is the existence of rollover fold. The faults at deeper level (FCP-1 to FCP-10) are synthetic to MFCP-1

and FCP-11 acting as antithetic that branches out from FCP-8. Although the most remarkable feature has been recognized along MFCP1 is the presence of drag fold which constitutes a syncline at the hanging and anticline at the footwall respectively *(fig. 3.15b)*. The faults situated at deeper level didn't influence the younger successions, so this disconnection represents that these both faulting was a result of different tectonic phase.

The lower fault terrace is bordered by MF2b and MF3b and generally reflections are dipping towards southeast. MF2b exhibits rotated fault blocks geometry along the planar faults. In lower terrace, the faults (f-1 & f-2) are synthetic to MF-2b whereas (f3 & f4) behaving as antithetic to MF-2b. Similarly, the faults (f-5 to f-8) are synthetic to MF-3b while some other faults (f-9 to f-17) behaving as antithetic to MF-3b. In addition, faults (f-13, f-14 & f15) have been branch out from MF-3 and acting as splay faults. The most remarkable feature has been examined at the hanging wall of MF3b is the development of drag fold *(fig. 3.15b)*. At this key profile the hanging wall of MF3b is more affected by the faulting as compared to others.

The succession ranging from the late Triassic to the late Cretaceous is absent both at the western corner of the Loppa High and in upper terrace of the fault complex. This implies an episode of erosion or non deposition in this age followed by uplifting. On the other hand a remarkable thickness has been observed between the intra Triassic successions and this is the only one reflection which is completely well preserved throughout the study area *(fig. 3.15b)*.

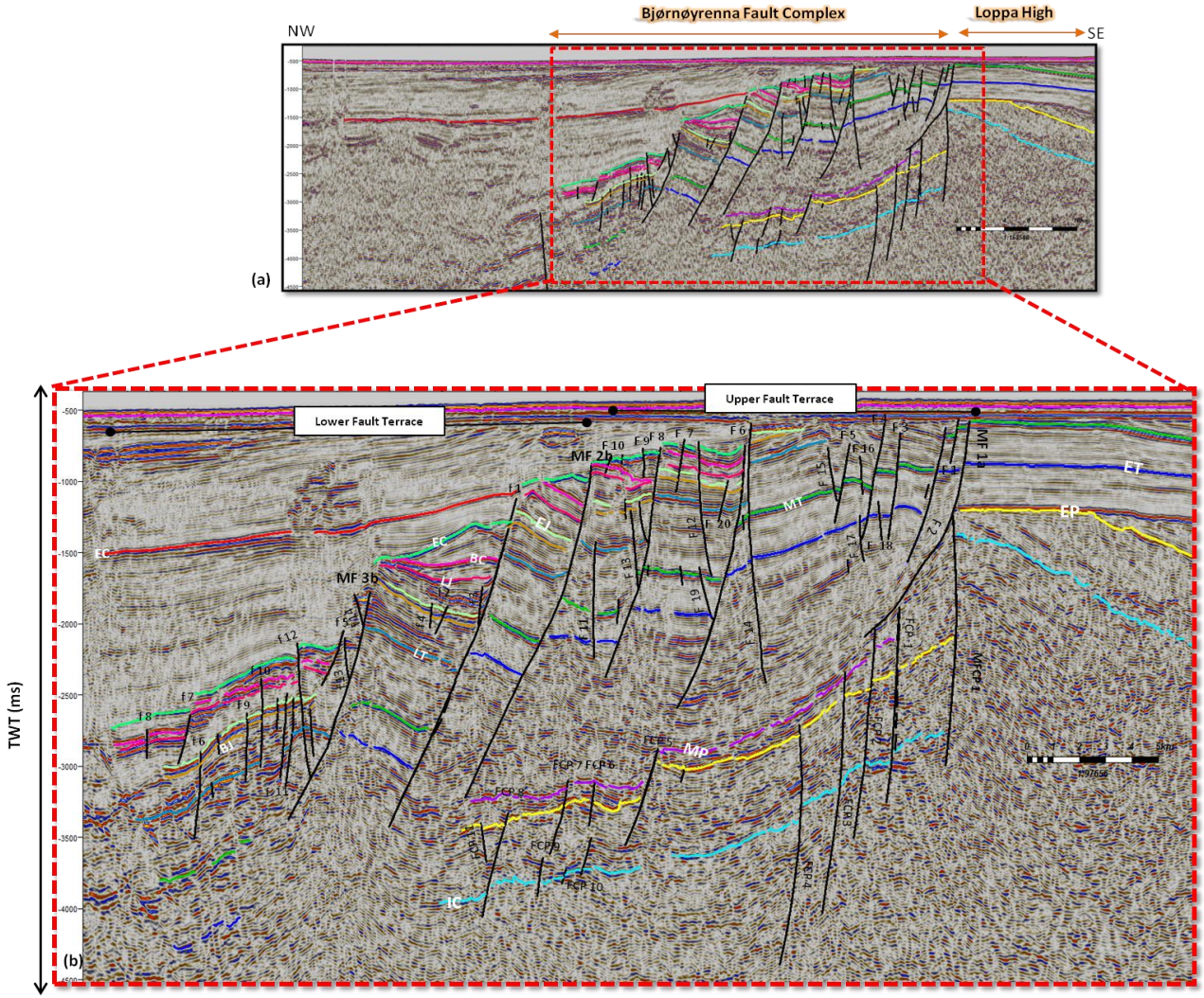


**Figure 3.15(a)**: Key Profile 5 along the fault segments MF1, MF2 & MF3. **(b)** Zoomed-in part of (a) shown by red square. See Figs. 3.8 & 3.9 for location of the line. EC: Early Cretaceous, BC: Base Cretaceous, LJ: Late Jurassic, EJ: Early Jurassic, BJ: Base Jurassic, LT: Late Triassic, MT: Mid Triassic, ET: Early Triassic, MP: Mid Permian, EP: Early Permian, IC: Intra Carboniferous.

### 3.4.6 Key profile 6

This 2D seismic line striking NW-SE, located at the central part of the study area in segment 2 *(fig. 3.8 & 3.9)*. The eastern main boundary fault MF-1a shows N-S structural trend with general westward dip that varies with depth. MF-1a exhibits a distinct diversity in fault geometry when the deeper and shallower levels are compared. Thus, its deeper level is indicated by a planar geometry and the shallowest level is dominated by a strong listric configuration *(fig. 3.16 a,b).* MF-1a shows a large vertical throw of about s 0.25 s TWT at mid-Triassic level and cut the stratigraphic succession from intra Triassic down to early Permian therefore it's termed as ***First*** *or* ***Second-class*** fault (Gabrielsen et al., 1984). On the other hand, at deeper level, MFCP-1 signifies a major role in the development of the Loppa High and this fault is seated up to basement level, hence it is termed as ***First class*** fault (*fig. 3.16 a,b)*(Gabrielsen et al., 1984).

MF-2b is indicated by planar fault geometry along rotated fault blocks. The fault is illustrated by a large vertical throw as compared to MF-1a. The vertical separation along MF-2a is estimated to be 0.13 s TWT at early-Jurassic level followed by NE-SW trend in strike dimension (*fig. 3.16 a,b).* MF-2a cut the stratigraphic succession from the early Cretaceous down to the Intra Triassic level *(Fig.3.16 a,b). A* wedge-shaped geometry has been examined between base Cretaceous to early Cretaceous level along MF2b which elaborate Syn-rift deposition. Similarly, MF-3b is characterized by planar normal fault and separating the western boundary of the fault complex by deep Bjørnøya Basin as mentioned earlier *(fig. 3.16 a,b).*

Comparatively, Upper terrace is highly faulted lower fault terrace. Most of the reflections in upper terrace are dipping toward southwest. The fault in upper terrace (F1 to F10) are synthetic to MF1a whereas, the faults (F11 to F19) acting as antithetic to MF1a. This seismic reflection profile is different because there is no rollover fold has been observed along the MF1a. the faults situated at deeper level (FCP1 to FCP8) are synthetic to MFCP1. The most prominent feature of drag fold has been observed along MFCP1 is the presence of syncline at the Hanging wall and anticline at the footwall.

The lower fault terrace is bordered by MF2a and MF3a, indicated by rotated fault blocks geometry. Mainly the reflections are dipping toward Southeast in this terrace. Most of the faults

in lower terrace (f1 & f11) are synthetic to MF3b whereas the faults (f12 and f13) are antithetic to the MF2b. Across this reflection profile a very noticeable feature is the presence of Horst structure bounded by f15 and f8 as shown in fig.

The frequency of faulting decreases toward the footwall where Loppa High is situated. Only intra Triassic sequences had experienced minor faulting and it shows planar geometry. Most of the faults (FLH-1 to FLH-2) are antithetic to the MF-1a while fault (FLH-3) are synthetic to MF-1a *(Fig. 3a,b).*

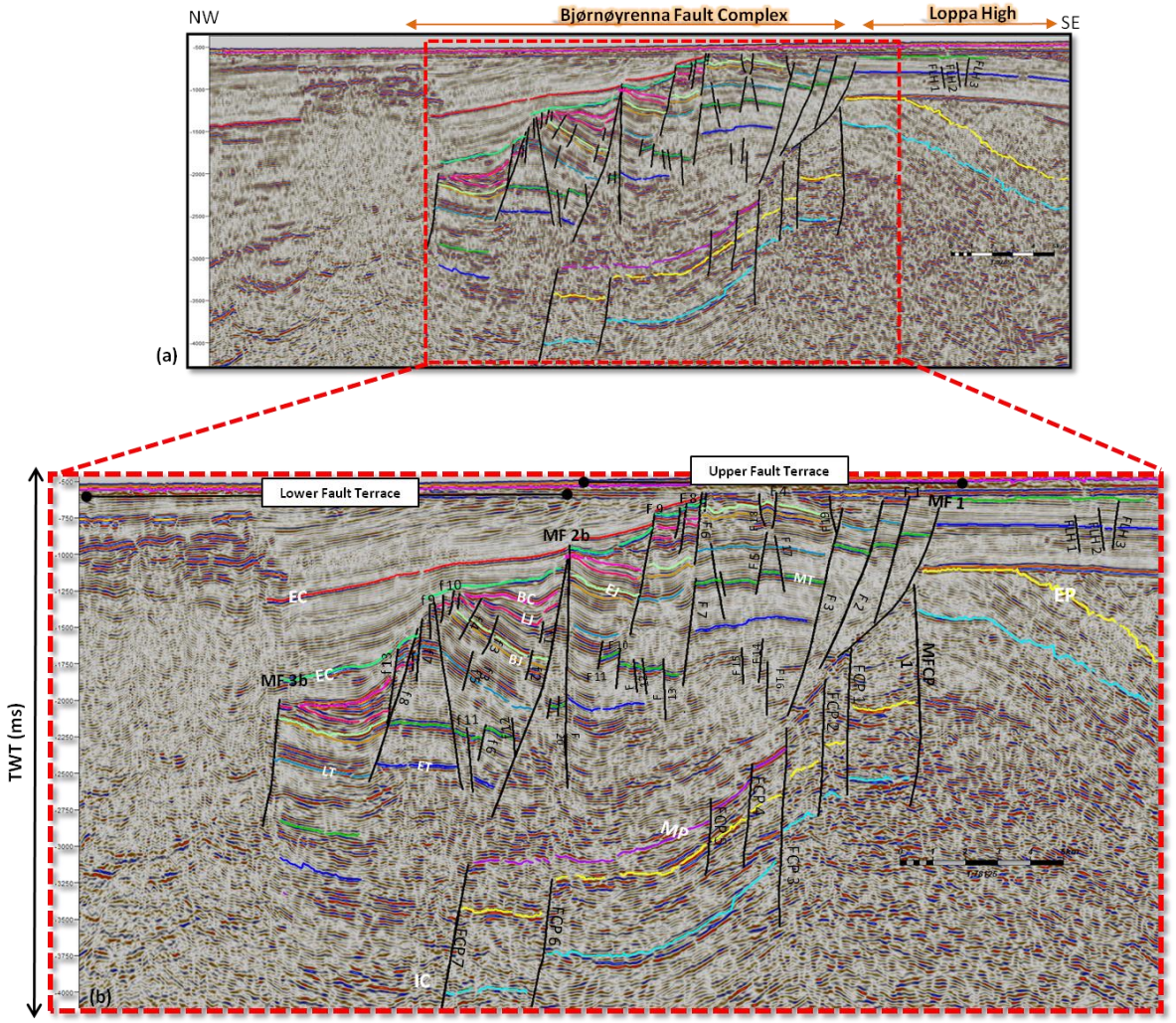


**Figure 3.16(a)**: Key Profile 6 along the fault segments MF1, MF2 & MF3. **(b)** Zoomed-in part of (a) shown by red square. See Figs. 3.8 & 3.9 for location of the line. EC: Early Cretaceous, BC: Base Cretaceous, LJ: Late Jurassic, EJ: Early Jurassic, BJ: Base Jurassic, LT: Late Triassic, MT: Mid Triassic, ET: Early Triassic, MP: Mid Permian, EP: Early Permian, IC: Intra Carboniferous.

### 3.4.7 Key Profile 7

The NW-SE trending 2D seismic line is located to the northern part of the study area in segment 3 (fig. 3.8 & 3.9). In this seismic reflection profile, MF1a doesnot cut the shallower stratigraphic succession which is quite different from other interpreted key profiles (1-6). MF1a demonstrate a distinct diversity in fault geometry when the deeper and shallower levels are compared. The deeper level is characterized by planar fault geometry whereas shallowest level is dominated strong listric configuration. Moreover, MFCP-1 demonstrate a major role in the development of the Loppa High and this fault is rooted up to basement level which indicate thick skin tectonics and therefore it is termed as ***First class*** fault (*fig. 3.17 a,b)*(Gabrielsen et al., 1984).

MF-2b exhibit planar fault geometry along rotated fault blocks. The fault shows a large vertical displacement particularly in this key profile as compare to MF-1a and it is estimated to be 0.95 s TWT with a reference to the late Triassic reflection *(fig. 3.17 a,b)* . MF-2b cut the stratigraphic succession from the early Cretaceous down-section to the Intra Triassic level *(Fig. 1 & 3 a,b). A* wedge-shaped geometry has been examined between the base Cretaceous to the early Cretaceous level along MF2b which elaborate Syn-rift deposition. Similarly, MF-3b is characterized by planar normal fault geometry, separating the western boundary of the fault complex by deep Bjørnøya Basin *(fig. 3.17 a,b).*

In upper terrace, the area between MF1a and MF2b becomes narrow in segment 3 and the dip of the reflection is dramatically changed from SW to SE in this key profile *(fig. 3.17b).* Fault (F1) is acting as synthetic to the MF1a whereas the faults (F2-F4) acting as antithetic to the MF1a. Moreover, this seismic reflection profile is different because there is no rollover fold has been observed along the MF1a. The faults located at deeper level (FCP1-FCP5) are synthetic to the MFCP1. . The most prominent feature of drag fold has been observed along MFCP1 is the presence of syncline at the Hanging wall and anticline at the footwall. In addition, prominent horst feature is interpreted in this key profile which separate the upper terrace form the lower terrace as seen in *(fig. 3.17b).*

Lower terrace is bordered by MF2a and MF3a, indicated by rotated fault blocks geometry. Mainly the reflections are dipping toward Southeast in this terrace. Most of the faults in lower terrace (f1 & f11) are synthetic to MF3b whereas the faults (f12 and f13) are antithetic to the MF2b.

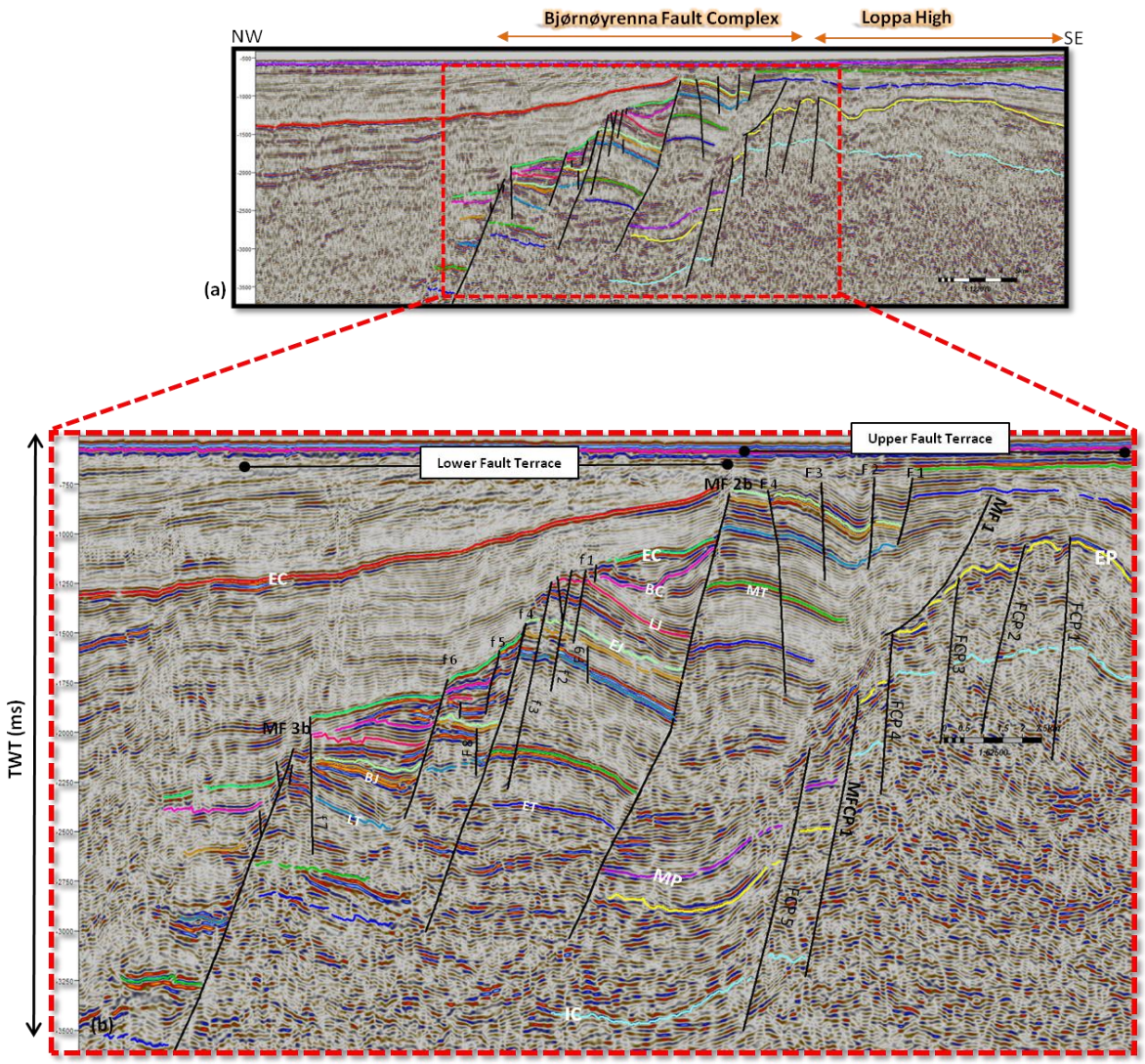


**Figure 3.17(a)**: Key Profile 7 along the fault segments MF1, MF2 & MF3. **(b)** Zoomed-in part of (a) shown by red square. See Figs. 3.8 & 3.9 for location of the line. EC: Early Cretaceous, BC: Base Cretaceous, LJ: Late Jurassic, EJ: Early Jurassic, BJ: Base Jurassic, LT: Late Triassic, MT: Mid Triassic, ET: Early Triassic, MP: Mid Permian, EP: Early Permian, IC: Intra Carboniferous.

## 3.5 Time structure (TWT) and Fault Maps

This section primarily focuses on illustrating the time-structure maps and the fault maps of the interpreted reflections. The changes in structural configuration of the fault segments along different features within the Bjørnøyrenna fault complex has been already described on the cross-sections in terms of key profiles (1-7). Intra-Triassic time-structural map and fault map have already been discussed above in order to prescribe the structural segmentation of the study area *(fig. 3.8 & 3.9).* This section predominantly, illustrates the time-structure and the fault map of intra-Permian, intra-Triassic, early Jurassic, base Cretaceous and early Cretaceous.

### 3.5.1 Intra Permian

The early Permian reflection is one of the two deepest reflections in the study area, interpreted across the Loppa High and the Bjørnøyrenna Fault Complex *(fig. 3.10 & 3.18)*. The time structure map of the early Permian reflection is generally characterized by westward deepening of the reflections as shown by the color variations from shallow to deep. The map shows a large vertical separation along MF1 and it can easily be observed by readily change in the color pattern from orange to green *(fig. 3.18)*. The deepest part is located in the southwestern corner of the study area shown by blue-purple color. Subsequently, the shallowest part of this reflection is situated towards the eastern part of the map indicated by least time values.

Fault map at the early Permian level is affected by two N-S trending master faults (MF1a & MFCP1) *(fig. 3.19)*. The behavior of the fault patterns at this level is quite different in contrast to other time intervals. Both interpreted master faults shows dip toward west *(fig. 3.19)*. Moreover, smaller normal faults have also been interpreted between these master faults which generally show dip toward west and are termed as synthetic to the master fault.

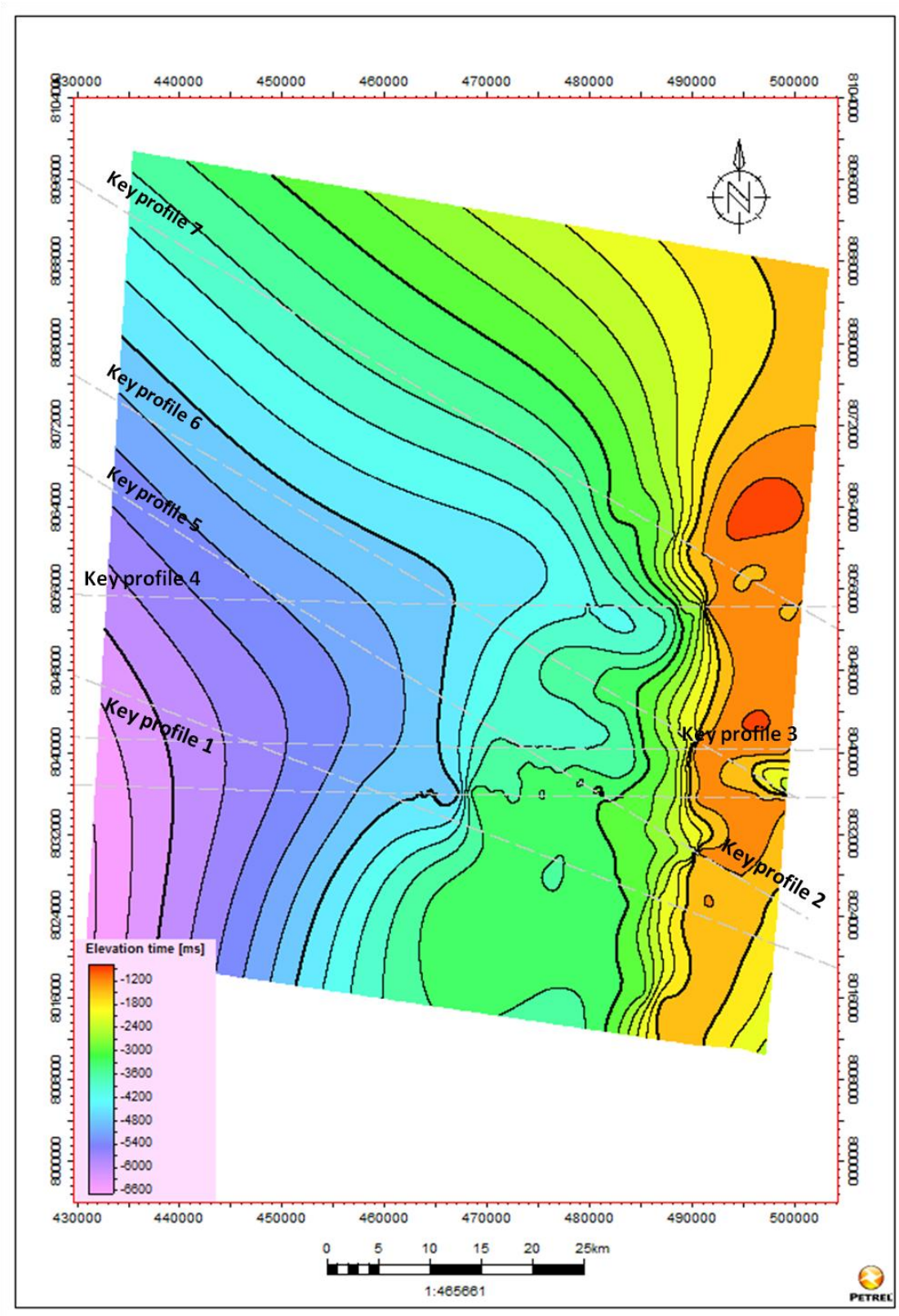


**Figure 3.18:** Time-structure map at the early Permian level. Location of the seismic lines already discussed as key profiles in the text.

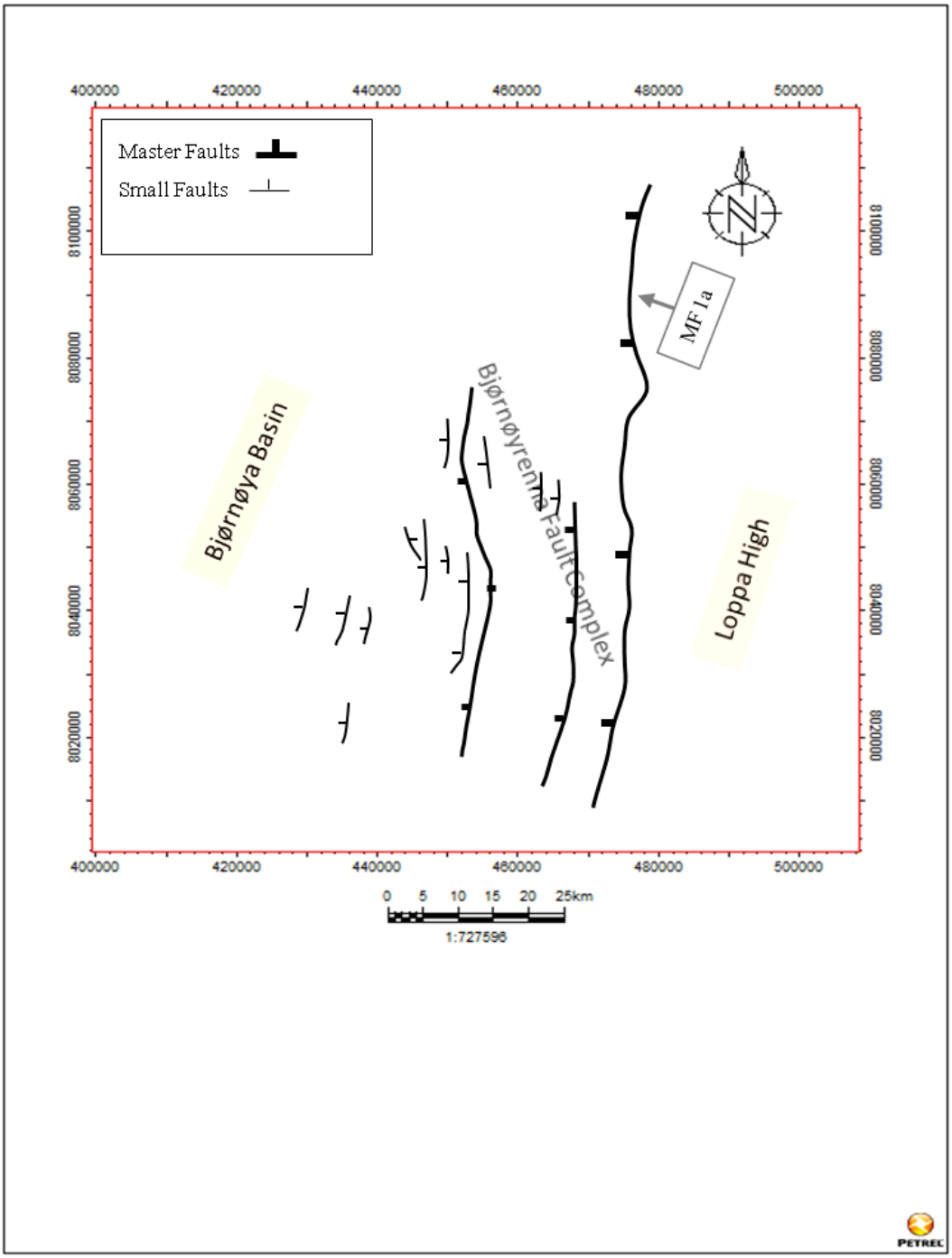


**Figure 3.19:** Fault map at the early Permian level showing the main structural segments of the Bjørnøyrenna Fautl Complex. Descriptions of the system for naming of the faults and the principles for identifying the main structural elements are described in the main text.

### 3.5.2 Base Jurassic

The base Jurassic reflection is only interpreted within the Bjørnøyrenna Fault Complex because of its disappearance at the Loppa High. Thus, the map shows those part of the study area where this stratigraphic succession is well preserved. The time structure map of base Jurassic reflection is characterized by the westward deepening of the reflection as illustrated by color variations *(fig. 3.20)*. The displacement pattern along master faults is not uniform and the greatest vertical separation is observed along MF-2 at base Jurassic level as interpreted on all the key profiles (1-7). The shape of array of master faults can be easily traced out on this time structure map as shown in *(fig. 3.20)*. The deepest part is located at the western corner of this map shown by light purple in color indicated by greatest time value. On the other hand, the shallowest part of this reflection is located at the southeast corner shown by least time values *(fig. 3.20)*.

The fault map at base Jurassic level is influenced by two main NE-SW trending master faults (MF-2 and MF-3). Thus each of the master faults is turn to be separate isolated segment termed as (MF-2a, Mf-2b and MF-3a, MF-3b, MF-3c) *(fig. 3.21)*. Although an overlapping relationship between MF2a and MF2b is observed and it seems to be hard-linked. Moreover, Small west-dipping normal faults are also interpreted between the fault segments MF-2a & MF-2b at key profiles 6, which bring both master faults in communication *(fig. 3.21)*. MF-2a shows its dip toward NW whereas; MF2b varies its dip from SW to NW. However MF-3 is throwing towards NW. A number of small normal faults also interpreted between these master faults which generally shows dip towards NW and W, are termed as synthetic with respect to master faults. The other set of small normal faults shows dip towards SE and E, are termed as antithetic with the reference of master faults *(fig. 3.21)*. The structure is more deformed at the footwall of the MF-2 by the synthetic and antithetic behavior of small normal faults particularly in structural segment 2.

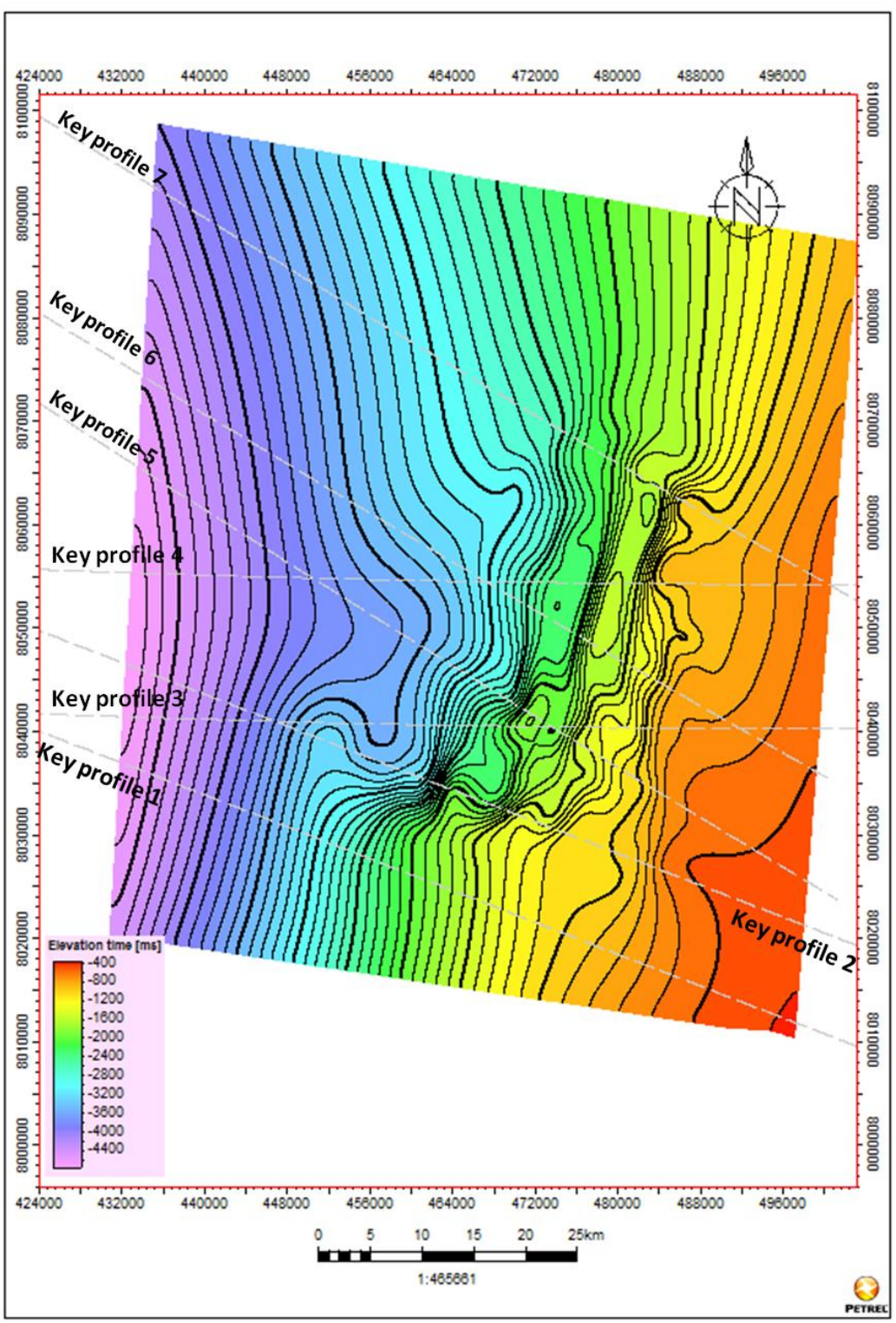


**Figure 3.20:** Time-structure map at the base Jurassic level. Location of the seismic lines already discussed as key profiles in the text.

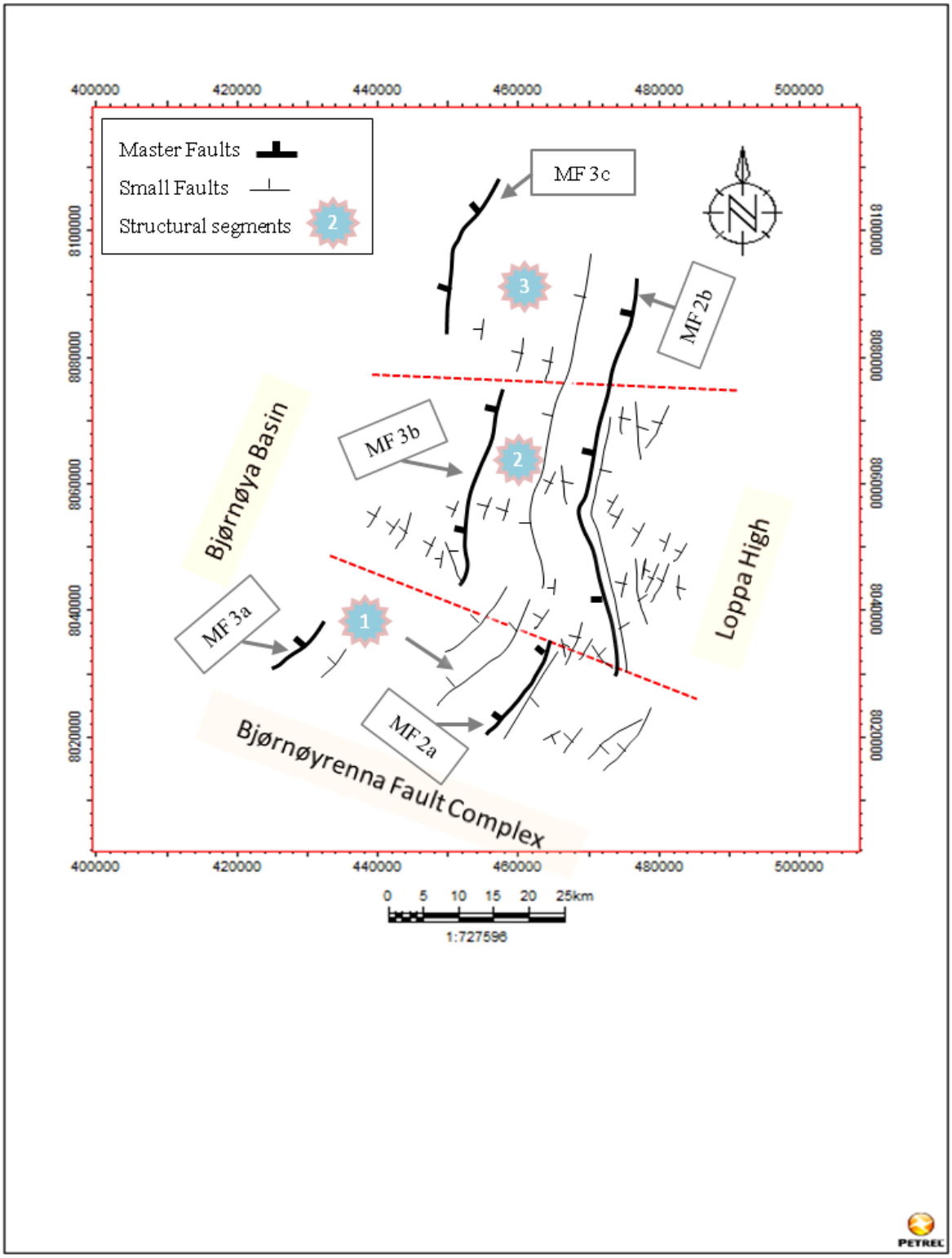


**Figure 3.21:** Fault map at the base Jurassic level showing the main structural segments of the Bjørnøyrenna Fautl Complex. Descriptions of the system for naming of the faults and the principles for identifying the main structural elements are described in the main text.

### 3.5.3 Early Jurassic

The early Jurassic reflection is only interpreted in the western part of the fault complex because stratigraphic succession is not present at the eastern corner of the fault complex and at the Loppa High due to extensive erosion or non deposition followed by uplifting. Thus, the map shows those parts of the study area where this stratigraphic succession is well preserved. The time structure map of the early Jurassic reflection is characterized by the westward deepening of the reflection as shown by color variation. The shallowest part is located at the eastern corner of the map shown by red color indicating less time values *(fig. 3.22)*. On the other hand, the deepest part is situated at the south-western part of the map shown by purple in color indicating greatest time values.

Generally, the structural elements in early Jurassic level are similar to the ones that observed at base Jurassic level *(fig. 3.21)*. The early Jurassic reflection is influenced by two main master faults (MF-2 and MF-3) trending NE-SW. The overlapping relationship between MF2a and MF2b is seems to be hard-linked *(fig. 3.23)*. Moreover, Small west-dipping normal faults are also interpreted between the fault segments MF-2a & MF-2b at key profiles 6, which bring both master faults in communication.

At early Jurassic level, the master faults, MF-2a shows dip toward NW whereas MF2b changes its dip from SW to NW *(fig. 3.23)*. However MF-3 is throwing towards NW in all three structural segments. A number of small normal faults are also interpreted between these master faults which generally shows dip towards NW and W, are termed as synthetic with respect to master faults. The other set of small normal faults shows dip towards SE and E, are termed as antithetic with the reference of master faults. The structure is more deformed at the footwall of the MF-2b by the synthetic and antithetic behavior of small normal faults particularly in structural segment 2 *(fig. 3.23)*. The main difference between this interval and base Jurassic interval is the presence of small normal faults at the footwall of MF2b in structural segment 3.

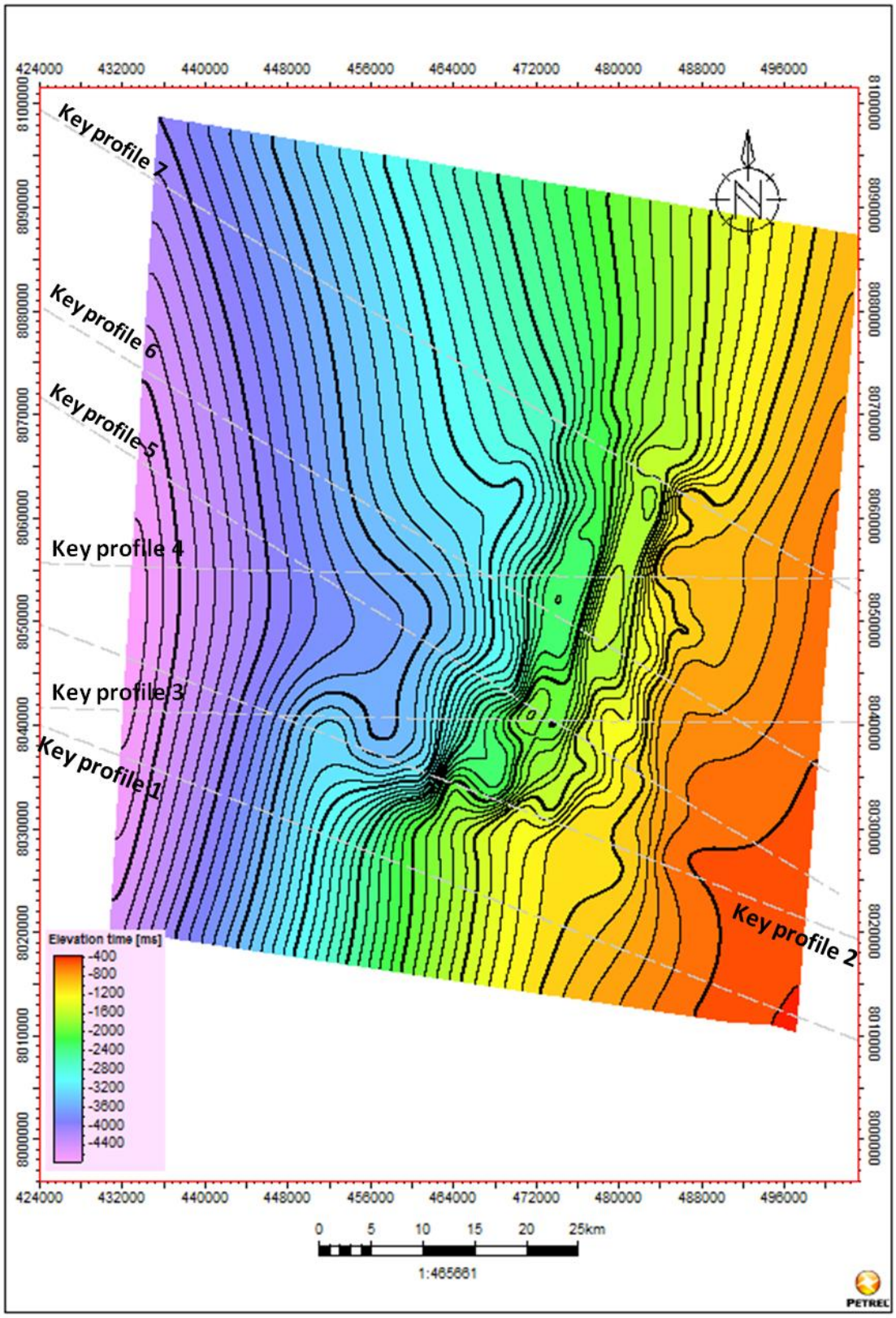


**Figure 3.22:** Time-structure map at the early Jurassic level. Location of the seismic lines already discussed as key profiles in the text.

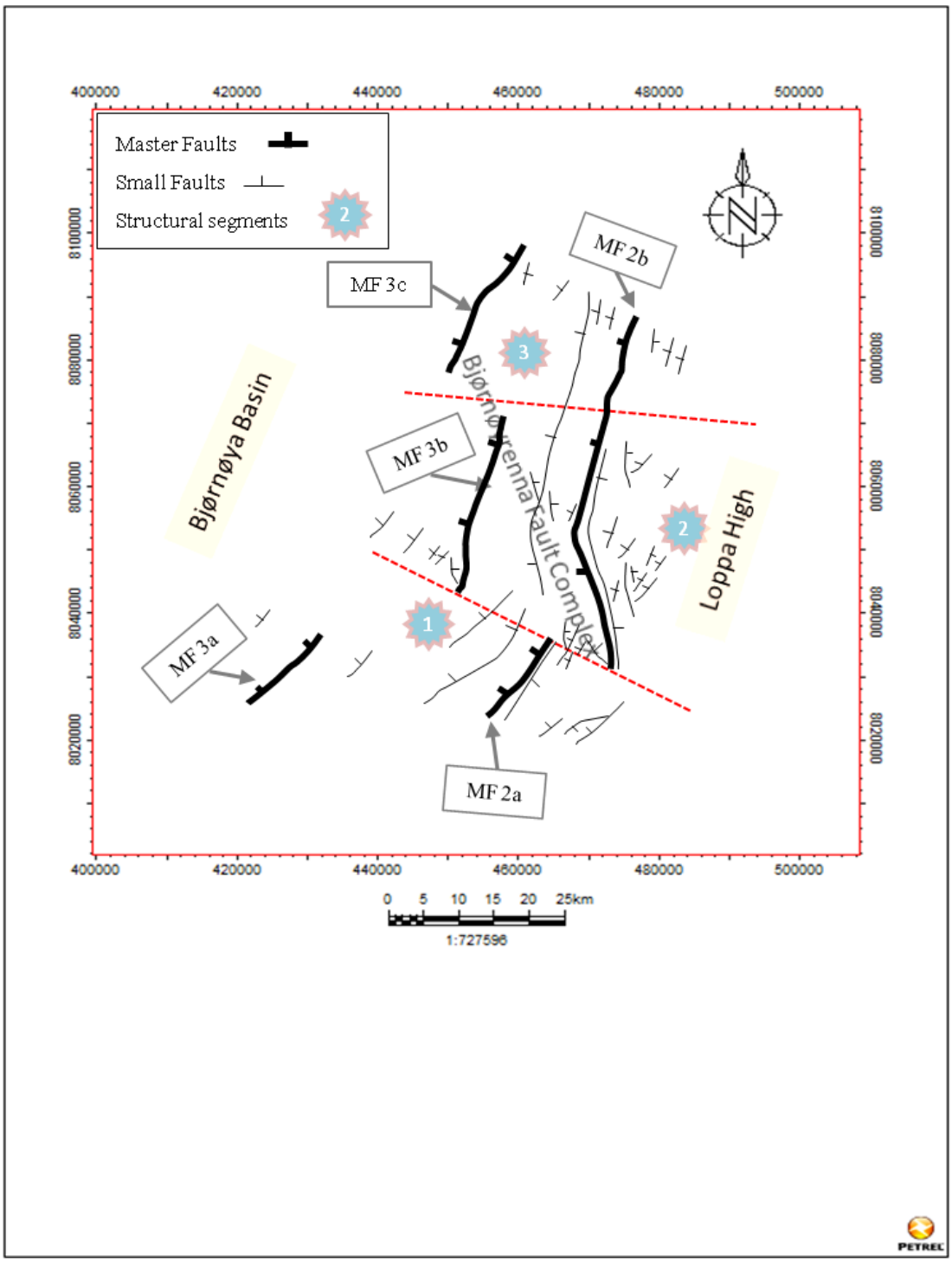


**Figure 3.23:** Fault map at the early Jurassic level showing the main structural segments of the Bjørnøyrenna Fault Complex. Descriptions of the system for naming of the faults and the principles for identifying the main structural elements are described in the main text.

### 3.5.4 Mid Jurassic

The upper mid Jurassic reflection is only interpreted within the Bjørnøyrenna Fault Complex, most particularly at the western part of the fault complex because this succession is not present at the eastern corner of the fault complex and at the Loppa High due to extensive erosion or non deposition followed by uplifting. Thus, the map shows those parts of the study area where this stratigraphic succession is well preserved. In general, the structural configuration in the mid Jurassic reflection remains similar to the ones observed in the early Jurassic *(fig. 3.23)*. The time structure map shows a general westward deepening of the upper mid Jurassic reflection as shown by color variation. However, the master faults can be easily seen on this time structure map as well. The shallowest most part is located at the north-eastern corner of the map shown by red color indicating less time values *(fig. 3.24)*. On the other hand, the deepest part is situated at the south-western corner of the map shown by light purple in color indicating greatest time values. Moreover, a half graben is observed towards the southwestern part of the map which is shown by maximum time values *(fig. 3.24)*.

The fault map at upper mid Jurassic level is characterized by the presence of two main master faults (MF-2 and MF-3) trending NE-SW. Thus, each of the master fault is turn to be separate isolated segment termed as (MF-2a, Mf-2b and MF-3a, MF-3b, MF-3c) *(fig. 3.25)*. Although, the overlapping relationship between MF2a and MF2b is seems to be hard-linked. Moreover, Small west-dipping normal faults are also interpreted between the fault segments MF-2a & MF-2b at key profiles 6, which bring both master faults in communication. In this reflection, MF-2a is dipping toward NW whereas MF2b changes its dip from SW to NW *(fig. 3.25)*. However MF-3 shows towards NW in the study area. A number of small normal faults also interpreted between these master faults which generally shows dip towards NW and W, are termed as synthetic with respect to master faults. The other set of small normal faults shows dip towards SE and E, are termed as antithetic with the reference of master faults. The structure is more deformed at the footwall of the MF-2b by the synthetic and antithetic behavior of small normal faults particularly in structural segment 2 *(fig. 3.25)*.

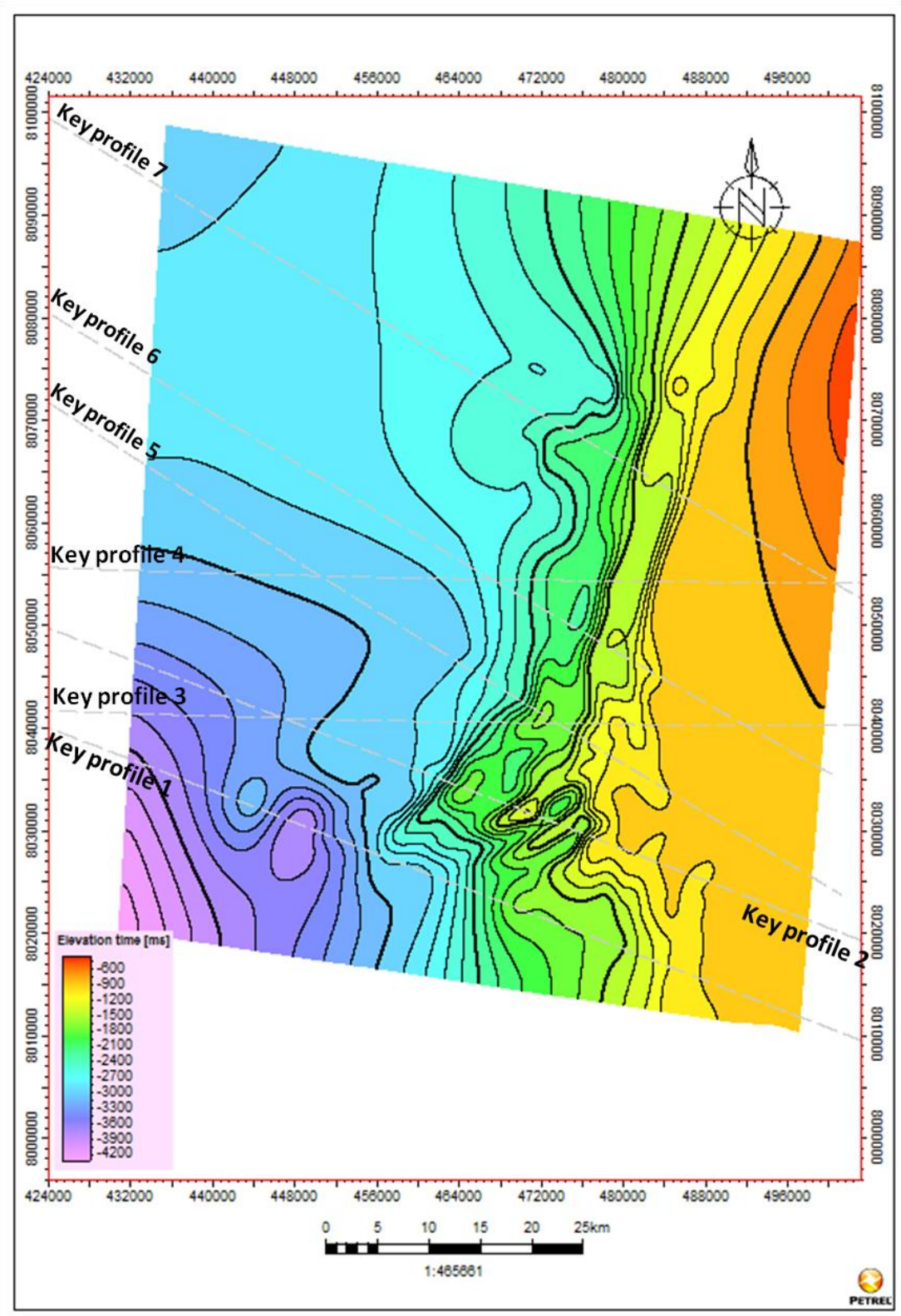


**Figure 3.24:** Time-structure map at the upper mid Jurassic level. Location of the seismic lines already discussed as key profiles in the text.

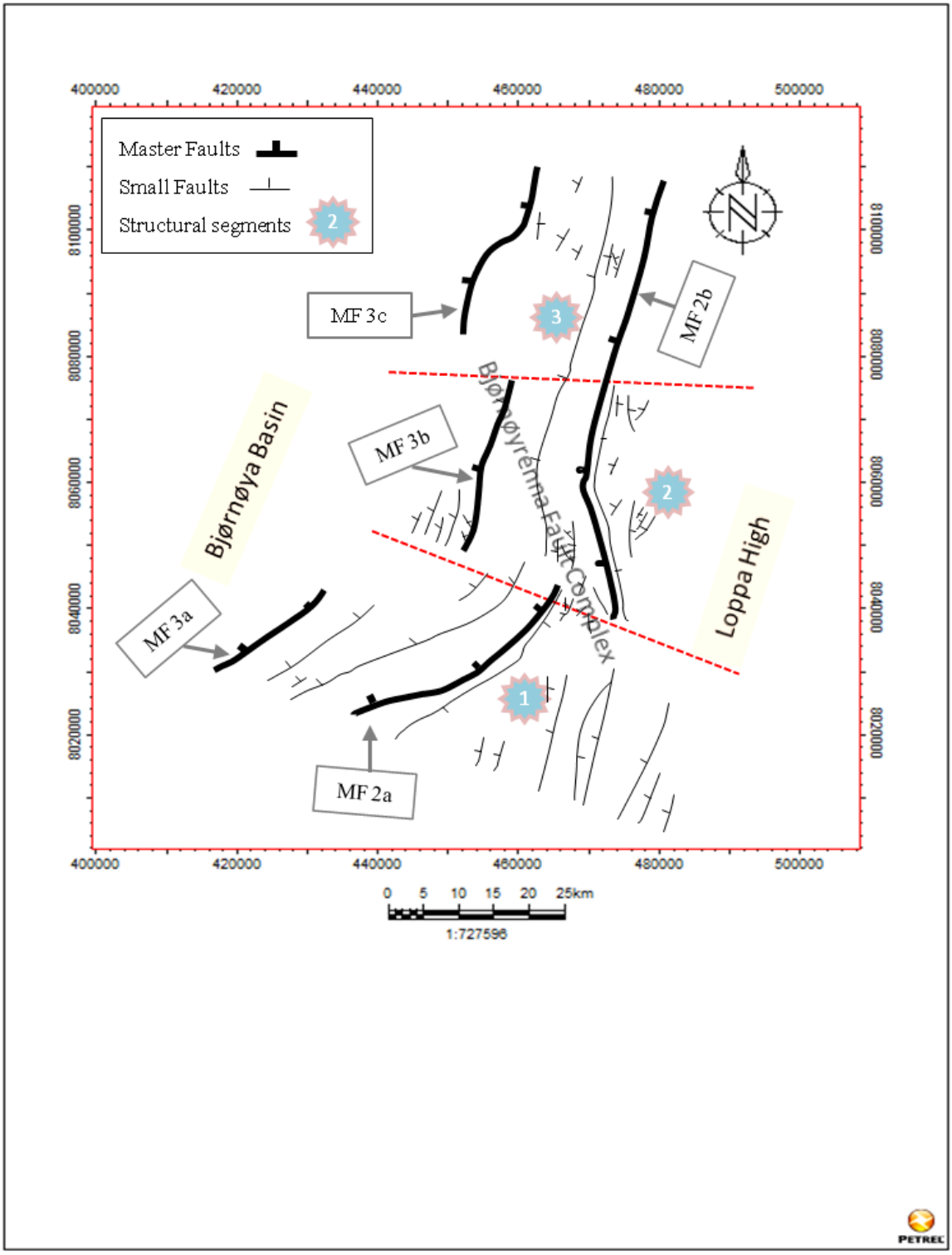


**Figure 3.25:** Fault map at the upper mid Jurassic level showing the main structural segments of the Bjørnøyrenna Fault Complex. Descriptions of the system for naming of the faults and the principles for identifying the main structural elements are described in the main text.

### 3.5.5 Base Cretaceous

The base Cretaceous reflection is only interpreted within the Bjørnøyrenna Fault Complex, most particularly at the western part (lower fault terrace) of the fault complex because this succession is not present at the eastern corner of the fault complex and at the Loppa High due to extensive erosion or non deposition followed by uplifting. Thus, the map shows those parts of the study area where this stratigraphic succession is well preserved. The time structure map shows a general westward deepening of the base Cretaceous reflection as shown by color variation from shallow to deep *(fig. 3.26)*. The shallowest most part is located at the eastern corner of the map termed as the Loppa High and shown by red color indicating less time values *(fig. 3.26)*. On the other hand, the deepest part is situated at the North-western corner of the map shown by light purple in color indicating greatest time values. In addition, a half graben is observed towards the basin in the southwestern quadrant of the map which is shown by maximum time values *(fig. 3.26)*.

The fault map at this level is characterized by decrease in the intensity of faulting and it also exhibit the presence of syn-sedimentary strata over this reflection already discussed in the key profiles (1-7). Furthermore, this reflection is influenced by two main master faults (MF-2 and MF-3) trending NE-SW. Thus, each of the master faults is turn to be separate isolated segments termed as (MF-2a, Mf-2b and MF-3a, MF-3b, MF-3c) *(fig. 3.27)*. Although, the overlapping relationship between MF2a and MF2b is seems to be hard-linked. Moreover, Small west-dipping normal faults are also interpreted between the fault segments MF-2a & MF-2b at key profiles 6, which bring both master faults in communication. In this reflection, MF-2a is dipping toward NW whereas MF2b changes its dip from SW to NW. However MF-3 shows towards NW in the study area *(fig. 3.26)*. A number of small normal faults also interpreted between these master faults which generally shows dip towards NW and W, are termed as synthetic with respect to master faults. The other set of small normal faults shows dip towards SE and E, are termed as antithetic with the reference of master faults.

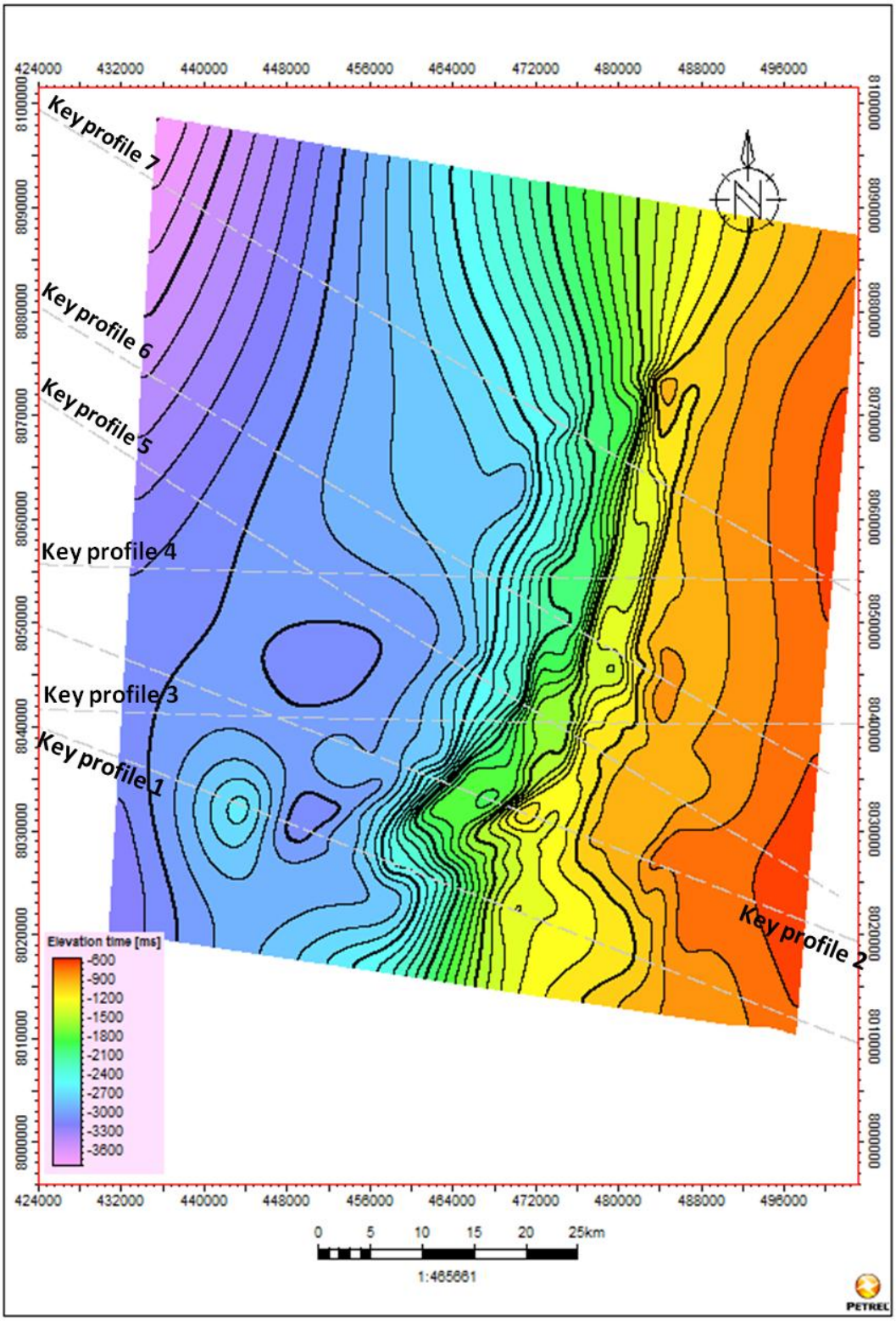


**Figure 3.26:** Time-structure map at the base Cretaceous level. Location of the seismic lines already discussed as key profiles in the text.

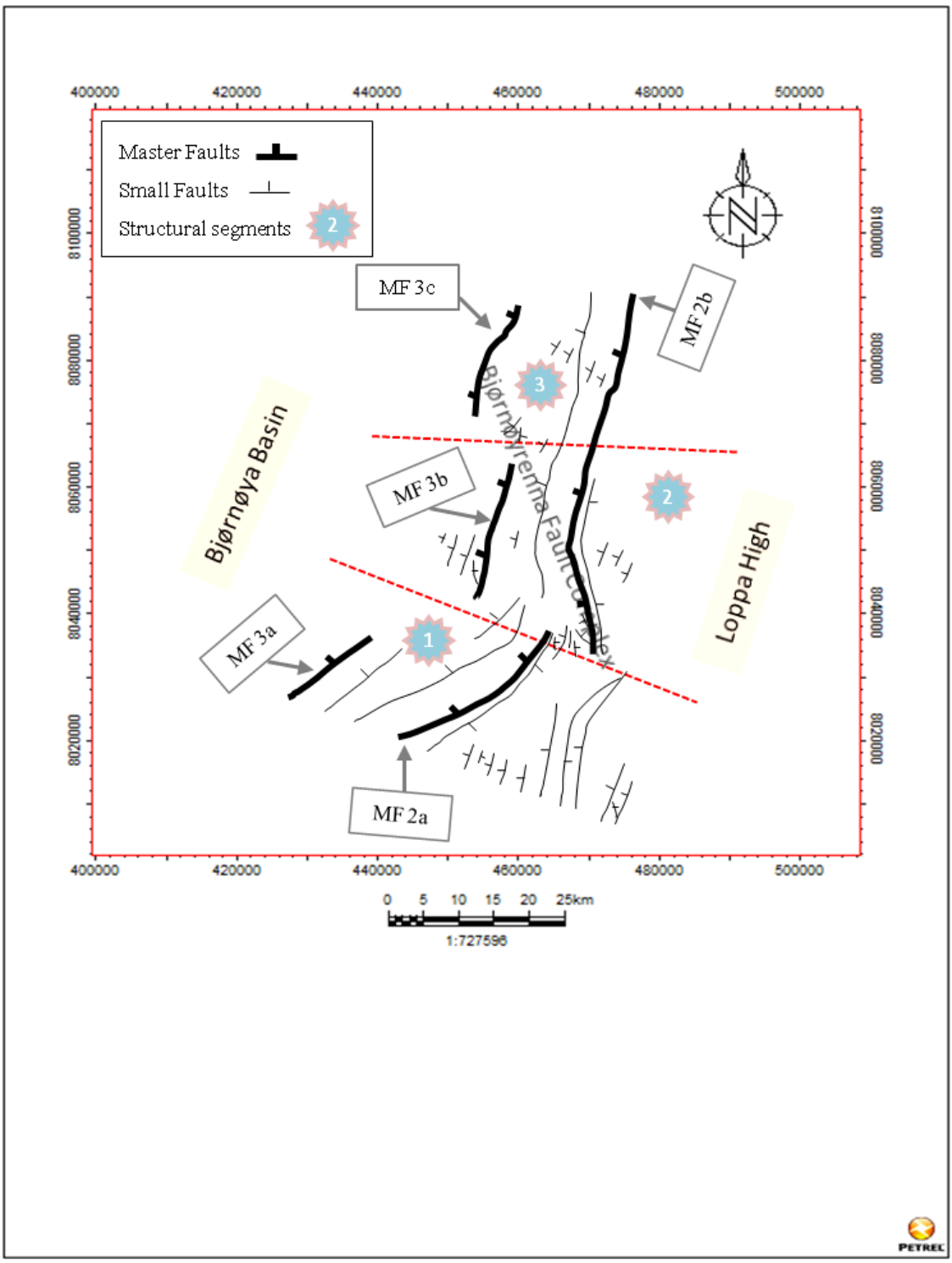


**Figure 3.27:** Fault map at the base Cretaceous level showing the main structural segments of the Bjørnøyrenna Fault Complex. Descriptions of the system for naming of the faults and the principles for identifying the main structural elements are described in the main text.

### 3.5.6 Early Cretaceous

The early Cretaceous reflection is also interpreted within the Bjørnøyrenna Fault Complex, most particularly at the western part (lower fault terrace) of the fault complex because of the absence in the eastern part and at the Loppa High which suggests an episode of extensive erosion or non deposition followed by uplifting at this time. Thus, the map shows those parts of the study area where this stratigraphic succession is well preserved. The time structure map at early Cretaceous level shows general deepening toward west as indicated by color variation from shallow to deep. The deepest part is located at the North-western corner of the map shown by light purple in color indicating maximum time values *(fig. 3.28)*.

The fault map at this level marked sudden decrease in the intensity of faulting as compare to the maps at the base Cretaceous and the upper mid Jurassic level *(fig. 3.25 & 3.27)*. The early cretaceous is the top most reflection interpreted in lower fault terrace and represents a sedimentary wedge between base cretaceous and the early cretaceous as prescribed in key profiles (1-7). It can recognize that wedge shaped geometry has been interpreted throughout the study area form south to North. Furthermore, this reflection is also influenced by two main master faults (MF-2 and MF-3) trending NE-SW *(fig. 3.29)*. Thus, each of these master faults turn to be separate isolated segments termed as (MF-2a, Mf-2b and MF-3a, MF-3b, MF-3c) *(fig. 3.29)*. Although, the overlapping relationship between MF2a and MF2b is seems to be hard-linked. Moreover, Small west-dipping normal faults are also interpreted between the fault segments MF-2a & MF-2b at key profiles 6, which bring both master faults in communication. In this reflection, MF-2a is dipping toward NW whereas MF2b changes its dip from SW to NW *(fig. 3.29)*. However MF-3 shows towards NW in the study area. A number of small normal faults also interpreted between these master faults which generally shows dip towards NW and W, are termed as synthetic with respect to master faults. The other set of small normal faults shows dip towards SE and E, are termed as antithetic with the reference of master faults *(fig. 3.29)*.

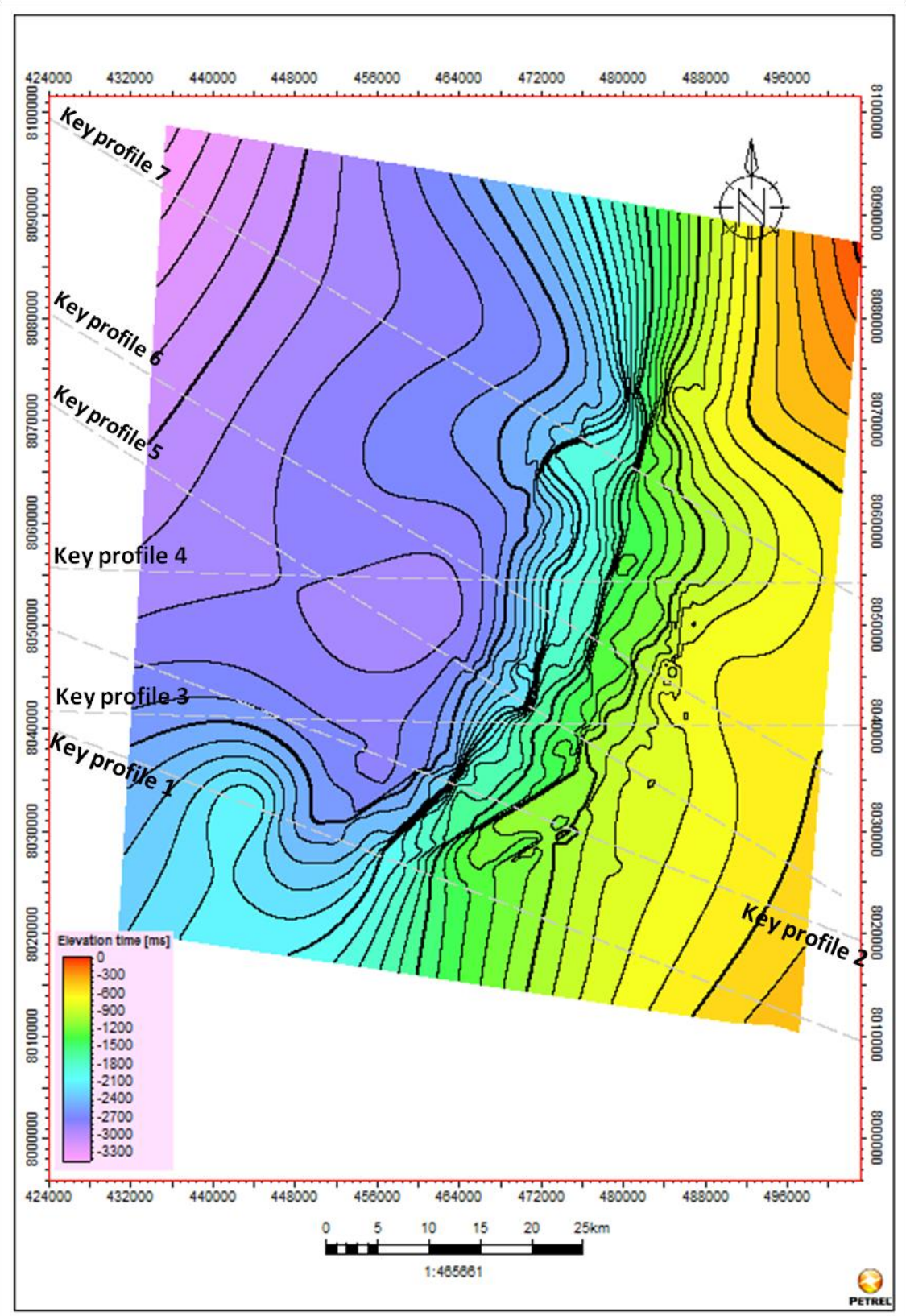


**Figure 3.28:** Time-structure map at the base Cretaceous level. Location of the seismic lines already discussed as key profiles in the text.

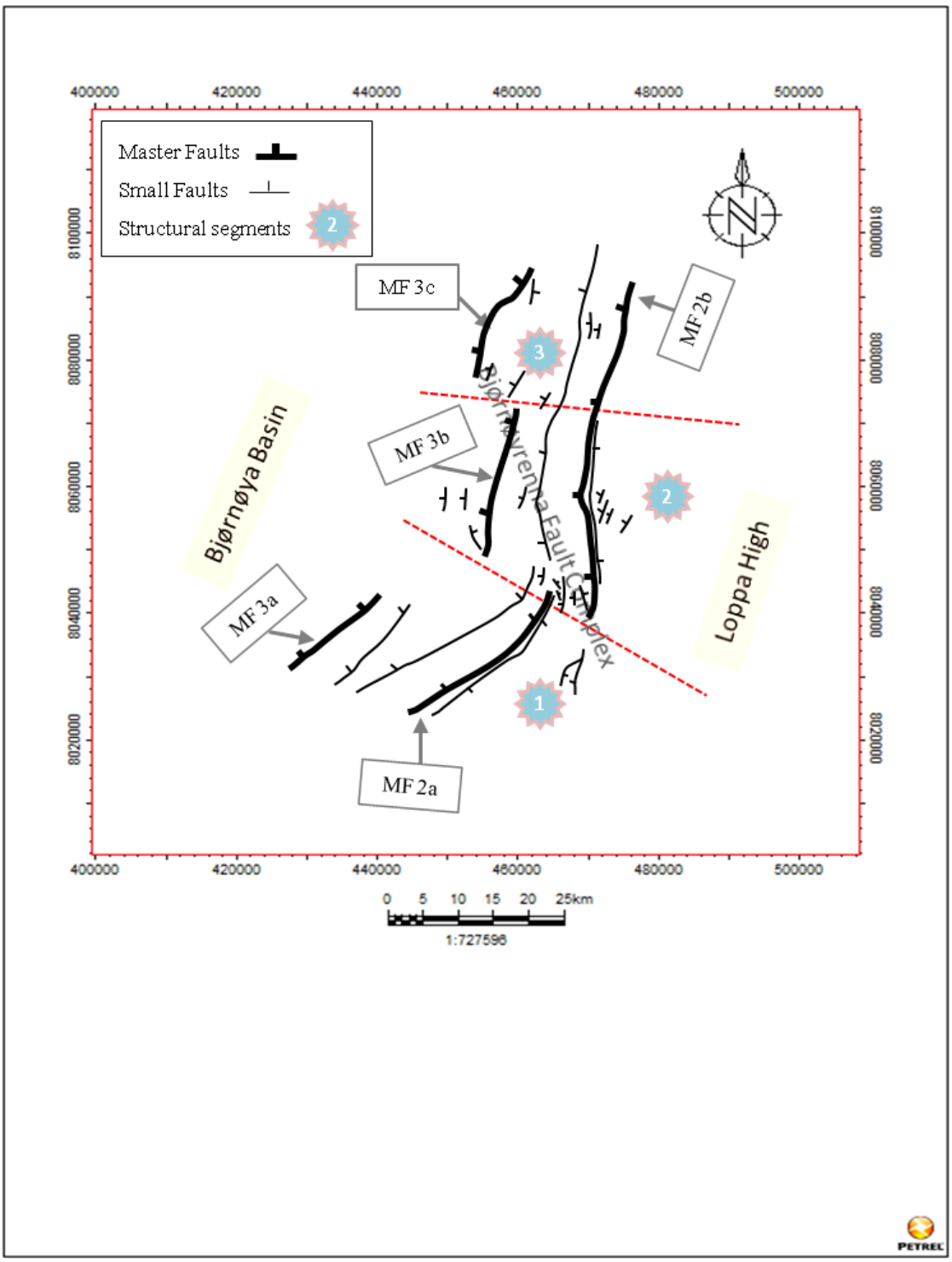


**Figure 3.29:** Fault map at early Cretaceous level showing the main structural segments of the Bjørnøyrenna Fault Complex. Descriptions of the system for naming of the faults and the principles for identifying the main structural elements are described in the main text.

## 3.6 Time thickness maps

The time thickness map (TWT) has been generated at several levels between interpreted reflections, in order to investigate the thickness variation along the master faults (MF1, MF2 and MF3).

### 3.6.1 Intra Triassic-Intra Permian

The time thickness map is constructed between the intra Triassic - intra Permian level across the Loppa High and within the Bjørnøyrenna Fault Complex. The intra Triassic is the only one reflection that is well preserved both at the Loppa High and within fault complex due to the appearance of strong lateral variation in thickness across the main boundary faults (MF1, MF2 and MF3) *(fig. 3.10*). Main boundary fault MF1 can be easily traced out at this level which distinguishes the Loppa High from the fault complex. Generally the thickness between this interval increased toward the south of the study area *(fig. 3.30)*. A remarkable thickness is observed at the hanging wall of MF1 which is shown by yellow in color while the thickness is gradually reduced towards MF2 as interpreted on key profiles (1-7) as well *(fig. 3.30)*. On the other hand, maximum value of thickness is recorded between both intervals toward the north of this map at key profile 3 & 6 as shown by red color *(fig. 3.30)*. Moreover, thickness is significantly reduced at the eastern and western part of this map as indicated by least time values.

### 3.6.2 Early Jurassic to Base Jurassic

The time thickness map between the early Jurassic and the base Jurassic is constructed only within fault complex because of disappearance of both the reflections towards the Loppa High. The map shows lateral variation in thickness across the main boundary faults (MF2 and MF3). Generally the thickness increases towards the North and NW corner of this map *(fig. 3.31)*. Both interpreted reflections show homogeneity in terms of thickness within fault complex while it diminished toward the Loppa High. The thickness variation along the MF2 is same throughout the study area as interpreted on the entire key profiles (1-7). On the other hand, the thickness variations along the MF 3 remain same but relatively increase in thickness has been observed at key profile 2 *(fig. 3.12)*.

### 3.6.3 Mid Jurassic to Early Jurassic

The time thickness map is only generated within fault complex due to disappearance around the vicinity of the Loppa High. Generally the thickness between these successions increased toward west while it reduced toward the North and SE of this map *(fig. 3.32)*. The thickness pattern along the master faults (MF2 and MF3) is also not uniform. The thickness variation along MF2 is relatively same throughout the study area. But some abnormalities have been observed at key profile 3 & 4 *(fig. 3.13 & 3.14)*, which is signifying pinch out character between both interval towards MF3.

### 3.6.4 Base Cretaceous to Mid Jurassic

The time thickness map generally shows lateral variations across the master faults. Generally the thickness of this map increased toward the South and attains maximum values at the SW corner while thickness reduced toward the north of this map *(fig. 3.33)*. Comparatively, this map is different from other thickness maps because a remarkable thickness is recorded between both intervals across the master faults (MF2 & MF3) at key profiles 1 & 2 *(fig. 3.11 & 3.12)*.

### 3.6.5 Early Cretaceous to Base Cretaceous

The time thickness map of this interval shows remarkable variations across the master faults (MF2 & MF3). The fault segments can be easily traced out on this map as well. Both reflections are only interpreted at the western part of the fault complex because of the absence of this interval toward the western part of the fault complex. Generally the thickness between both intervals increased toward NE and SW corner of this map *(fig. 3.34)*. The centre part of this map indicates homogeneity in thickness. In addition, Syn-rift sedimentary sedimentation has been interpreted between both intervals as marked on the entire key profiles (1-7).

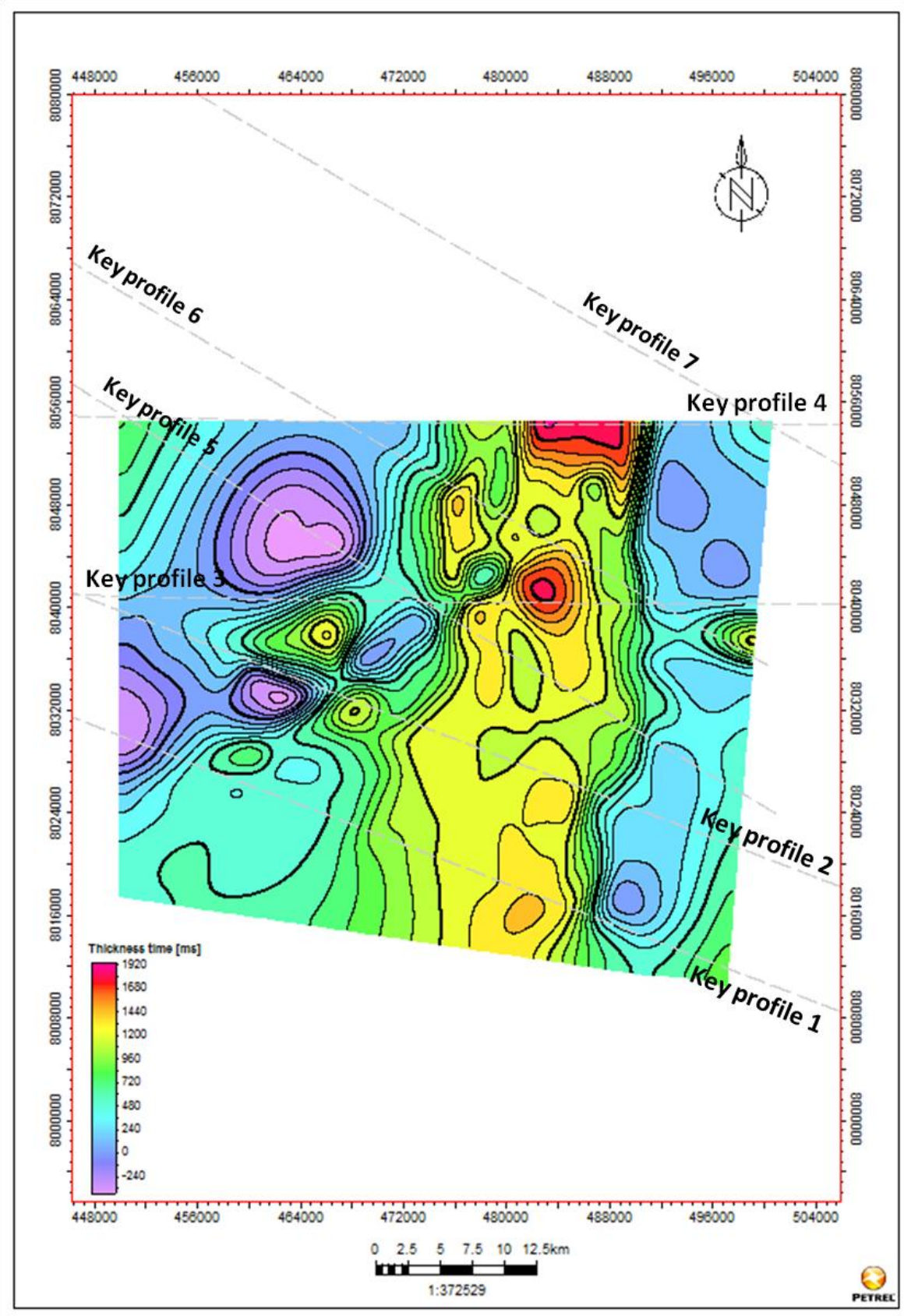


**Figure 3.30:** Time thickness map between the interpreted Intra Triassic-Intra Permian reflections.

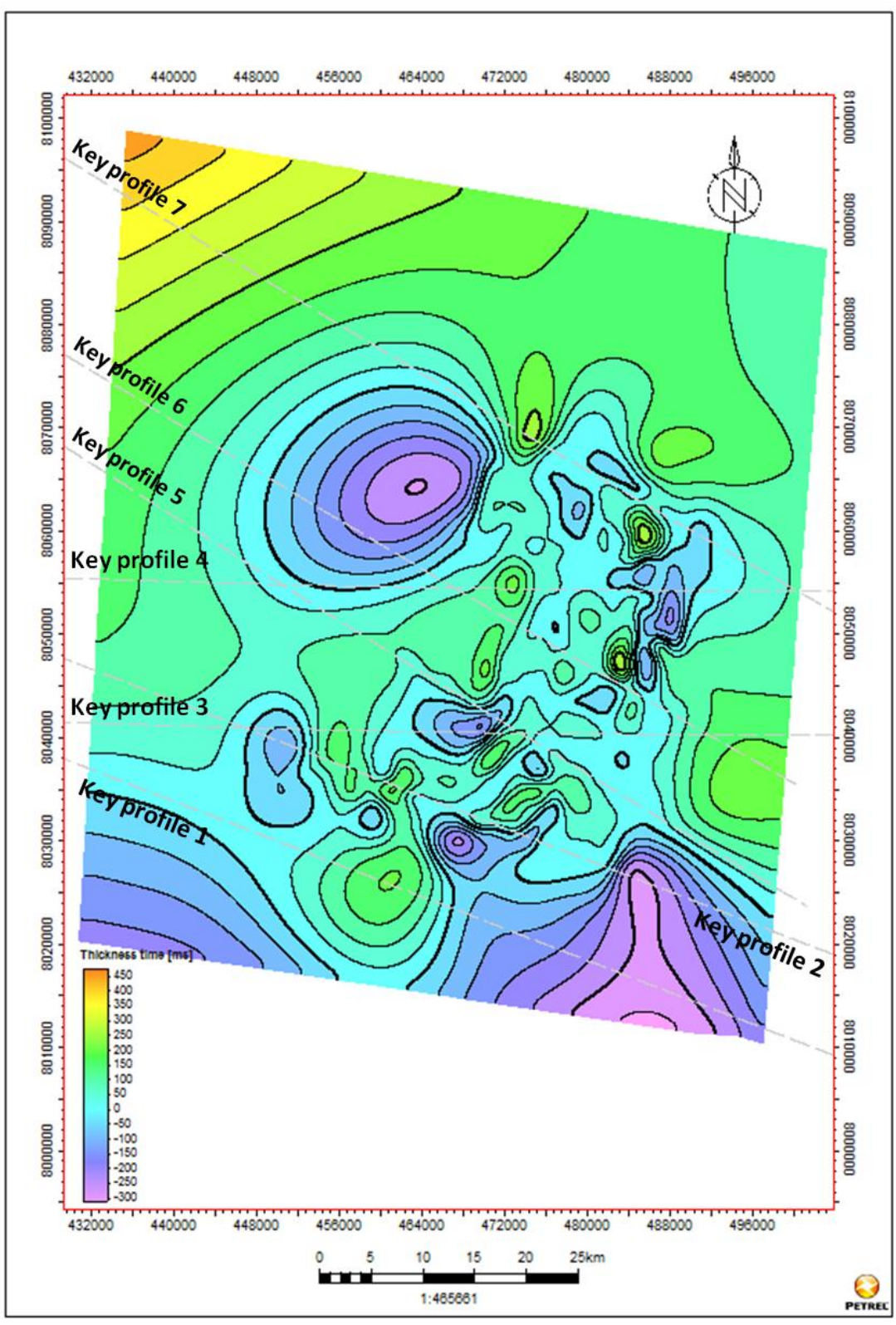


**Figure 3.31:** Time thickness map between the interpreted early Jurassic to the base Jurassic reflection.

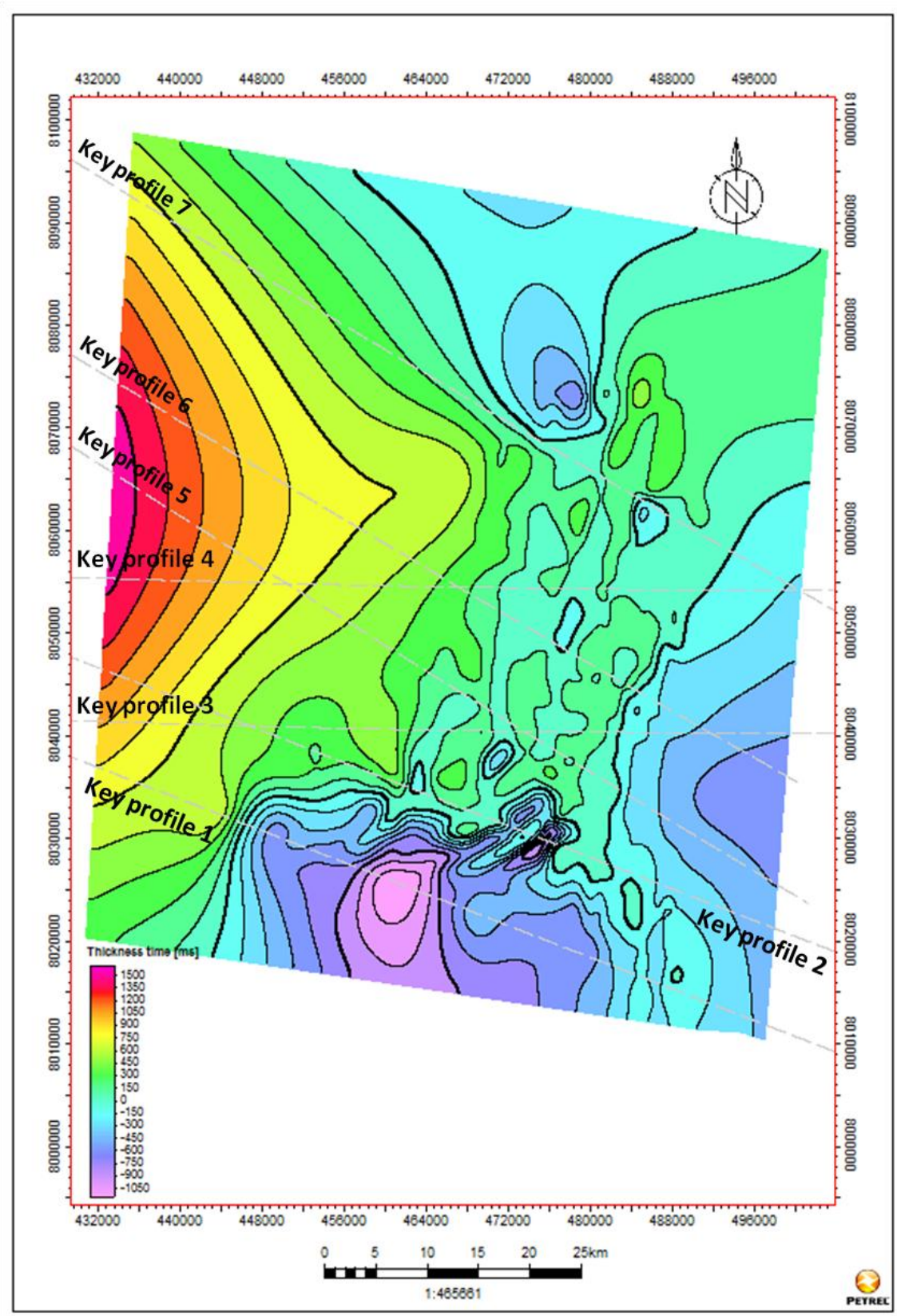


**Figure 3.32**: Time thickness map between the interpreted mid Jurassic to the early Jurassic reflection.

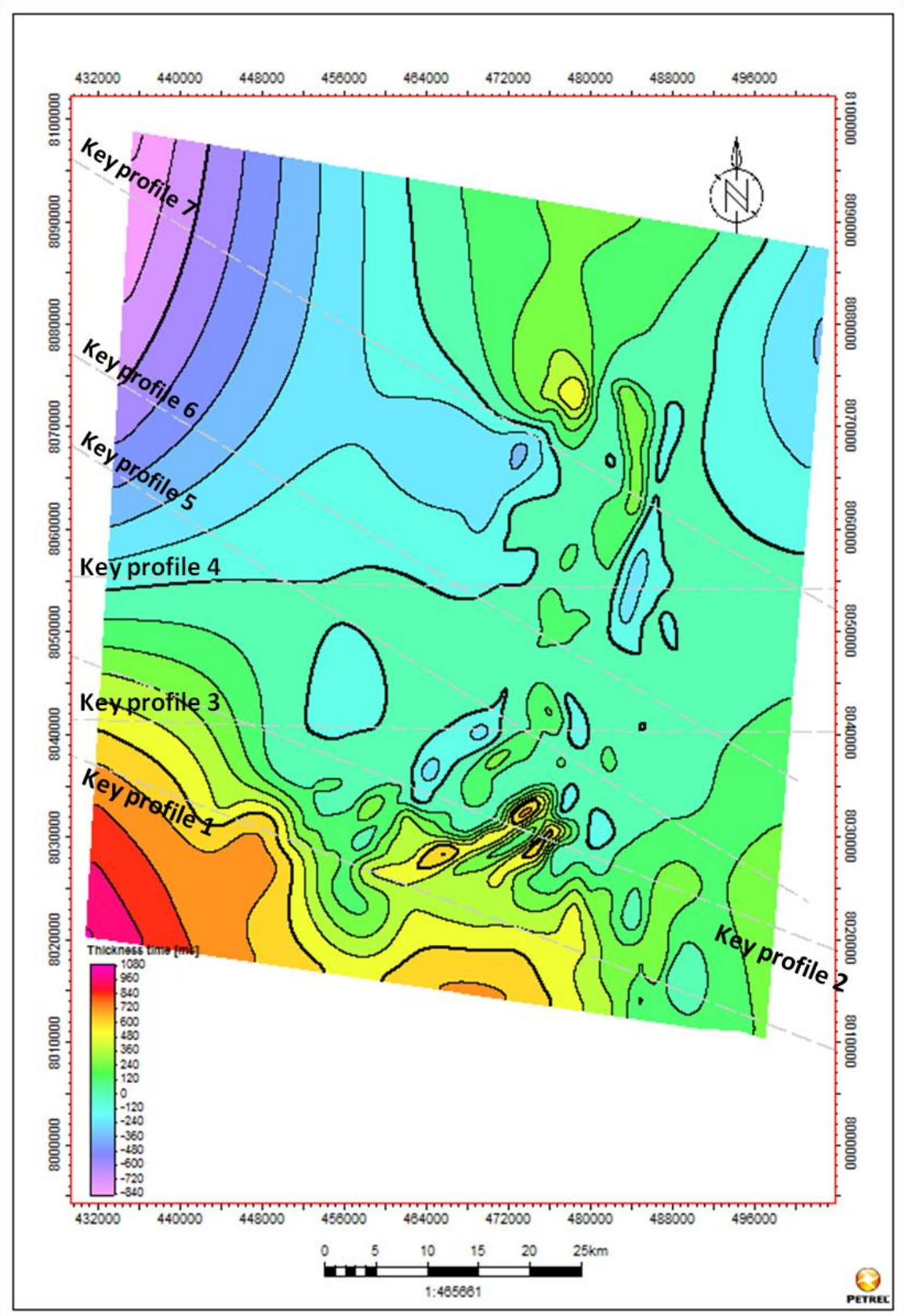


**Figure 3.33:** Time thickness map between the interpreted base Cretaceous to the mid Jurassic reflection.

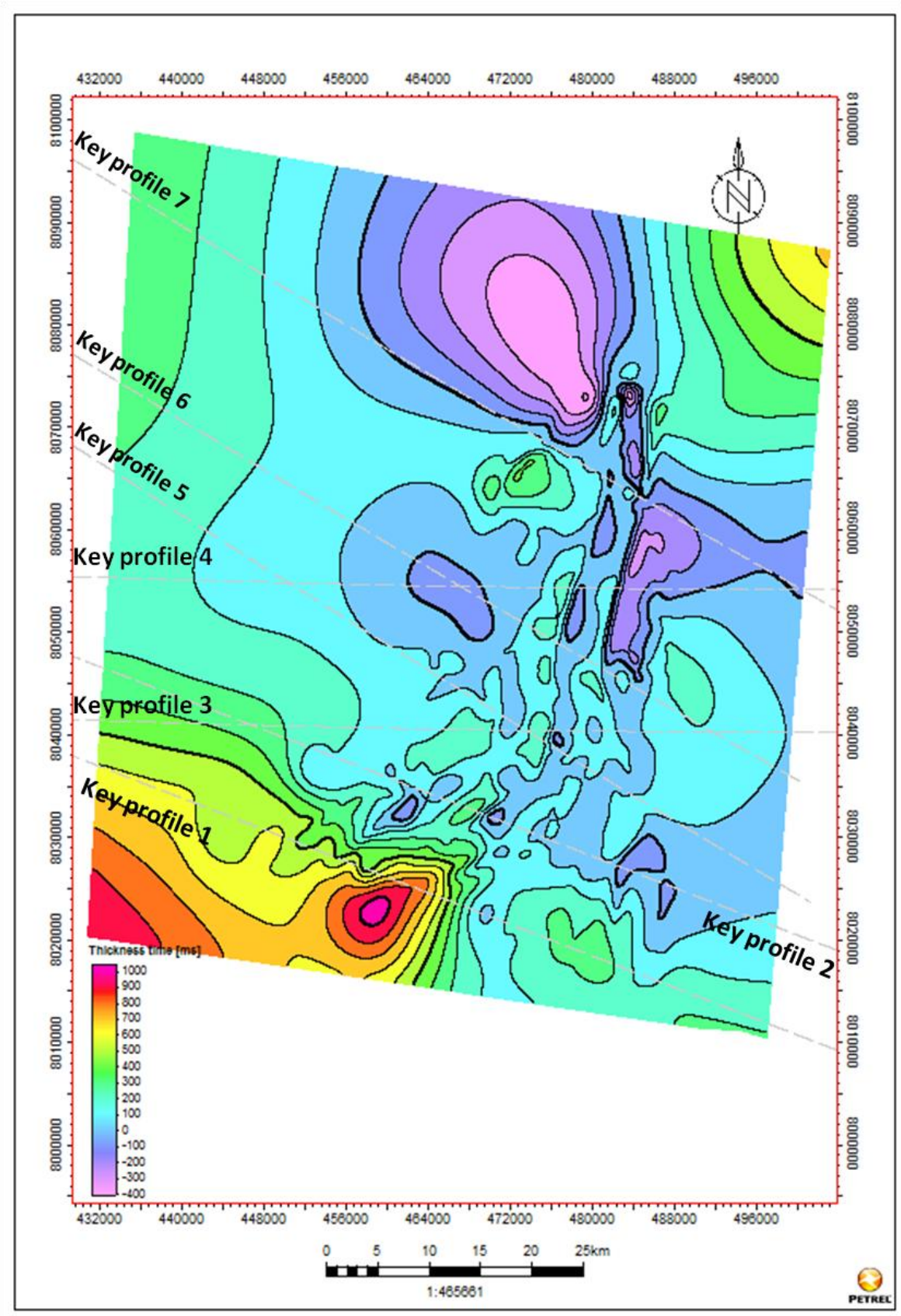


**Figure 3.34:** Time thickness map between the interpreted **e**arly Cretaceous to the base Cretaceous reflections.

# CHAPTER 4

# DISCUSSION

This chapter is mainly related to stage 3 of the study in which detailed structural investigation of the Bjørnøyrenna Fault Complex has been carried out on the basis of data described in the previous chapters. The main topics of discussion are (1) fault classification (2) fault geometry (3) fault Dating (4) detachments (5) structural inversion and (6) geological evolution of the Bjørnøyrenna Fault Complex.

## 4.1 Fault Classification

The Bjørnøyrenna Fault complex comprised of three main master faults (MF1, MF2 & MF3) and further characterized by different segments on the basis of strike (MF-1a, MF-1b; MF-2a, Mf-2b and MF-3a, MF-3b, MF-3c) in the study area. These segments are demonstrating linked fault system *(fig 4.2)*. The segment linkage is an important mechanism for the fault growth (Peacock, 191; Peacock and sanderson, 1991; Cartwright et al., 1995; Willemse et al., 1996; Kim et al., 2000, 2001b; Wilkins and Gross, 2002). Generally linked fault segments can be classified by three main stages as mentioned below (Y.-S. Kim & D.J. Sanderson 2005).

a) Isolated or unlinked faults **(Stage 1)**:

They propogate each other but evolve without obvious connection.

b) Hard-Linked faults **(Stage 2)**:

The fault surfaces are linked on the scale of map or cross sestion.

c) Soft-linked faults **(Stage 3)**:

Mechanical and geometric persistence is attained by ductile strain of the rock volume between fault segments.

A linked fault system is one of the most important elements of upper-crustal deformation. It is prescribed as a bunch of branching faults over contemporaneous level which linked through a length scale much larger than individual fault segments *(fig. 4.1)* (Davison, 1994). Linked faults are really branchout rather than cross-cut each other (Davison, 1994). Its mainly divided into two types:

1. Conjugate
    a. Convergent
    b. Divergent
2. Synthetic

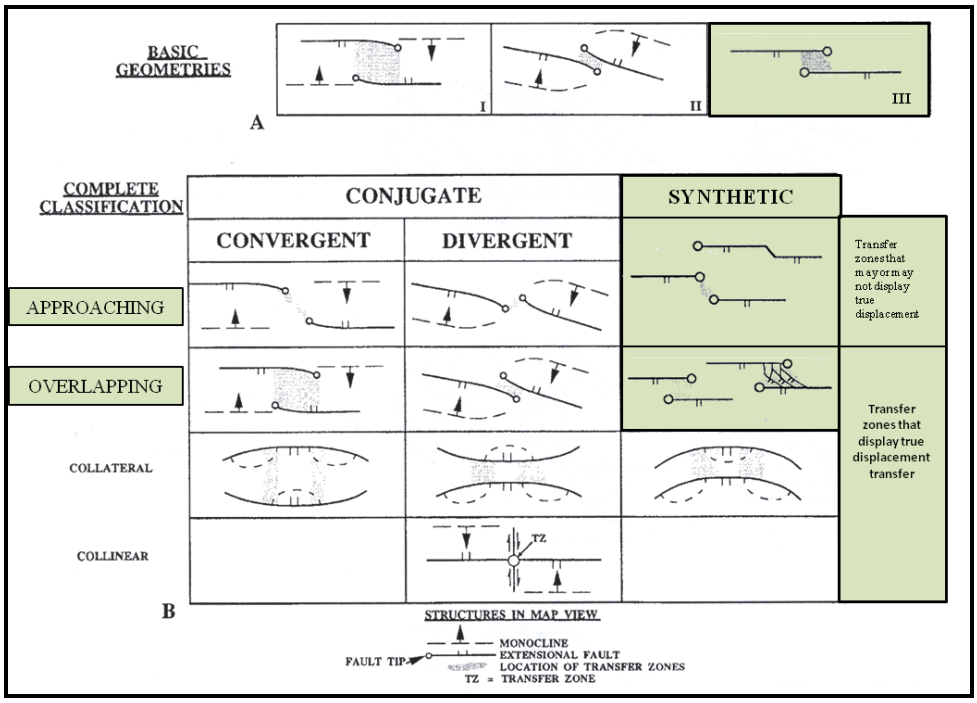


**Table 4.1:** Classification of transfer zones between the unlinked and linked faults following Morley et al., (1990) (modified from Davison, 1996). Following this classification, the linkage between master fault segments of the Bjørnøyrenna Fault Complex is termed as "Approaching & Overlapping-Synthetic Fault Segments".

On the basis of transfer zone geometry, these both types are further categorized into: Approaching, Overlapping, Collinear, Collateral (*table 4.1*) (Davison, 1994). Consequently, hard-linked fault segment (MF2a & MF2b) is indicated by synthetic overlapping transfer zone whereas two soft-linked fault segment (MF1a & MF1b) demonstrating synthetic approaching transfer zone *(fig. 4.1).*

The linkages between faults are established by spatial growth and connection between individual fault segments. Therefore, the overlapping relationship has been noticed between each of these master faults (MF 1 & MF 2)*(fig. 4.1).* The connection between MF-1a & MF-1b is soft-linked whereas MF 2a & MF 2b are dominated by hard-linking (*fig 4.1*). On the other hand, linkages between MF 3a, MF 3b and MF 3c cannot be both linked and unlinked.

Furthermore, small synthetic and antithetic faults are identified between these master fault branches and these are apparently unlinked *(fig 4.1)*.

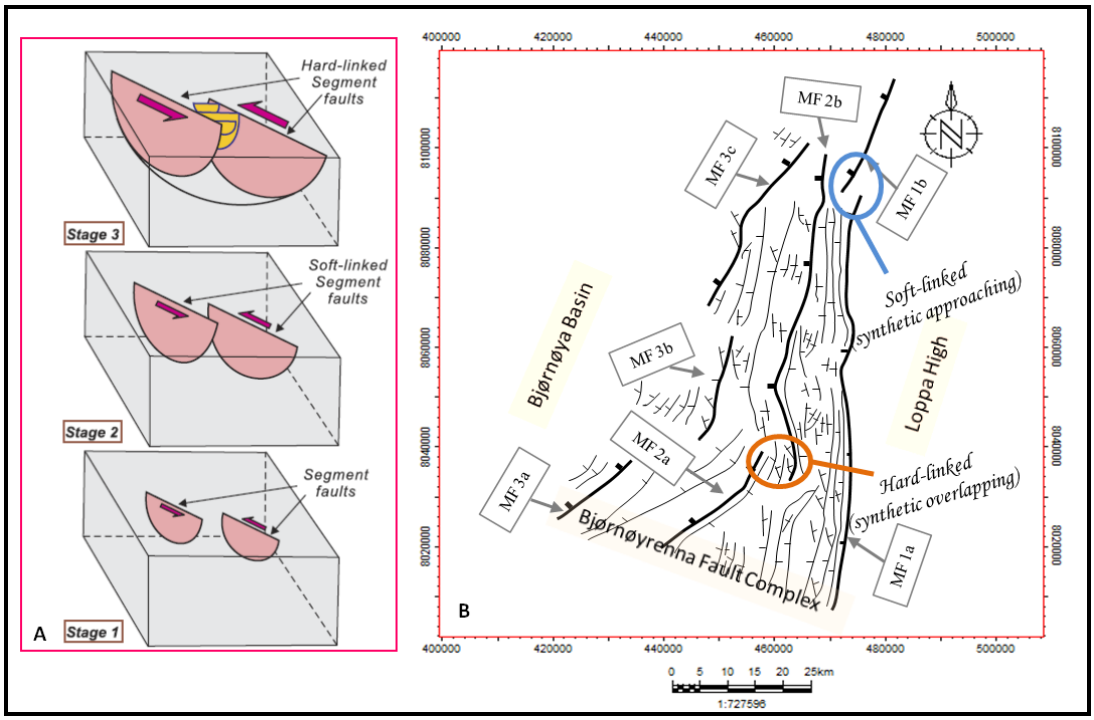


**Figure 4.1:** Faults segmentation and linkages. (A) Faults evolve from isolated faults to interacting faults through linkage (modified from Kim, Y.-S., Sanderson, D.J., 2004). (B) Fault map at intra Triassic level demonstrating linkages between fault segments with different colored circles. Orange: Hard-linked segment, Blue: soft-linked.

In a cross-sectional view, the extensional fault geometries exhibits two main styles: (1) Domino faults which is indicated by planar fault geometries along rotated bedding planes *(Wenricke & Burchfiel 1982, Davison 1989)*; (2) linked listric faults commonly shallow out in a detachment horizon along a weak horizon mainly shale or salt (*Davison 1989*).

Gabrielsen, (1984), classified the faults into three main classes on the basis of geometry, appearance, age and different tectonics *(table 4.2)*. The most important criteria are to classify each class is the involvement of basement.

1. First class
2. Second class
3. Third class

| | | | | |
|---|---|---|---|---|
| **First class** | Basement involved | Regional significance | Reactivated | Separate areas of different tectonic outline |
| **Second class** | Basement involved | Semi regional | Reactivated/not reactivated | Separate areas of different tectonic outline |
| **Third class** | Basement detached | Local significance | Not reactivated | Does not separate areas of different tectonic outline |

**Table 4.2:** Classification of fault systems into first, second and third classes (modified from Gabrielsen, 1984).

In the study area, MF1a & MF1b distinguish the eastern boundary of the fault complex by the Loppa High where as MF3 separates the western boundary of the fault complex by deep Bjørnøya Basin (*fig 4.3*). On the other hand, two distinct units that classify as platform and sub-platform in the terminology of Gabrielsen, (1984) are separated by a horst as discussed earlier. At deeper level, MFCP1 clearly cuts the stratigraphic succession from the early Permian to the basement demonstrating its thick skin nature and regional significance, hence fitting the definition of a first class fault in the terminology of Gabrielsen, (1984). On the other hand, master fault (MF1a & MF1b) cuts the stratigraphic section from the intra Triassic to the early Permian (*fig. 3.8*) whereas; MF2a & MF2b cuts the stratigraphic interval from the early Cretaceous to the intra Triassic level *(fig. 3.8)*. Therefore, both fault segments (MF1a, MF1b, MF2a & MF2b) are not basement involved but shows reactivation with time and have a regional significance so it could be termed as a combination of first or second class fault (Gabrielsen, 1984).

## 4.2 Structural Architecture of the Bjørnøyrenna Fault Complex

During present study, the interpreted geometries of the master faults, position of terrace and location of the high along master faults may reflect the real image of the principal sketch presented by Gabrielsen, (2010) (*fig 4.2*). This principal sketch generally elaborates the development of structural elements in an extensional regime. Therefore, key profile 2 from segment 1 (fig 3.6) has been selected to present the architectural elements in the study area.

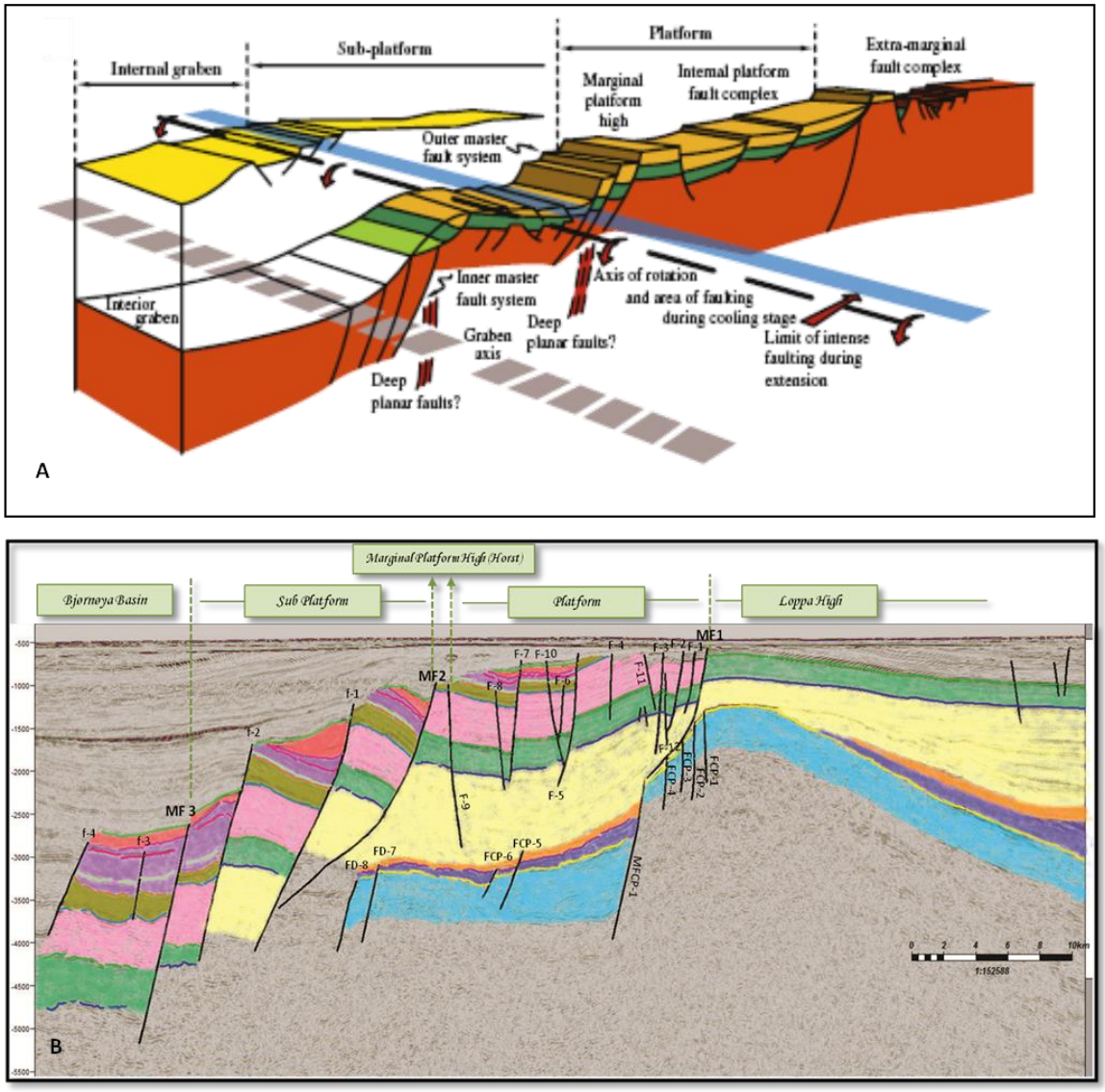


**Figure 4.2:** Comparison of structural architecture in extensional regime (A) Principal sketch of major structural elements in graben systems (Modified from Gabrielsen, 2010). (B) Interpreted structural elements of the Bjørnøyrenna Fault Complex.

It can be observed in cross-section *(fig 4.2)* that a horst could be termed as the marginal platform high separating the quiet platform from much more heavily faulted sub platform. The faults situated at the platform exhibit relatively small vertical throws except the major boundary faults which separate the Loppa High from the fault complex (*fig 4.2)*. On the other hand, the faults located in the sub platform indicating domino fault geometries along rotated fault blocks with large vertical throw as compare to the faults located in platform. According to Gabrielsen, (2010), the platform may show direct contact with the internal basin but in some cases the platform or the platform marginal high may be absent and it could be

recognized in the fault complex that horst feature get terminated towards the north of the study area (*fig 4.3*). This is due to the discrepancy indicating the structural or lithological inhomogeneties in the basement and dominating variations in strain rate or bulk extension along the basin axis (Gabrielsen, 2010).

## 4.3 Fault Geometry of the Bjørnøyrenna Fault Complex

### 4.3.1 Lateral Configuration

The NE-SW and N-S trending Bjørnøyrenna Fault Complex is dominantly an extensional fault system demonstrating a platform and sub platform framework in the study area *(fig 3.6; 4.2, 4.3)*. On the fault map the platform and sub platform is dominantly distinguished by narrow horst marked by orange in color *(fig 3.6, 4.3A)*. This fault complex can be specifically categorized into three main lateral segments based on the fault geometry and structural trends, namely segment 1, 2 and 3 *(fig 4.3)*. The southern corner of the fault complex constitutes of three main master faults with distinct strike dimension. The N-S oriented, MF1a qualifies as an unbroken master fault which can be trace into segment 2 and 3 as well. On the other hand, MF2a and MF3a are embedded in the structural sub platform with strike NE-SW. Segment 2 in the central part exhibits three main master faults (MF1a, MF2b & MF3b). MF1a is oriented N-S whereas MF2a changes its strike from NNW-SSE to NE-SW. Moreover, MF3b is dominating NE-SW structural trend. In the north, segment 3 is also symbolized by three master faults (MF1b, MF2b & MF3c). MF1a is characterized by change in orientation from N-S to NE-SW whereas, MF2b & MF3c is dominating NE-SW structural trend. In addition, the population of interpreted small number of antithetic and synthetic normal faults is higher in the platform as compare to sub platform. Moreover, toward the north the segment is abolished at the eastern margin of the Fingerdjupet sub basin. Similar structural trend and segmentation of Bjørnøyrenna Fault Complex have been also presented by Gabrielsen et al., (1997) (*fig 4.3c*).

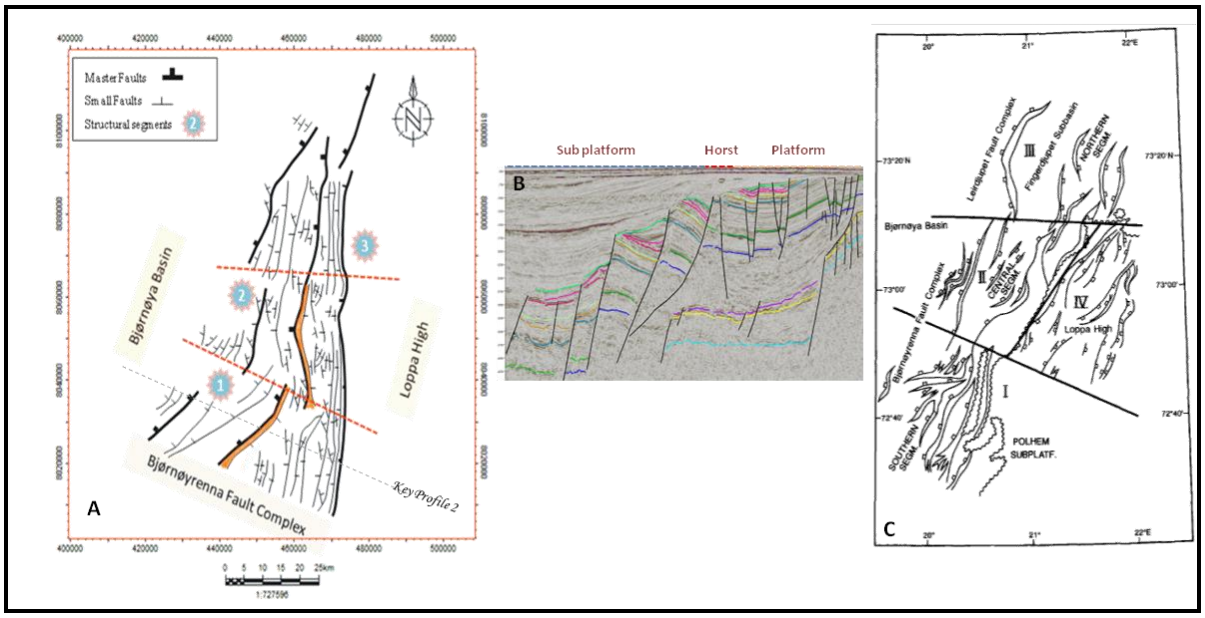


**Figure 4.3:** comparison of Structural maps view (A) Fault map of the interpreted mid Triassic level shows structural segments. (B) Cross-sectional view of key profile 2. (C) Structural map of the Bjørnøyrenna Fault Complex indicating structural subarea (Modified from Gabrielsen et al., 1997).

### 4.3.2 Fault associated features

The detailed investigation of the fault geometries and associated structures in the hanging-wall of the master faults (MF1, MF2 & MF3) can be describes as follows *(fig 4.4)*. A distinct contrast exists in fault geometries between deep (late-Carboniferous-early Permian) and shallower (intra Triassic-Cretaceous) stratigraphic level in a cross-sectional view (fig 3.8, 4.4). Thus, it can be divided into several depth dependent segments, namely late Carboniferous-early Permian, late Permian-mid Jurassic and base Cretaceous-early Cretaceous. Late Carboniferous-early Permian time is represented by set of planar normal faults, whereas late Permian-mid Jurassic is characterized by listric faulting, rotated fault blocks and sag sediment packages particularly observed in the hanging wall between the mid Permian to the early Triassic. Wedge shape geometry is also observed between the base Cretaceous-early Cretaceous which dominate syn-rift sedimentary packages *(fig. 4.4)*. Moreover, a narrow fold is examined in sub-platform between the late Jurassic to the base Cretaceous which probably related to mild inversion *(fig. 4.4)*.

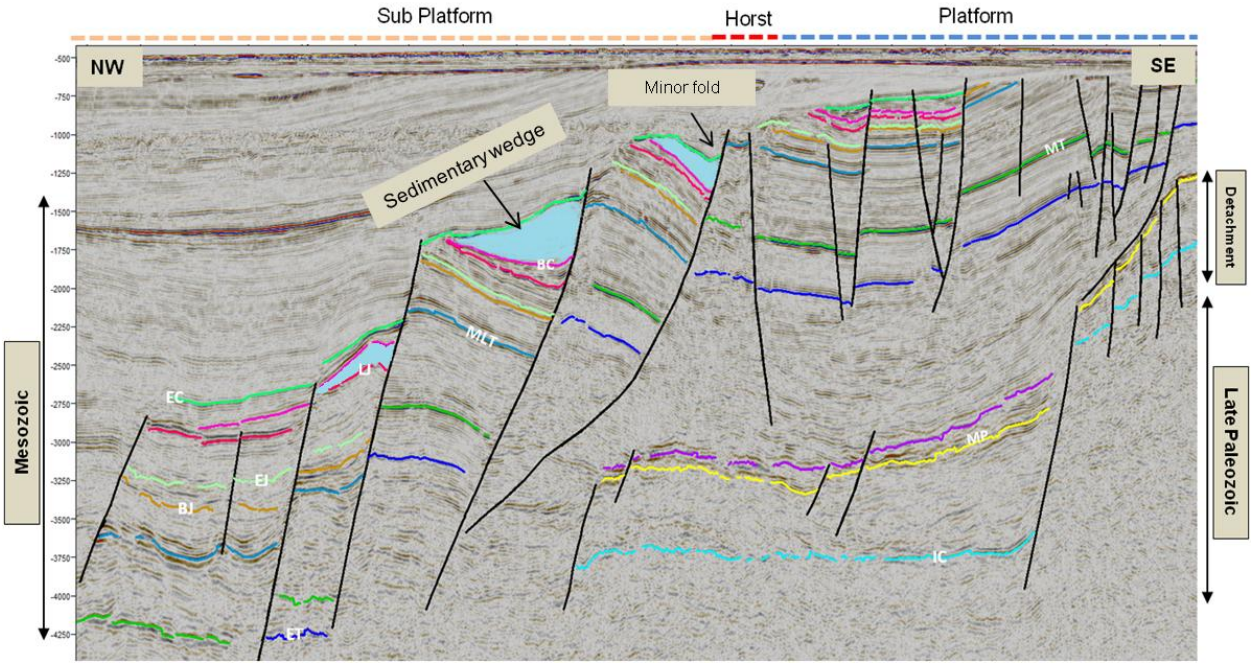


**Figure 4.4:** Cross section elaborating fault associated features in depth dependent segments. Black arrows are indicating minor fold and sedimentary wedge as shown by light blue in color.

#### 4.3.2.1 Late Carboniferous-Early Permian

The deep seated faults at late Carboniferous to early Permian level constitute a set of planar normal faults *(fig 4.4)*. These faults are defining a half graben in the hanging wall towards basin. The thickness of sedimentary succession increased toward the faults and it dominates subsidiary fault movements during Permian. The main boundary faults separating the western part of the Loppa High were also active in Permian times (Gudlaugsson et al., 1998). Thickness of sediments toward the fault is characteristic of extensional basin. At this level, MFCP1 define as a First class fault in the terminology of Gabrielsen (1984). Moreover, a syncline feature is observed at the hanging wall while anticline is examined at the footwall of the MFCP1 which is clear indication of normal drag fold and this feature is consistently observed on all the key profiles 1-7 *(fig. 3.8, fig. 4.4).*

#### 4.3.2.2 Late Permian-Mid Jurassic

The geometry of the Bjørnøyrenna Fault Complex at Mesozoic level proposed by Gabrielsen et al., (1997), presented that the faults are predominantly listric. The southern segment of the fault complex is indicated by number of rotational fault blocks. The reflections are dipping

toward southeast in the fault blocks. The oldest reflection which is affected by listric faulting is the Ladinian and the youngest reflection is represented by intra Barremian.

The present study supplements the observations made by Gabrielsen et al., (1997). The presence of one major listric fault (MF1a & MF1b) in the platform distinguishes the western part of the Loppa High from the fault complex. The hanging wall of MF1 is highly influenced by the synthetic and antithetic behavior of normal faults as seen on the key profiles (1-7) (fig 4.3, 4.4). Moreover, a rollover fold has been examined in the vicinity of MF1a & 1b and it can be clearly seen in segment 1 at key profile 1 & 2 *(fig 3.6, 3.9 & 3.10)*. Rollover folds, resulting from slip along listric normal faults that are detached in the sedimentary section or in the basement (Bally et al., 1981). The presence of rollover fold is a good clue that the associated fault is listric (Hamblin, 1965). Rollover and reverse drag anticlines are mostly exhibit similar geometries (Schlische, 1995). Reverse drag erroneously interpreted as rollover fold and the associated faults falsely assume to be listric (Barnett et al, 1987). The existence of reverse drag folds doesn't intimate the possibility of listric faults. Generally reverse drag fold are affiliated with planar or only mildly listric faults. The rollover and reverse drags are distinguished on the basis of the following reasons:

1. Rollover folds are affiliated with detached normal faults and anticipated in thick sedimentary successions.
2. Reverse-drag folds are developed in both hanging wall and footwall while rollover folds are established in the hanging wall of the normal fault.

In sub platform, rotational fault blocks have been observed along planar normal faults (MF2a & MF2b) which can be an indication of domino fault blocks geometries (fig 3.8, 4.4). The domino fault blocks are a common type of normal fault observed in many extensional basins (Mascle & Martin 1990; Jackson *et al.* 1988; Montadert *et al.*1979). During extension there is a net rotation of each fault block accommodating regional extension. Fault blocks are assumed to rotate rigidly with a diffuse accommodation zone at their base (Waltham et al., 1993). All dominoes are required to move simultaneously. Other models allow for 'soft' dominoes which deform during extension (Walsh & Watterson 1991) or allow compaction of a soft domino during extension and rotation (Iliffe *et al.* 1990, Waltham et al., 1993).

Additionally, the stratigraphic succession ranging from late Triassic to Cretaceous level in platform is eroded due to an extensive uplifting along MF1. On the other hand, stratigraphic succession is well preserved with valuable thickness at the foot wall and hanging wall of MF2 and MF3 in sub platform.

#### 4.3.2.3 Base Cretaceous-Early Cretaceous

The existence of fault blocks which rotated away from the basin axis (*fig. 4.6*) dominating a wedge shape geometry between base Cretaceous to early Cretaceous along MF2a & 2b *(fig. 4.4 & 4.7)*. This wedge shape geometry is clear indication of syn-rift sedimentation (*fig. 4.5 & 4.7)*. Moreover, fault escarpments have been observed along rotational fault blocks. These are the ambiguous area of graben system and signifying uplift in the area (sensu Gabrielsen, 2010). In addition, mild inversion may further confer to the uplift of fault block along basin margin *(fig 4.4*). The wedge shape geometry is consistently observed throughout the area along MF2a & MF2b and thickness of sediments increased toward the fault (*fig 4.7*).

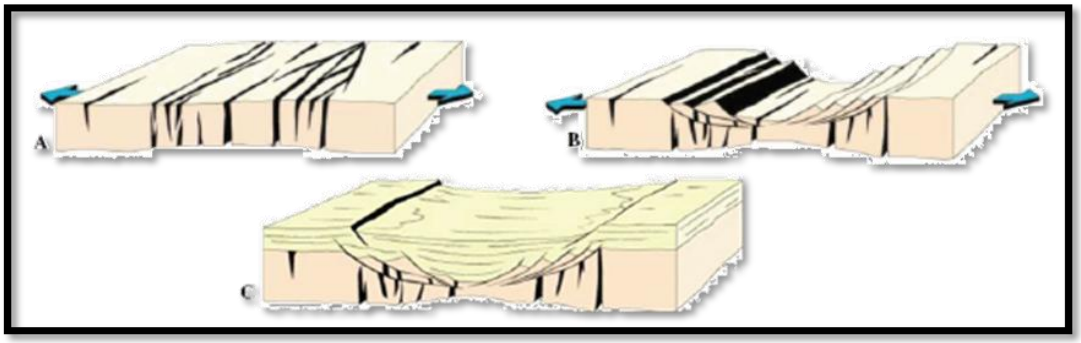


**Figure: 4.5:** Three major stages in the development of extensional basins (modified from Gabrielsen, 2010).

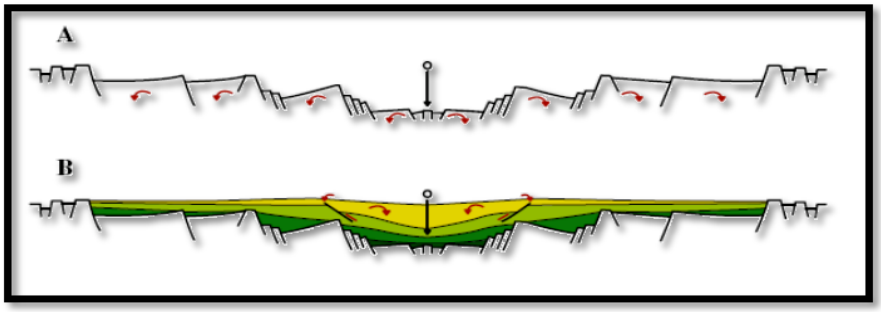


**Figure 4.6:** Pattern of rotation of sedimentary units (A) Synrift (B) Post rift stages (modified from Gabrielsen, 2010).

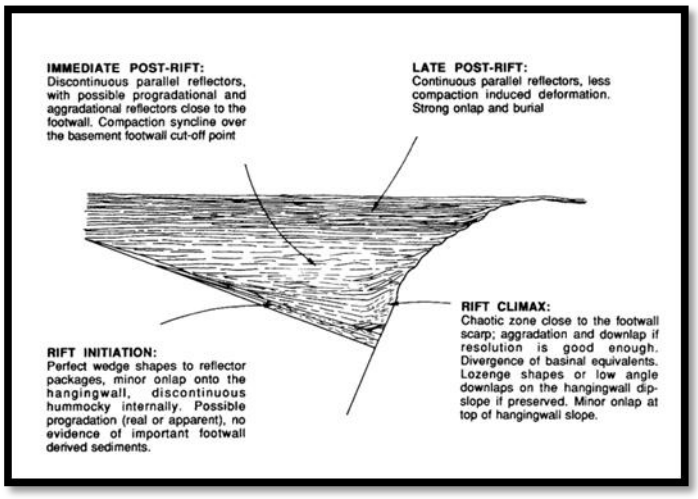


**Figure 4.7:** An idealized figure of syn sedimentary wedge (modified from Prosser, 1993).

## 4.4 Dating of structural events

In the present study, following three methods were used to examine the behavior of fault movement and sedimentation.

1. Expansion (Growth) index
2. Throw/depth Plot Analysis
3. Stratigraphic Dating

The method used to quantify expansion index or growth is the ratio of the stratigraphic thickness of each unit between the upthrown and downthrown blocks (Thorsen, 1963). Growth faults are formed by the result of faulting and sedimentation and generally describes by abrupt increase in thickness of corresponding strata across the fault on the downthrown blocks (Hardin and Hardin 1961, Edwards, 1976). The expansion index gives valuable information about the time of significant growth (Edwards, 1995) as it describe in ratio, so it doesn't show concrete information about absolute slip or slip rate (Cartwright et al., 1988). Therefore, the rate of sedimentation across the fault shows variation in growth index with the same slip amount.

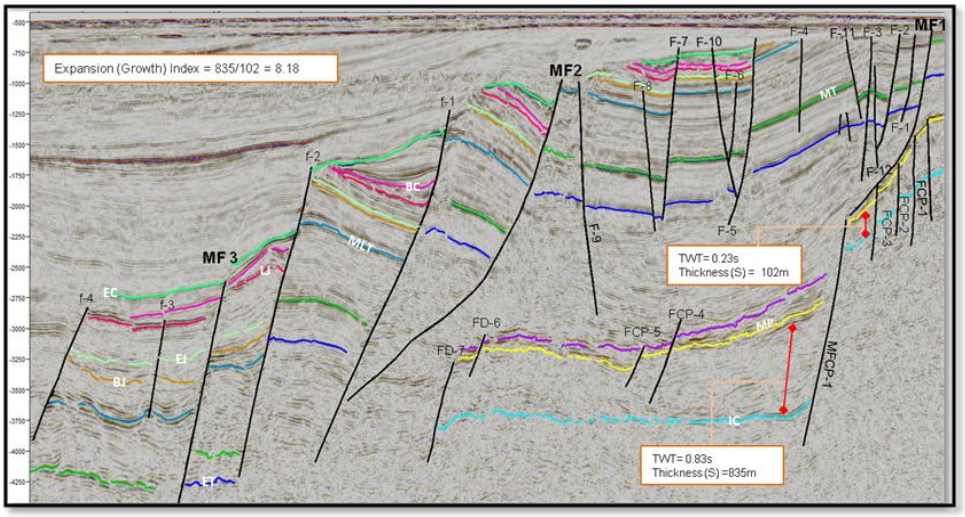


**Figure 4.8:** Application of the expansion index (E.I) to understand the growth fault behavior, E.I =1 suggests non-growth and E.I > 1 represents growth faulting.

In present study, the fault dating is only performed along MFCP1, MF 1a, MF 2a & MF2b segments. The expansion index of MF1a was not possible to calculate because the strata ranging from the mid late Triassic to the Cretaceous were eroded due to an extensive uplifting of the Loppa High. Therefore, two cross-sections have only been selected to examine the expansion index of MFCP1, MF2a & MF2b between mid Triassic- late Triassic and late Carboniferous to early Permian *(fig 4.8, 4.10 & 4.11).* Both sections illustrate expansion index greater than 1 which signifies that the faults are related to growth strata. The expansion index method did not explain the absolute displacement of the fault because of measurement in ratio. Thus it doesn't resolve the issue of absolute growth strata. In addition, Edwards, (1976) proposed the presence of growth faulting in Triassic succession in the vicinity of Svalbard as shown in *fig (4.9).*

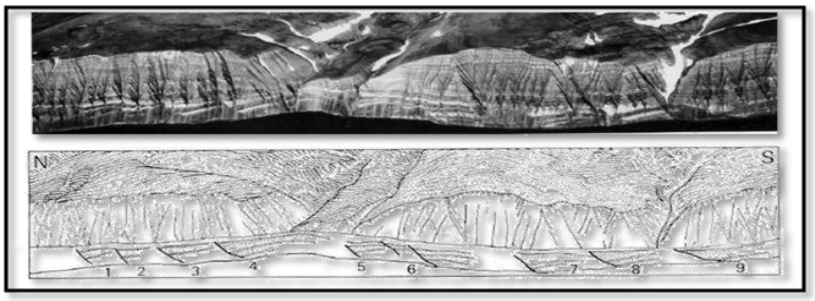


**Figure 4.9:** Oblique aerial sketch showing the growth faults in the upper Triassic sediment in Kvalpynten, Svalbard. Numbers refer to the growth fault (Edwards, 1976).

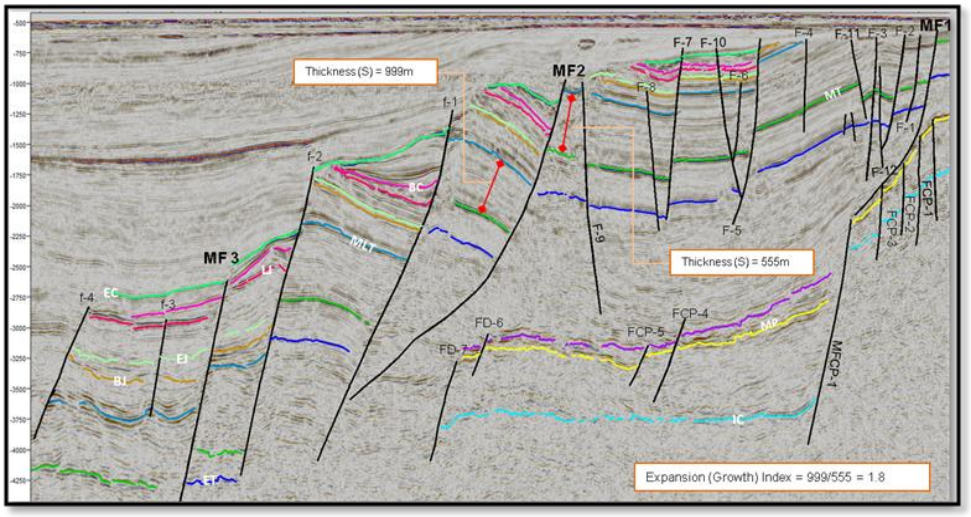


**Figure 4.10:** Application of the expansion index (E.I) to understand the growth fault behavior, E.I =1 suggests non-growth and E.I > 1 represents growth faulting.

The second method to identify growth strata across the master faults is the vertical displacement versus depth plot (Cartwright et al 1998; Castelltort et al., 2004; Back, et al., 2006; Tearpock and Bischke, 1991, 2003). It is a powerful visualization method that can detect growth where growth is not obvious in the seismic data. Unfortunately, this method was also not possible to perform in the current studies because it requires dense well data across the master faults.

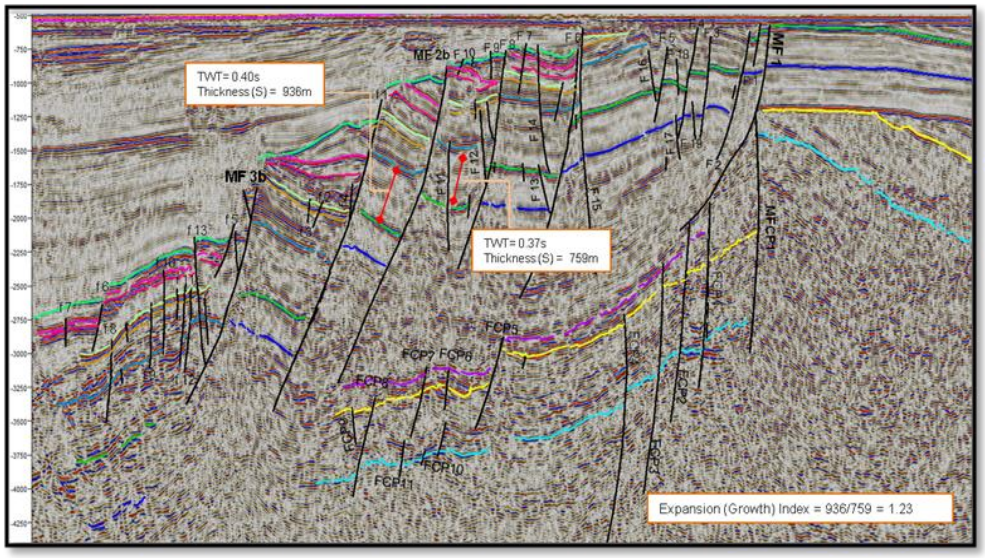


**Figure 4.11:** Application of the expansion index (E.I) to understand the growth fault behavior, E.I =1 suggests non-growth and E.I > 1 represents growth faulting.

Subsequently, stratigraphic dating has been taken into account to determine the ages of rock formation either affected by faulting or unaffected by faulting (Angelier, 1994). In the study area, syn-depositional faults are recognized on the entire key profiles (1-7) and it shows noticeable information because the age of formation could be same as that of faulting (Angelier, 1994). Syn-depositional faulting can be exactly reconstructed, when fault movement and deposition have interacted during a long time interval. Consequently, three zoomed in cross-section for the master faults (MFCP1, MF2a & MF2b) *(fig. 4.12a,b,c)* and one for MF 1a have been selected *(fig 4.12d)* from already prescribed seismic sections.

The N-S trending MFCP1 has been interpreted between late Carboniferous-early Permian as seen in the key profile 1-7 (*fig. 3.6, fig. 3.9*). The thickness of strata increases in the hanging wall towards MFCP1 and it demonstrate that the growth strata is affiliated between the interpreted intra Carboniferous and the early Permian reflection (4.12a). Hence, an age of this fault could be related to intra carboniferous-early Permian.

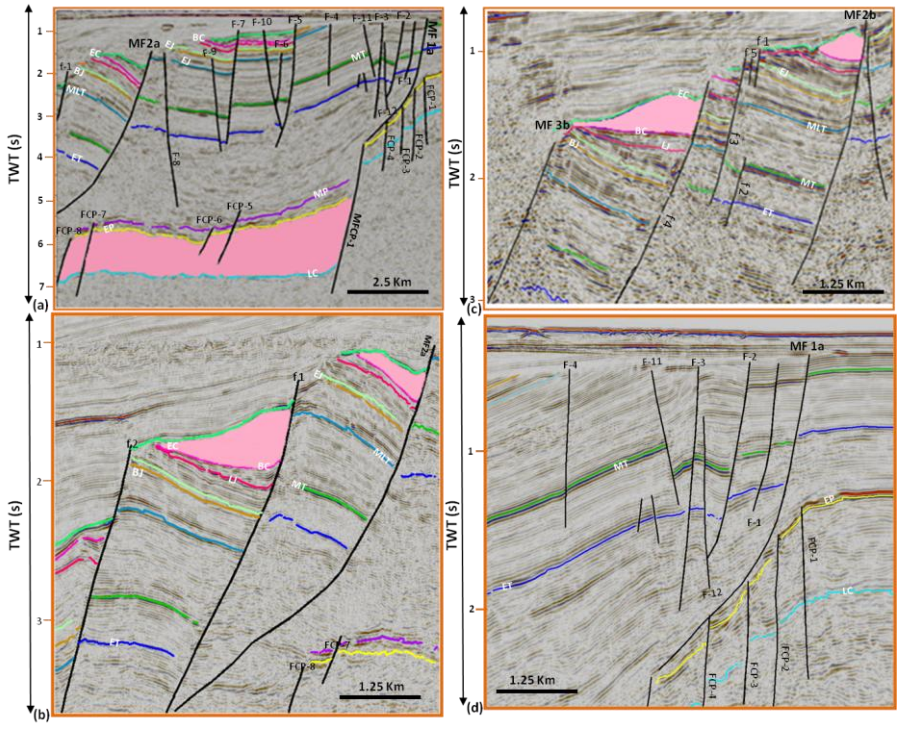


**Figure 4.12:** Pink highlighted area illustrating fault growth strata on pre described key profiles (1,4). For color codes view figure 3.2. EC: Early Cretaceous, BC: Base Cretaceous, LJ: Late Jurassic BJ: Base Jurassic, MLT: Mid Late Triassic, MT: Mid Triassic, ET: Early Triassic, MP: Mid Permian, EP: Early Permian, IC: Intra Carboniferous.

The NE-SW trending master fault segment MF2a has been interpreted in segment 1 at key profiles 1 & 2 (Fig. 3.6, 3.9 & 3.10). MF2a exhibits the existence syn-sedimentary wedge between the interpreted base Cretaceous and the early Cretaceous reflection (4.12 b). Therefore, an age of mid/late Jurassic-early Cretaceous has been assigned to this master fault segment.

The NE-SW master fault MF2b is interpreted in segment 2 & 3 in the key profile 3-7 *(fig. 3.6, 3.11*) affirm the existence of syn-sedimentary wedge between base Cretaceous to early Cretaceous. The growth strata is found to be associated between mid Jurassic to early Cretaceous (Fig 4.12 c). Therefore, an age of mid/late Jurassic- early Cretaceous has been assigned to this master fault segment.

It can be observed that extensive amount of uplifting eroded mid late Jurassic to Cretaceous sequences along MF1a in the vicinity of platform. Therefore, it is not possible to predict exact movement of the master fault MF1a. On the other hand, a valuable constant thickness has been observed across MF1 in the intra Triassic succession (Fig. 4.12 d). Thus, an age of MF1a could be younger than the mid Triassic reflection.

## 4.5 Detachments

The detachments usually occur along listric faults (*Fig 4.13*) as observed in the key profiles (1-7) *(Fig. 3.9 & 3.11).* Listric faults are usually shallow out in a common detachment along a weak horizon such as over pressured shale or salt (Davison, 1989). The most extensional detachments dipped in the same direction as the surface topography when faulting was active. It has become apparent, that most of the faults in seismic reflection profile shows curved or listric form and are concave upward (Bally, 1984 & Williams, 1987). Such types of faults tend to flatten downwards and this results in dominantly horizontal movements above detachment (William, 1987). Many listric faults show curvature indicating that their 3-D geometry is spoon shaped. Three basic detachment geometries have been indicated by Mclay, (1989); (a) Uniform extension (b) simple listric detachment (c) Ramp/flat detachment. The most typical characteristics of detachment are as follows:

- It has no root.
- It usually takes place along a weak, stratigraphic horizon.
- Younger rocks will lie on older, often with a stratigraphic or metamorphic gap.

- Faults and brecciation are pervasive in the hanging wall and may be lacking in the footwall.
- Tight, overturned and recumbent, eventually faulted folds are common in incompetent strata.

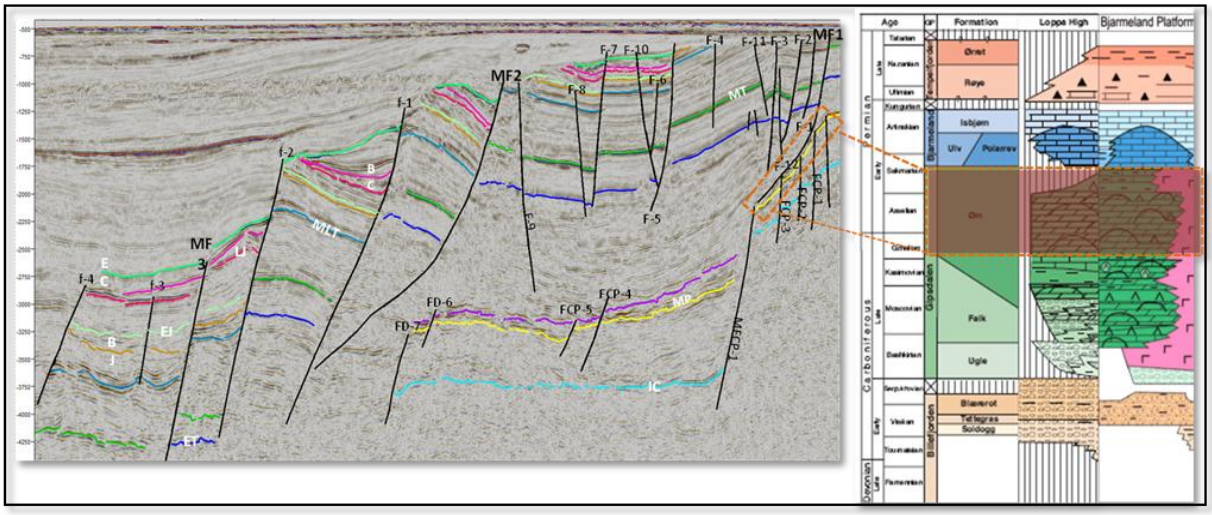


**Figure 4.13**: Orange rectangle demonstrating interpreted detachment within Permian strata see *(fig.3.6)* for location of line. Stratigraphic column modified from Worsley, (2008).

Faleide et al., (1993) documented that the Bjørnøyrenna Fault Complex is indicated by listric faulting and shows similar detachment within the Permian rocks. The present study supplements the observation of Faleide et al., (1993). During present study, the conversion of time sections to depth section was not possible, due to lack of well data (check shots & interval velocities). Therefore, the detachment in above *(fig. 4.13)* is displaced in TWT (ms) interval. A relatively simple listric detachment is interpreted along MF1 within the Permian succession *(fig. 4.13)*. This detachment also exhibits distinct contrast in fault geometries which distinguished depth dependent segments. The detachment at this particular level could be a result of mechanical weak lithology mainly carbonates & evaporate sequences as reported in Ørn Formation *(Fig. 4.13)*.

## 4.6 Structural Inversion

According to Glennie & Boegner (1981), the term structural inversion is simply defined as conversion of a basin area into structural high. The inversion can be considered as positive or negative. The term "positive inversion" inherently corresponds to uplift whereas the term "negative inversion" substantially related to basin subsidence.

The most common characteristics of positive inverted system are reverse reactivation of extensional faults, generation of new, low angle fault traces, development of secondary contractional structures (fold, reverse faults, thrusts), uplift of basin margins and uplift of central parts of basins (Gabrielsen, 2010). All these defined characteristics are not found in the study area but the existence of fold along can be a strong indication of mild inversion.

Gabrielsen et al., (1997) proposed the presence of structural inversion at early Cretaceous level due to dextral shear transtension? *(fig. 4.16)*.

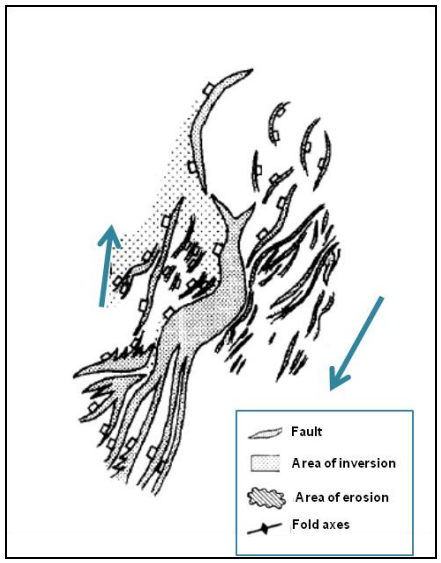


**Figure 4.16**: Structural pattern of the Bjørnøyrenna Fault Complex indicating early Cretaceous dextral shear (transtension?) (modified from Gabrielsen et al., 1997).

The present study supplements the observation of Gabrielsen et al., (1997). For this purpose, a general observation has been carried out in order to investigate the inversion either related to head-on contraction or strike-slip movement. Due to limitation of time in thesis work, it is not possible to map out this narrow fold on a fault map. The head-on contraction is delineated by parallel fold axis to the master fault whereas inversion related to strike-slip movement constitutes a fold axis strike obliquely to the master fault. The analysis suggests that dextral strike-slip event is responsible for the generation of mild inversion *(fig. 4.15*). Moreover, a narrow fold in the hanging wall of f-2 has been interpreted between late Jurassic to the base Cretaceous reflections *(fig. 4.15)* while the early Cretaceous reflection also influenced by structural inversion. Therefore, the present study places this episodic event in

the late Jurassic to the early Cretaceous, on the basis of related structural configuration *(fig. 4.15)*.

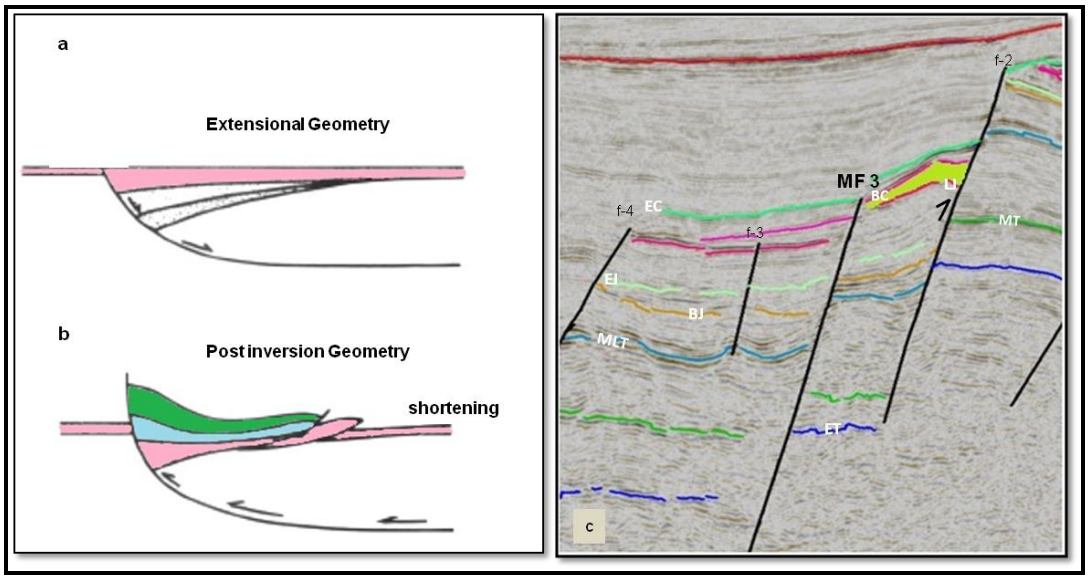


**Figure 4.15:** Comparison of principal sketch of inversion with an interpreted example of the study area. (a) formation of asymmetric half graben in extensional geometry (b) Accommodation structure developed during inversion of the half graben (modified from Hayward & Graham, 1989)(c)Light green color highlighting the positive structural inversion.

## 4.7 Geological Evolution of the Bjørnøyrenna Fault Complex

The generalized geological history of the study area with comparison of regional events can be seen in fig. 4.18.

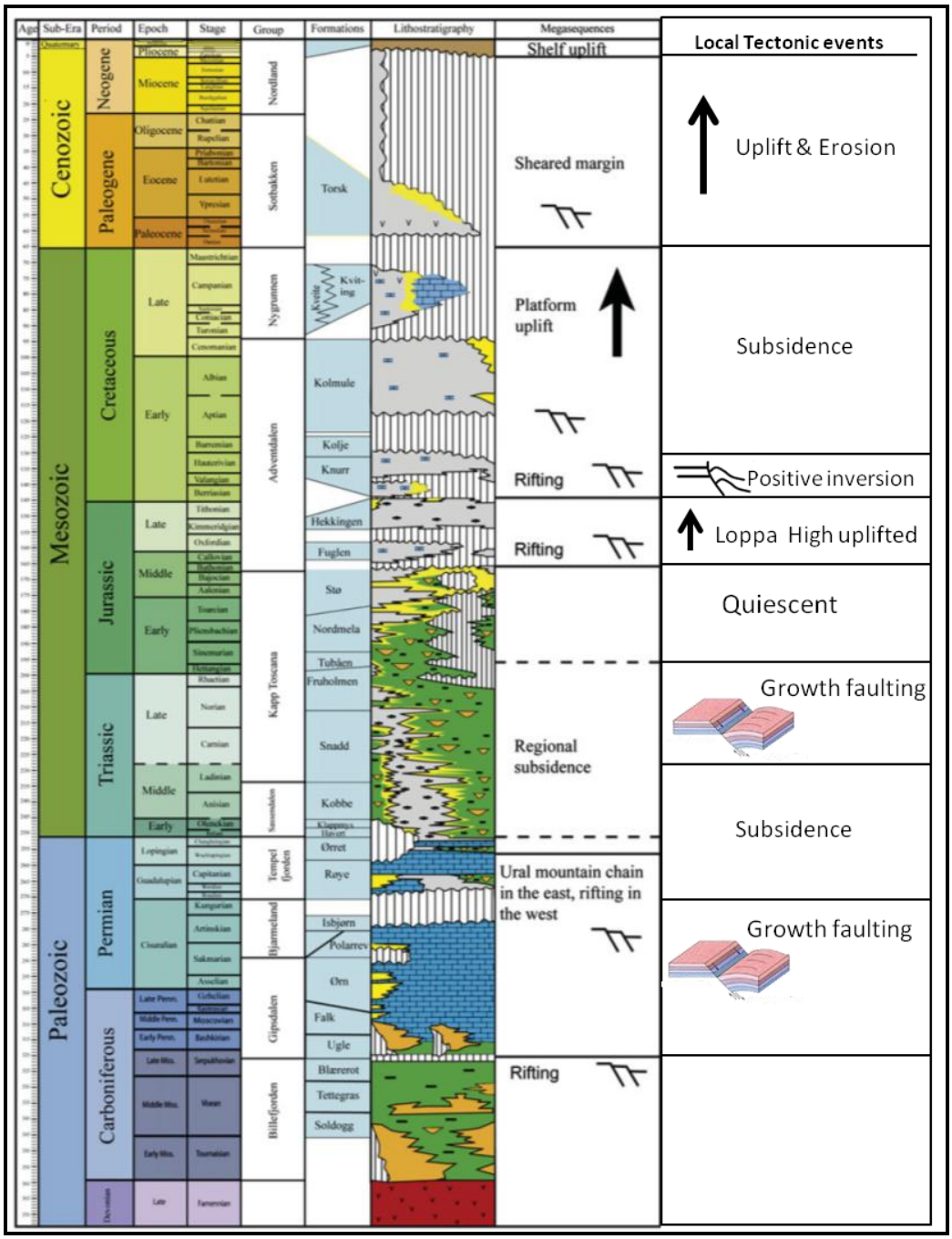


**Figure 4.18:** Comparison of regional tectonic evolution in SW Barents Sea (modified from Glørstad-Clark et al., 2011) to the local tectonic events in study area.

The NNE-SSW trending Bjørnøyrenna Fault Complex exhibits a junction between the Loppa High and the Bjørnøya Basin. The faults within this province are of Paleozoic and older provenance and were reactivated several times during the Mesozoic and Tertiary.

1. Late Carboniferous-Early Permian
2. Late Permian-Early Triassic
3. Mid/Late Triassic-Early Jurassic
4. Mid Jurassic-Early Cretaceous
5. Early Cretaceous-Recent

### 4.7.1 Late Carboniferous-Early Permian

The evolution of the Bjørnøyrenna Fault Complex is started by the late Carboniferous extensional rifting. In the study area it can be observed that the fault at this interval is termed to be growth fault. The interval shows a significant thickness towards the fault which demonstrates subordinate movement during that time. The main boundary faults limiting the Loppa High to the west were also active in Permian times. Similarly, both Carboniferous and Permian fault movements occurred on Bjørnøya Basin located on the Stappen High (Worsely, 1990). During this time period, an extensive amount of post-rift carbonate platform was established with evaporite deposition in local basins (Faleide et al., 1984; Larssen et al., 2002).

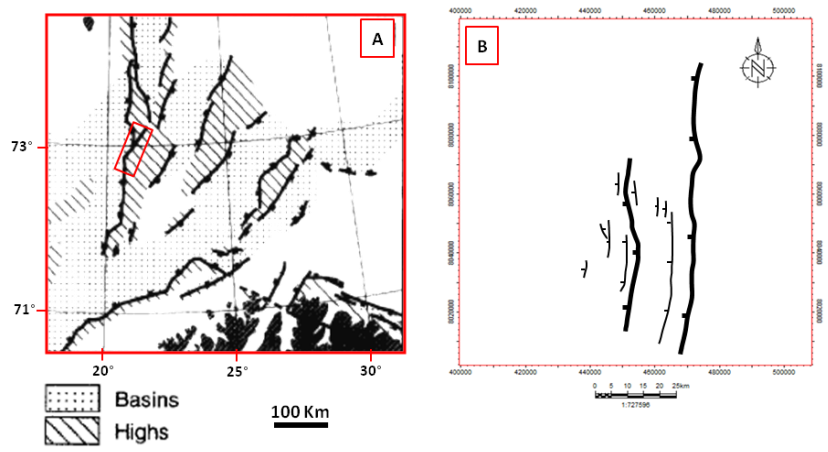


**Figure 4.17:** Comparison of fault pattern in map view (A) regional structures of late Paleozoic rift system (modified from Gudlaugsson et al., 1998) (B) interpreted fault map of the early Permian reflection in the study area.

### 4.7.2 Late Permian-Early Triassic

The late Permian-early Triassic event is characterized by the presence of N-S and NE-SW structural trend and by the pronounced uplift of the Loppa High at Permian-Triassic boundary and accelerated subsidence in the fault complex as shown in the vicinity of the Platform (Fig. 3.8, 4.2 & 4.4). Ziegler, (1988) suggested that the rejuvenation of the Loppa High was due to thermal doming.

This time period was marked by significant extension (Gudlaugsson et al., 1998; Johansen et al., 1994, 1993; Wood et al., 1989; Ziegler, 1988), contributing to Triassic subsidence in the western Barents Sea and exaggerate the relief of the Paleo-Loppa High (Glørstad-Clark et al., 2010). Normal faulting along the western margin of the Loppa High as well as the uplift, tilting and erosional truncation of the high itself (Johansen et al., 1994a) are of sufficient magnitude to indicate a significant Permian-Early Triassic rift phase affecting the north-south structure trend. Evidence of fault movements is found as from north as the Fingerdjupet Basin.

During the late Permian time, the Norwegian Greenland rift system was developing and a continuous seaway opened between the Arctic in the north and the northwest European basins in the south, but during the Triassic the seaway to the south was closed (Faleide et al., 1984; Müller et al., 2005; Nøttvedt et al., 2008). A transition to clastic deposition occurred in the Late Permian as a result of uplift of the Uralian Mountains in the southeast and landmasses to the south (Johansen et al., 1993; Larssen et al., 2002).

In the study area, the early Mesozoic sedimentation was markedly influenced by the paleo topography from the late Paleozoic rifting, particularly the Loppa High acting as a barrier to the west to sediments prograding from south and southeast (Faleide et al., 1984; Skjold et al., 1998; van Veen et al., 1993; Worsley et al., 2001).

The present day wide Loppa High is a Late Mesozoic structure (Gabrielsen et al., 1990), whereas the Late Paleozoic high was a narrow ridge trending north-south under the western part of the present day Loppa High.

### 4.7.3 Mid/Late Triassic-Early Jurassic

The mid-late Triassic time is characterized by growth faulting in the study area. On the other hand, the late Triassic to early Jurassic time period was tectonically quiescent and marked by reduced in subsidence compared to that seen for the early-mid Triassic (Bergan, M. & Knarud, R., 1993; Worsley, D., 2008), which may have been due to a change in tectonic configuration /or a shift source area from the Uralian orogeny to the Baltic shield in the south. By the middle Ladinian times, accommodation space east of the paleo-Loppa High was filled in, and sediments were deposited on the west of the high. By Late Triassic times, the paleo-Loppa High was a major depocenter (Larssen et al., 2002; Glørstad-Clark et al., 2010).

In general, it seems that accommodation space generated in the Triassic was partly controlled by rejuvenation of Late Paleozoic structures (Glørstad-clark, E. et al., 2010) such as subsidence associated with the reactivation of deep seated fault zones.

### 4.7.4 Mid Jurassic-Early Cretaceous (Late syn-rift )

The structural development during mid Jurassic- early Cretaceous in the study area is marked by the removal of 1000m of sediments (Middle Jurassic-Triassic). Some 750m of this erosion is attributable to foot wall uplift, whilst the remaining 250m of uplift is associated with thermal doming via lateral heat transfer from the development of rift basins to the south and west (Wood et al., 1989).

Moreover, the presence of positive inversion demonstrates reversely reactivation of the early cretaceous growth related fault *(Fig. 4.15)*. This positive inversion is indicated by the existence of minor fold at the upper most part of the hanging wall. Due to lack of time, the direction of the fold axis was not possible to map out but the interpreted mild inversion could be a result of dextral strike slip movement.

Regionally, the process responsible for the inversion of the Loppa High is not well understood. Rotated fault block and footwall uplift as described by Wood et al. (1989) is sufficient to explain the inversion of the broader feature. Far field stresses associated with the increased tectonic activity in the Arctic and North Atlantic have caused inversion of the Triassic basin over the selis ridge in early Cretaceous (Glørstad-clark et al., 2011). However

it cannot explain uplift of entire Loppa high structural features. The pattern of NW-SE extension was, however accompanied by strike slip that was focused along deep seated structural lineaments, and the development of deep basins west of the Loppa High. Loppa High became uplifted in the Late Jurassic-earliest Cretaceous, which inverted the late Triassic to the middle Jurassic depocentre (Glørstad-clark et al., 2011).

### 4.7.5 Early Cretaceous-Recent

The westernmost part of the Barents Sea region developed into a sheared margin in Early Cenozoic times, related to rifting and continental break-up in the west and north, followed by seafloor spreading in the Norwegian-Greenland Sea and Eurasia Basin (Faleide et al., 1991, 1993b). The Cenozoic was dominated by regional uplift and erosion in the Barents Sea region, with maximum uplift increasing from south to north and west to east, creating a north-south tilting of the crustal block of the region (Faleide et al., 1993a,b; Wood et al., 1989). The region became tectonically quiet during the Oligocene, but basin-wide Neogene uplift resulted in deposition of a large sedimentary wedge comprising mainly Late Pliocene-Pleistocene glacial deposits to the west (Faleide et al., 1996).

# CHAPTER 5

# CONCLUSION

This thesis is based on the interpretation of 2D seismic with focus on the structural outline and history of the Bjørnøyrenna Fault Complex. Seven 2D seismic lines termed as key profiles have been selected from three different structural segments of the Bjørnøyrenna Fault Complex, to investigate the fault geometry, dating of structural events and temporal evolution.

The NE-SW and N-S trending, Bjørnøyrenna Fault Complex is comprised of three main master faults (MF1, MF2 & MF3) in the study area. MF1 separates the eastern boundary of the fault complex from the Loppa High whereas, MF3 distinguishes western boundary of fault complex from the deep Bjørnøya Basin. This large array of master faults, further characterized by different segments are termed as (MF1a, MF1b; MF2a, MF2b; MF3a, MF3b & MF3c) which constitute linked fault system with variable soft-linked and hard-linked elements. The mutual relationship between these fault segments is found to be synthetic-overlapping and synthetic approaching transfer zones in the terminology of Davison, (1984). In a cross-sectional view, the fault geometries exhibit a distinct contrast between deepest (late Carboniferous-early Permian) and shallowest (intra Triassic -Cretaceous) stratigraphic levels. Additionally, MFCP1 cut the stratigraphic succession from the early Permian down to the basement, demonstrating its thick-skin nature and regional significance. Therefore, it is qualified as a "**First class"** fault. On the other hand, MF1 & MF2 are not basement involved but shows reactivation with time and exhibits a regional significance. Hence, it could be termed as a combination of "**First or Second class"** fault.

Subsequently, two distinct units classified as platform and sub platform on the basis of intrinsic fault frequency, pattern and dip dimensions of the reflection packages distinguished by horst. On the platform, the presence of detachment within the Permian succession separated the deepest and shallowest level of fault geometries. Additionally, the fault at deeper level MFCP1 is characterized by planar fault geometry whereas; MF1 at shallowest level is dominated by strong listric configuration. However, rotated fault blocks geometry has been recognized along planar normal faults (MF2a & MF2b) in sub platform. Moreover,

Narrow fold is recognized which is found to be associated along f-2 in sub-platform and it could be an evidence of positive structural inversion in the present study. The analysis of such feature suggests that the strike slip movement could be responsible for the generation of this mild inversion. Therefore, an age of inversion structure can be related to the late Jurassic to the early Cretaceous.

Fault dating was performed by using the methods of expansion growth index and recognition of syn-rift sedimentation. The value of expansion index is greater than 1 for the sedimentary packages between the mid Triassic-late Triassic and the late Carboniferous-early Permian across the master faults MFCP1, MF2a & MF2b which shows that the fault related growth strata is associated with these ages. The N-S striking, MFCP1 was active in the late Carboniferous-early Permian on the basis of interpreted growth sequence. In contrast, NE-SW striking master fault MF2a & MF2b demonstrate an age of mid/late Jurassic – early Cretaceous, based on the presence of interpreted syn- sedimentary wedge between base Cretaceous-early Cretaceous.

The temporal evolution of the Bjørnøyrenna Fault Complex in the study area is summarized below:

- Late Carboniferous-early Permian defining a half graben in the hanging wall towards basin. The increased in thickness toward faults demonstrates subsidiary fault movement during Permian time.
- Late Permian-early Triassic period is characterized by the pronounced uplift of the Loppa High and significant subsidence observed in the fault complex.
- Mid-late Triassic time period is characterized by growth faulting.
- Late Triassic-early Jurassic period is tectonically quiescent.
- Mid Jurassic-early Cretaceous time period is marked by an extensive erosion of sediments situated at the Loppa High and the foot wall of MF1 followed by uplifting. This uplifting could be associated with thermal doming.
- Early Cretaceous time is indicated by the presence of positive inversion resulting in dextral strike slip movement.
- Late Cretaceous time is followed by Post rift subsidence.

# References

Amogu, D. K., Filbrandt, J., Kadipo, K. O., & Onuoha, K.,, 2011, Seismic interpretation, structural analysis, and fractal study of the Greater Ughelli Depobelt, Niger Delta basin, Nigeria: Leading Edge, v. 30, p. 640-648.

Angelier, J., 1994, Fault slip analysis and paleostress reconstruction. In: Hancock, P.L., (Ed.) Continental Deformation, Pergamon Press, Oxford, p. 53-100.

Bally, A. W., D. Bernoulli, G. A. Davis, and L. Montadert, 1981, Listric normal faults: Oceanologica Acta, v. 4, supplement, p. 87-101.

Barnett, J. A. M., J. Mortimer, J.H.Rippon, J.J. Walsh, and J. Watterson, 1987, Displacemnt geometry in the volume containing a single normal fault: AAPG Bulletin, v. 71, p. 925-937.

Back, S., C. Hocker, M. B. Brundiers, and P. A. Kukla, 2006, Threedimensional-seismic coherency signature of Niger Delta growth faults: integrating sedimentology and tectonics: Basin Research, **18**, no. 3, 323–337, doi:10.1111/j.1365-2117.2006.00299.x.

BALLY, A. W. 1984. Tectonogenese et sismique reflection:*Bulletin de la Socidte G(ologique de France,* 26, 279-286.

Bally, A. W. 1984. Seismic expression of structural styles. *Am. Ass. Petrol. Geol.*

Berglund, L. T., Augustson, J., Faerseth, R., Gjelberg, J., & Ramberg-Moe, H. (1986) The evolution of the Hammerfest Basin. In : A. M. Spencer (Ed.), Habitat of Hydrocarbons on the Norwegian Continental Shelf (pp. 319-338). London: Graham and Trotman.

Bergan, M., Knarud, R., 1993. Apparent changes in clastic mineralogy of the TriassiceJurassic succession, Norwegian Barents Sea: possible implications for palaeodrainage and subsidence. In: Vorren, T., Bergsager, E., Dahl-Stamnes, Ø.Holter, E., Johansen, B., Lie, E., Lund, T. (Eds.), Arctic Geology and Petroleum Potential. Norwegian Petroleum Society (NPF), Special Publication, vol. 2. Elsevier, Amsterdam, pp. 481e493.

Breivik, A. J., Gudlaugsson, S. T., & Faleide, J. I. (1995) Ottar Basin, Sw Barents Sea : a major Upper Paleozoic rift basin containing large volumes of deeply buried salt. Basin Research 7, 299-312.

Bugge, T., & Fanavoll, S. (1995) The Svalis Dome, Barents Sea – a geological playground for shallow stratigraphic drilling. First Break 13, 237-251.

Bruce. J. R., & Toomey, D. F. (1993) Late Paleozoic bioherm occurrences of the Finnmark shelf, Norwegian Barents Sea: analogues and regional significance. In : *Arctic Geology and Petroleum Potential*, T. O. Vorren, E. Bergsager, ø. A. Dahl-Stamnes, E. Holter, B. Johansen, E. Lie, & T. B. Lund (Eds). *Norwegian Petrol. Soc. Spec. Publ. No. 2* (pp. 377-392).

Cecchi, M., Markello, J., & Waite, L. (1995) Sequence stratigraphy architecture of Carboniferous-Permian sedimentary systems of the Norwegian Barents Sea with comparison to coeval systems in the USA. In : Sequence Stratigraphy on the Northwest European Margin, R. J.

Steel, V. L. Felt, E. P. Johannessen, & C. Mathieu (Eds), Norwegian Petrol. Soc. Spec. Publ. No. 5 (pp. 545-569). Amsterdam: Elsevier.

Cartwright, J.A., Trudgill, B.D., Mansfield, C.S., 1995. Fault growth by segment linkage: an explanation for scatter in maximum displacement and trace length data from the Canyonlands

Grabens of SE Utah. Journal of Structural Geology 17, 1319– 1326.

Cartwright, J., Bouroullec, R., James, D., & Johnson, H., 1998, Polycyclic motion history of some Gulf Coast growth faults from high-resolution displacement analysis: Geology, Geological Society of America, v. 26; no. 9, p. 819–822.

Castelltort, S., S. Pochat, and J. Van Den Driessche, 2004, Using T-Z plots as a graphical method to infer lithological variations from growth strata: Journal of Structural Geology, **26**, no. 8, 1425–1432, doi:10.1016/j.jsg.2004.01.002.

Cecchi, M. (1993) Carbonate sequence stratigraphy : application to the determination of play models in the upper Paleozoic succession of the Barents Sea, offshore northern Norway. In : Arctic Geology and Petroleum Potential, T. O. Vorren, E. Bergsager, ø. A. Dahl-Stamnes, E. Holter, B. Johansen, E. Lie, & T. B. Lund (Eds), Norwegian Petrol. Soc. Spec. Publ. No. 2 (pp. 419-438).

Dalland, A. (1981) Mesozoic sedimentary succession at Andoya, northern Norway, and relation to structural development of the North Atlantic. In: Geology of *the North At/antic Borderlands* (Eds J. W. Kerr and A. J. Fergusson), *Can. Sot. Petrol. Geol. Mem. No. 7,* pp. 563-584.

Dalland, A., Worsley, D., & Ofstad, K.,, 1988, A lithostratigraphic scheme for the Mesozoic and Cenozoic succession offshore mid- and northern Norway: Norwegian Petroleum Directorate, Bulletin no.4, p. 1-65.

Davison, I., 1994, Linked fault systems; extensional, strike-slip and contractional. In: Hancok, P.L., (Ed.) Continental Deformation, Pergamon Press, Oxford, p. 121-142.

Davison, I. 1989. Extensional domino faulting: kinematics and geometrical constraints. Ann. Tecton. 3, 12-24.

Dengo, C.A., & Røssland, K.G. (1992) Extensional tectonic history of the western Barents Sea. In : *Structural and Tectonic Modelling and its Application to Petroleum Geology,* R.M. Larsen, H. Brekke, B. T. Larsen, & E. Talleraas (Eds). *Norwegian Petrol. Soc. Spec. Publ. No. 1* (pp. 91-107). Amsterdam: Elsevier.

Doré, A.G., 1995, Barents Sea geology, petroleum resources and commercial potential, Arctic 8, 207-221.

Edwards, M.B., 1976, Growth faults in upper Triassic deltaic sediments, Svalbard, TheAmerican Association of Petroleum Geologist Bulletin, v.60(3), 341-355.

Edwards, M. B., 1995, Differential subsidence and preservation potential of shallow-water Tertiary sequences, Northern Gulf Coast Basin, USA. In: Plint, A. G., (Ed.), Sedimentary facies analysis: International Association of Sedimentologists, Special Publication v. 22, p. 265–281.

Eldholm, O., Faleide, J. I. and Myhre, A. M. (1987) Continentocean transition at the western Barents Sea/Svalbard continental margin Geology 15, *1118- 1122.*

Faleide, J.I., Tsikalas, F., Breivik, A.J., Mjelde, R., Ritzmann, O., Engen, O., Wilson, J. And Eldholm, O., 2008, Structure and evolution of the continental margin of Norway and Barents Sea, Episodes 31, 82-91.

Faleide, J. I., Bjørlykke, K., & Gabrielsen, R. H., 2010, Geology of the Norwegian Continental Shelf. In: K. Bjørlykke (Ed.). Petroleum Geoscience: From Sedimentary Environment to Rock Physics, Springer, Berlin, p. 467-501.

Faleide, J.I., Vågnes, E., / Gudlaugsson, S.T. (1993) Late Mesozoic-Cenozoic evolution of the south-western Barents Sea in a regional rift-shear tectonic setting. *Mar. Petrol. Geol. 10, 186-214.*

Faleide, J. I., Gudlaugsson, S. T., Eldholm, O., Myhre, A. M. and Jackson, H. R. (1991) Deep seismic transects across the sheared western Barents Sea-Svalbard continental margin *Tectonophysics 189, 73-89.*

Faleide, J. I., Myhre, A. M. and Eldholm, 0. (1988) Early Tertiary volcanism at the western Barents Sea margin. In: *Ear/y Tertiary Volcanism and the opening of the NE Atlantic* (Eds A. C. Morton and L. M. Parson), *Spec. Pub/. Geol. Sot. fond. No. 39,* pp. 135-146.

Faleide, J.I., Gudlaugsson, S.T., & Jacquart, G. (1984) Evolution of the western Barents Sea. *Mar. Petrol. Geol. I, 123-150.*

Gabrielsen, R. H., Grunnaleite, I, and Ottesen, S. (1992) Reactivation of fault complexes in the Loppa High area, southwestern Barents Sea. In *Arctic Geology and Petroleum Potential* eds T. O. Vorren, E. Bergsager, 0. A. DahI-Stamnes, E. Holter, B. Johansen, E. Lie and T. B. Lund, pp. 631-641. *Norwegian Petroleum Society Special Publication No. 2,* Elsevier, Amsterdam.

Gabrielsen, R.H., Færseth, R.B., Jensen, L.N., Kalheim, J.E. & Riis, F. 1990: Structural elements of the Norwegian continental shelf. Part I: The Barents Sea. *Norwegian Petroleum Directorate Bulletin 6*, 1-33 pp.

Gabrielsen, R.H. 1984: Long-lived fault zones and their influence on the tectonic development of the south-western Barents Sea. *Journal of the Geological Society, London 141,* 651-662.

Gabrielsen, R.H., 2010, The structure and hydrocarbon traps of sedimentary basins, In: Bjørlykke, K. (ed.), Petroleum geoscience from sedimentary environments to rock physics, Springer, Berlin, 299-327.

Gabrielsen, R. H., Grunnaleite, I., & Rasmussent, E., 1997, Cretaceous and Tertiary inversion in the Bjornoyrenna Fault Complex, south-western Barents Sea: Marine and Petroleum Geology, v. 14 No. 2, p. 165-178.

Gerard, J., & Buhrig, C. (1990) Seismic facies of the Barents Shelf: analysis and interpretation. Mar. Petrol. Geol. 7, 234-252.

Glørstad-Clark, E., Faleide, J. I., Lundschien, B. A. & Nystuen, J. P. , 2010, Triassic seismic sequence stratigraphy and paleogeography of the western Barents Sea area: Marine and Petroleum Geology, v. 27, p. 1448-1475.

Glørstad-Clark, E., Birkeland, E. P., Nystuen, J. P., Faleide, J. I., and Midtkandal, I., 2011, Triassic platform-margin deltas in the western Barents Sea: Marine and Petroleum Geology, v. 28, p. 1294-1314.

GLENNIE, K. W. & BOEGNER, P. L. E . 1981. Sole Pit inversion tectonics . In: ILLING, L. V. & HOBSON, G. D. ( e d s ) Petroleum Geology o f the Continental Shelf o f N W Europe. Institute of Petroleum, London, p p. 110-120

Gudlaugsson, S.T., Faleide, J.I., Johansen, S.E., Breivik, A.J., 1998. Late Palaeozoic structural development of the South-western Barents Sea. Marine and Petroleum Geology 15 (1), 73–102.

HARLAND, W. B. 1973. Tectonic evolution of the Barents Shelf and related plates. Bull. Am. Assoc. Petrol. Geol. 19, 599-608.

Hardin, F. R., and Hardin, G. C, Jr., 1961, Contamporaneous Normal Faults of Gulf Coast and their relation to Flexures: American Assoc. of Petroleum Geologists Bull., v. 45, pp. 238-248.

Hayward, A.B., & Graham, R. H., 1989, Some geometrical characterstics of inversion. In: M. A. Cooper & G. D.Williams, (Eds.) Inversion Tectonics . Special Publication, Geological Society London, v. 44, p. 17-40.

Hamblin, W. K., 1965, Origin of "reverse-drag" on the downthrown side of normal faults: Geological Society of American Bulletin, v. 76, p. 1145-1164.

ILIFFE, J. E., LERCHE, I. & NAKAYAMA, K. 1990. Structural implications of compactional strain caused by fault block rotation: evidence from two-dimensional numerical analogues. In KNIPE, R. J. & RUTTER, E. H. (eds) Deformation Mechanisms, Rheology and Tectonics. Geological Society, London, Special Publication, 54, 501-508.

JACKSON, J. A., WHITE, N. J., GARFUNKEL, Z. & ANDERSON, H. 1988. Relations between normal-fault geometry, tilting and vertical motions in extensional terrains: an example form the southern Gulf of Suez. Journal of Structural Geology, 10, 155-170.

Jensen, L. N., & Sørensen, K. (1992) Tectonic framework and halokinesis of the Nordkapp Basin. In: *Structural and Tectonic Modelling and its Application to Petroleum Geology,* R. M. Larsen, H. Brekke, B.T. Larsen, & E. Talleraas (Eds). *Norwegian Petrol. Soc. Spec. Publ. No.1* (pp. 109-120).

Jensen, L.N., & Broks, T. M. (1988) Late movement on the Trollfjord-Komagelv fault zone and rifting in the Nordkapp basin (abstract). In: VI. *Annual Tectonic and Structural Geology Studies Group Meeting, Norwegian Geological Society, Oslo, 17-18 November 1988, Program with Abstracts, Internal* Rep. Ser. No. 54, Dept. Geol., Univ. Oslo (pp. 24-25).

Johansen, S.E., Ostisty, B.K., Birkeland, O., Fedorovsky, Y.F., Martirosjan, V.N., Christensen, O.B., Cheredeev, S.I., Ignatenko, E.A., Margulis, L.S., 1993. Hydrocarbon potential in the Barents Sea region: play distribution and potential. In: Vorren, T., Bergsager, E., Dahl-Stamnes, Ø., Holter, E., Johansen, B., Lie, E., Lund, T. (Eds.), Arctic Geology and Petroleum Potential.

Norwegian Petroleum Society (NPF), Special Publication, vol. 2. Elsevier, Amsterdam, pp. 273e320.

Johansen, S.E., Gudlaugsson, S.T., Svånå, T.A., Faleide, J.I., 1994. Late Paleozoic evolution of the Loppa High, Barents Sea. Part of unpublished PhD thesis, University of Oslo, Oslo, p. 25.

Johansen, S. E. Gudlaugsson, S. T., Svånå, T. A., & Faleide, J. I. (1994a) Late Paleozoic evolution of the Loppa High, Barents Sea. In : Geological Evolution of the Barents Sea, with special Emphasis on the Late Paleozoic Development, S. E. Johansen (Ed.), Dr. Scient. Thesis, University of Oslo, 25 pp.

Kim, Y.-S., Andrews, J.R., Sanderson, D.J., 2000. Damage zones around strike–slip fault systems and strike–slip fault evolution, Crackington Haven, southwest England. Geoscience Journal 4, 53– 72.

Kim, Y.-S., Andrews, J.R., Sanderson, D.J., 2001. Reactivated strike–slip faults: examples from north Cornwall U.K.. Tectonophysics 340, 173– 194.

Kim, Y.-S., Sanderson, D.J., 2004. The relationship between displacement and length of faults: Earth Science Reviews 68 (2005) 317-334.

Larssen, G. B., Elvebakk, G., Henriksen, L. B., Kristensen, S. E., Nilsson, I., Samuelsberg, T.A., Stemmerik, L., & Worsely, D., 2002, Upper Paleozoic lithostratigraphy of the southern Norwegian Barents Sea: Norsk Geologisk Undersøkelser, Bulletin 444, 43. Geological Survey of Norway, Trondheim.

Lippard, S.J. & Roberts, D. 1987: Fault systems in Caledonian Finnmark and the southern Barents Sea. *Norges geologiske undersøkelse Bulletin 410*, 55-64.

MASCLE, J. & MARTIN, L. 1990. Shallowstructure and recent evolution of the Aegean Sea: A synthesis based on continuous reflection profiles. Marine Geology, 94, 271-299.

McCLAY 1989. Analogue models of inversion tectonics. Geological Society, London, v. 44; p41-59.

Müller, R., Nystuen, J.P., Eide, F., Lie, H., 2005. Late Permian to Triassic basin infill history and palaeogeography of the mid-Norwegian shelf e East Greenland region. In: Wandas, B.T.G., Nystuen, J.P., Eide, E., Gradstein, F. (Eds.), Onshoreeoffshore Relationships on the North Atlantic Margin. Elservier, Trondheim, pp. 165e789.

Morley, C. K., Nelson, R. A., Pattion, T. L., & Munn, S. G., 1990 Transfer zones in the East African Rift System and their relevance to hydrocarbon exploration in rifts: AAPG Bulletin, v. 74, p. 1234-1253.

MONTADERT, L., ROBERTS, D.G., DE CHARPEL, O. & GUENNOC, P. 1979. Rifting and subsidence of the northern continental margin of the Bay of Biscay. In: MONTADERT, L. & ROBERTS, D.G. (eds) Initial Reports of D.S.D.P., 48, 1025-1060.

Nilsen, K. T., Henriksen, E., & Larssen, G. B. (1993) Exploration of the Late Paleozoic carbonates in the southern Barents sea – a seismic stratigraphy study. In *: Arctic Geology and Petroleum Potential*, T. O. Vorren, E. Bergsager, ø. A. Dahl-Stamnes, E. Holter, B. Johansen, E. Lie, & T. B. Lund (Eds), Norwegian Petrol. Soc. Spec. Publ. No. 2 (pp. 393-403).

Nøttvedt, A., Johannessen, E.P., Surlyk, F., 2008. The Mesozoic of western Scandinavia and east Greenland. Episodes 31, 59e65.

Nøttvedt, A., Cecchi, M., Gjelberg, J. G., Kristensen, S.E., Lønøy, A., Rasmussen, A., Rasmussen, E., Skott, P. H., & van Veen, P. M. (1993a) Svalbard-Barents Sea correlation : a short review. In : *Arctic Geology and Petroleum Potential*, T. O. Vorren, E. Bergsager, ø. A. Dahl-

Stamnes, E. Holter, B. Johansen, E. Lie, & T. B. Lund (Eds). *Norwegian Petrol. Soc. Spec. Publ. No. 2* (pp. 33-361).

Peacock, D.C.P., 1991. Displacement and segment linkage in strike–slip fault zones. Journal of Structural Geology 13, 1025–1035.

Peacock, D.C.P., Sanderson, D.J., 1991. Displacement and segment linkage and relay ramps in normal fault zones. Journal of Structural Geology 13, 721–733.

Prosser, Sarah, 1993, Rift-related linked depositional systems and their seismic expression, Tectonics and Seismic Sequence Stratigraphy, Geological Society Special Publication 71, 35-66.

Reemst, P., Cloetingh, S. and Fanavoll, S. (1994) Tectonostratigraphic modelling of Cenozoic uplift and erosion in the south-western Barents Sea. *Marine and Petroleum Geology* 11,478-490.

Reksnes, P. A. and Vagnes, E. (1985) Evolution of the Greenland Sea and Eurasia Basin *Cand. Scient. Thesis***,** University of Oslo, 136 pp.

Riis, F., Vollest, J., & Sand, M. (1986) tectonic development of the western margin of the Barents Sea and adjacent areas. In: *Future Petroleum provinces of the world,* M. T. Halbouty (Ed.), Am. Assoc. Petrol. Geol. Mem. 40 (pp. 66-675).

Rønnevik, H. and Jacobsen, H.P., 1984. Structural highs and basins in the western Barents sea. In: A.M. Spencer et al. (Editors), Petroleum Geology of the North European Margin. Norw. Pet. Soc., Graham and Trotman, London, pp. 98-107.

Schlische, R. W., 1995, Geometry and origin of fault-related folds in extensional settings:AAPG Bulletin, V. 79, No. 11, p. 1661-1678.

Stemmerik, L., Nilsson, I., & Elvebakk, G. (1995) Gzelian-Asselian depositional sequences in the western Barents Sea and north Greenland. In : *Sequence Stratigraphy on the Northwest European Margin*, R. J. Steel, V. L. Felt, E. P. Johannessen, C. Mathieu (Eds), *Norwegian Petrol. Soc. Spec. Publ. No. 5* (pp.529-544).

Skjold, L.J., van Veen, P.M., Kristensen, S.E., Rasmussen, A.R., 1998. Triassic sequence stratigraphy of the southwestern Barents Sea. In: de Graciansky, P.-C., Hardenbol, J., Jacquin, T., Vail, P.J. (Eds.), Mesozoic and Cenozoic Sequence Stratigraphy of European Basins. Society for Sedimentary Geology, Special Publication, No. 60. Society for Sedimentary Geology (SEPM), Tulsa, pp. 651e666.

Stemmerik, L., & Larssen, G. B. (1992) Upper Paleozoic carbonates in the Loppa high area, western Barents Sea. IKU Report No. 23.1438.00/08/92, IKU Petroleum Research, Trondheim, 29 pp.

Stemmerik, L., & Worsley, D. (1989) Late Paleozoic sequence correlations, North Greenland, Svalbard and the Barent Shelf. In : *Correlation in Hydrocarbon Exploration*, J. D. Collinson (Ed.). *Norwegian Petroleum Society* (pp. 99-111). London: Graham and Trotman.

Stemmerik L. & Worsley D. 2005. 30 years on—Arctic Upper Palaeozoic stratigraphy, depositional evolution and hydrocarbon rospectivity. *Norwegian Journal of Geology 85*, 151–168.

Tearpock, D. J. and R. E. Bischke, 1991, Applied subsurface geological mapping: Prentice-Hall.

Tearpock, D. J. and R. E. Bischke, 2003, Applied subsurface geological Mapping second edition: Prentice-Hall, New Jersey.

Thorsen, C. E., 1963, Age of growth faulting in Southeast Louisiana: Transactions - Gulf Coast Association of Geological Societies, v. 13, p. 103–110.

van Veen, P.M., Skjold, L.J., Kristensen, S.E., Rasmussen, A., Gjelberg, J., Stolan, T., 1993. Triassic sequence stratigraphy in the Barents Sea. In: Vorren, T., Bergsager, E., Dahl-Stamnes, Ø., Holter, E., Johansen, B., Lie, E., Lund, T. (Eds.), Arctic Geology and Petroleum Potential. Norwegian Petroleum Geolgists (NGF), Special Publication, vol. 2. Elsevier, Amsterdam, pp. 515e538.

Walsh, J. J., &Watterson, J., 1991, Geometric and kinematic coherence and scale effects in normal fault systems. In: A. M., Yielding, G., and Freeman, B., (Eds.), The geometry of normal faults: Geological Society of London Special Publication, v. 56, p. 193-206.

Waltham, D. A., Hardy, S. and Abousetta, A. (1993) Sediment geometries and domino faulting. In: Tectonics a n d Seismic Sequence stratigraphy (Eds G. D. Williams and A. Dobb), Spec, PubL Geol. Soc. London. No 71, 6 7 - 8 5

Wenricke, B. & Burchfiel, C. 1982. Modes of extensional tectonics. J. Struct. Geol. 4, 105-115.

Willemse, E.J.M., Pollard, D.D., Aydin, A., 1996. Three-dimensional analyses of slip distributions on normal fault arrays with consequences for fault scaling. Journal of Structural Geology 18, 295– 309.

Wilkins, S.J., Gross, M.R., 2002. Normal fault growth in layered rocks at Split Mountain, Utah: influence of mechanical stratigraphy on dip linkage, fault restriction and fault scaling. Journal of Structural Geology 24, 1413– 1429.

Worsley, D., 2008, The post-Caledonian geological development of Svalbard and the Barents Sea, Polar Reasearch 27, 298-317.

Worsley, D., Agdestein, T., Gjelberg, J., Steel. R., & Kirkemo, K, (1990). Late Palaeozoic basinal evolution of Bjørnøya: implications for the Barents Shelf (abstract) Geonytt I, 124-125.

Worsley, D., Agdestein, T., Gielberg, J.G., Kirkemo, K., Mork, A., Nilsson, I., Olaussen, S., Steel, R.J., Stemmerik, L., 2001. The geological evolution of Bjornoya, Arctic Norway: implications for the Barents shelf. Norsk Geologisk Tidsskrift 81, 195e234.

Wood, R.J., Edrich, S.P., Hutchison, I., 1989. Influence of north Atlantic tectonics on the large-scale uplift of the Stappen high and Loppa high, western Barents shelf. In: Tankard, A.J., Balkwill, H.R. (Eds.), Extensional Tectonics and Stratigraphy of the North Atlantic Margins. American Association of Petroleum Geologists, Memoir, vol. 46. Canadian Geological Foundation and AAPG, Tulsa, pp. 559e566.

Zielger, P. A. (1989) Evolution of Laurussia. Kluwer, Dordrecht, 102 pp.

Zielger, P. A. (1988a) Evolution of the Arctic-North Atlantic and the western Tethys Am. Assoc. Petrol. Geol. Mem. 43, 198 pp. (and 30 plates).

Zielger, P. A. (1988b) Laurussia—The Old Red Continent. In: Devonian of the world, eds N.J. McMillan, A.F. Embry, & D.J. Glass, Can. Soc. Petrol. Geol. Mem. 14, 15-48.

Ziegler, P. A. (1978) North Western Europe : tectonics and basin development Geol. *Mijnb*. 57, 589-626.

http://en.wikipedia.org/wiki/File:Barents_Sea_map.png. Last accessed 20th April, 2012.

http://factpages.npd.no/factpages/Default.aspx?culture=en. Last accessed 20th May, 2012.

http://www.slb.com/services/software/geo/petrel.aspx. Last accessed 20th May, 2012.